

Physiological traits associated with increasing grain number in wheat (*Triticum aestivum* L.) and their genetic regulation.



James Norton Garner

School of Biosciences

Sutton Bonington Campus, University of Nottingham

Thesis submitted to the University of Nottingham for the degree of

Doctor of Philosophy

March 2022

Abstract

Previous studies suggest that genetic variation in grain yield potential in wheat is associated with grain sink strength under favourable conditions, which is mainly determined by grain number. Even in suboptimal conditions, increasing grain sink strength raises yield potential and attainable yield in wheat. Therefore, the elucidation of novel grain number traits such as fruiting efficiency (FE, ratio of grain number to spike dry weight at anthesis) and grain dry matter partitioning in wheat is crucial for genetic gains and food security. However, the physiological and genetic basis of these traits is not fully understood. The objectives of this study were, using a winter wheat KWS panel, to identify novel grain number and partitioning traits for increased harvest index and grain yield, and to determine marker-trait associations and candidate genes through a genome wide association study. The association panel of 138 KWS winter wheat genotypes was phenotyped for grain number and partitioning traits in field experiments at anthesis and physiological maturity in two seasons near Cambridge, UK. A subset of eight genotypes representative of field variation for FE was grown in the glasshouse under well-watered conditions at the University of Nottingham, UK in two years for analysis of flag-leaf gas exchange traits and their association with grain number traits and grain yield. To examine if specific plant organs and stem internodes were competing with the spike at anthesis, samples were taken in the field and glasshouse where the plants were separated into their component parts (ear, stem (including stem internodes), leaf sheath and leaf lamina).

Results showed genetic variation in grain yield correlated with grain number and harvest index in the field experiments. The increase in grain number amongst genotypes was associated with an increase in FE. The stem internode component which was competing most with spike growth was the stem-internode 3 as

indicated by a negative association between stem-internode 3 partitioning index and spike partitioning index, suggesting reducing stem-internode 3 length could increase spike dry matter at anthesis. Fourteen traits were analysed in a genome-wide association study and 78 putative marker-trait associations were identified, while 50 potential candidate genes were suggested. These included the *GNI-1* gene on chromosome 2A for Fruiting efficiency, a known gene associated with increased grain number, and *NFYB4* for spike partitioning index, a gene associated with increased spikelet fertility on chromosome 1A. Next steps include validating the associations and developing markers for these key traits to incorporate into plant breeding programs.

Acknowledgements

I would like to thank my Supervisors John and Sean for their endless patience and knowledge imparted. My fellow students, with whom I commiserated often, Bethany, Laura, Jas, and Patrick. Finally, I would like to thank the BBSRC and KWS for funding my work.

Table of contents

Abstract	2
Acknowledgements	4
List of figures	8
List of tables	12
List of abbreviations	16
Chapter 1. General Introduction	21
1.1. Global wheat production.....	21
1.2. Wheat demand and usage	24
1.3. Evolution of bread wheat	26
1.5. Previous genetic gains in yield potential	28
1.5. Genetic analysis of wheat yield potential traits.....	31
1.6. Overall objectives.....	32
Chapter 2. Literature Review	33
2.1. Genetic progress in grain yield potential	33
2.2. Physiological basis of genetic gains in grain yield potential	35
2.3. Crop development	37
2.3.1. Major genes for flowering time	39
2.3.2. Key development phases related to grain number	39
2.4. Grain number model.....	43
2.4.1. Crop growth rate	45
2.4.2. Spike partitioning index	45
2.4.3. Fruiting efficiency.....	48
2.5. Genetic variation in wheat.....	49
2.6. Genome Wide association studies in wheat.....	50
2.7. Project objectives and hypotheses	57
Chapter 3. General Materials and Methods	59
3.1. Field Experiments	59
3.1.1. Experimental design, treatments and crop management.....	59

3.2.	Glasshouse experimental design.....	60
3.2.1	Crop and plant measurements	60
3.3.	Statistical analysis	61
Chapter 4. Dry matter partitioning and associations with grain number and yield in an elite doubled-haploid winter wheat panel		62
4.1.	Introduction.....	62
4.2.	Materials and methods	64
4.2.1.	Plant material and experimental design.....	64
4.2.2.	Crop measurements.....	66
4.2.3.	Statistical analysis	68
4.3.	Results.....	69
4.3.1.	Grain yield and yield components traits in the KWS panel.....	69
4.3.2.	DM partitioning traits at anthesis in KWS panel	76
4.3.3.	True-stem internode der-matter partitioning at anthesis for subset 1	81
4.3.4.	NDVI senescence and leaf chlorophyll fluorescence traits	84
4.3.4.1.	Leaf photosynthesis and canopy senescence parameters	85
4.4.3.	Correlations between leaf photosynthetic and senescence traits.	87
4.5.	Discussion.....	91
Chapter 5. Genetic analysis of physiological traits to improve grain partitioning and yield in an elite UK winter wheat association panel ...		103
5.1.	Introduction.....	103
5.2	Materials and methods.....	106
5.2.1.	Plant material and experimental design.....	106
5.2.2.	Crop measurements.....	106
5.3.	DNA extraction and genotyping.....	107
5.3.1.	Results.....	107
5.3.1.	Distribution of significant markers.....	108
5.3.2.	Genome wide association analysis	110
5.3.3.	Candidate gene analysis.....	125
5.4..	Discussion.....	131

5.5.	Supplementary material	Error! Bookmark not defined.	38
5.5.1	Combined year GWAS output.....		138
Chapter 6 Source/Sink traits and association with HI and grain yield in a subset of a UK KWS winter wheat association panel in glasshouse experiments			
			140
6.1.	Introduction		140
6.2.	Materials and Methods.....		141
6.2.1	Experimental design and growth conditions.....		141
6.2.2	Crop measurements.....		142
6.2.3	Spike sampling and RNA extraction.....		143
6.3.	Results		144
6.3.1	Genetic variation in experiments.....		144
6.3.2	Correlation between variation in glasshouse traits and field experiments.....		148
6.4.	Discussion.....		150
Chapter 7. General Discussion			Error! Bookmark not defined.
			53
7.1.	Summary of hypotheses.....		153
7.2	Implications for breeders.....		156
7.3	Future work.....		156
7.3.1	Optimising spike partitioning and validation of physiological relationships.....		156
7.3.2	Further exploration of Fluorescence parameters.....		157
7.3.3	Validation of potential candidate genes.....		157
8.	References.....		159

List of Figures

Figure 1.1. Annual Global wheat yield in tonnes per hectare 1961 – 2012. Data from FAOSTAT (statistics division of the Food and agriculture organisation of the United Nations	23
Figure 1.2. Average wheat yields for different regions by tonne per hectare as of 2014. Data from FAOSTAT (statistics division of the Food and agriculture organisation of the United Nations, http://www.faostat.fao.org/	24
Figure 1.3. Global area cultivated for cereal crops by year in million hectares, 1961 – 2020. Data from FAOSTAT (statistics division of the Food and agriculture organisation of the United Nations, http://www.faostat.fao.org/.....	25
Figure 1.4. Phylogeny of hexaploid wheat <i>Triticum aestivum</i> L, adapted from Feullet et al. (2008)	27
Figure 2.1. Diagram of wheat developmental stages and their relation to yield components. Taken from Sreenivasulu, N. & Schnurbusch, T. (2012)	41
Figure 3.1. Image of plots for the 2017/18 field trial, June 2018	1
Figure 3.2. Image of plots for the 2017/18 field trial, Jan 2019	1

Figure 4.1. Cross-year Linear regressions of grain yield with biomass and yield components in the KWS association panel for 2017/18 and 2018/19 field trials. A) Yield versus Above ground dry matter g per m⁻² (AGDM) - R² = 0.287, P = <.001. B) Yield versus Harvest index R² = 0.142, P = <.001 C) Yield g m² versus fruiting efficiency (Anthesis) - R² = 0.057, P = 0.003. D) Yield g m² x Fruiting efficiency (chaff) - R² = 0.01, P = 0.7)71

Figure 4.2. Cross-year linear regressions of yield with grain traits. A) Yield versus Thousand grain weight R² = 0.054, P = 0.005. B) Yield g m⁻² x Grains per m⁻² - R² = 0.0320, P = 0.03.72

Figure 4.3. A) Yield x Thousand grain weight for 2017/18 field trial of the KWS association panel. R² = 0.127, P = <.001). B) Yield x Grains per m⁻² for the 2018/19 field trial of the KWS association panel. R² = 0.1487, P = <.001).....73

Figure 4.4. A) Fruiting efficiency x Grains m⁻² for the KWS association panel combined means. R² = 0.332, P = <.001. B) Spike partitioning index x Grains m⁻² for the KWS association panel combined means. R² = 0.053, P = 0.005.74

Figure 4.5. Yield 2017/18 g m⁻² x Yield 2018/19 g m⁻² for the KWS association panel. R² = 0.1228, P = <.00173

Figure 4.6. Pearson's correlation matrix of key grain partitioning and plant component partitioning indices, yield, and other traits. Internode lengths (cm), Anthesis components dw m^{-2} , anthesis component partitioning indices, Above ground dry matter g m^{-2} , TGW, Yield g m^{-2} , Harvest index, grains m^{-2} , fruiting efficiency calculated with anthesis biomass, fruiting efficiency with chaff at harvest. Values shown are for the combined field trials.75

Figure 4.7. Annual Linear relationships between dry matter partitioning indices. A) Spike partitioning index versus Lamina partitioning index – $R^2 = 0.035$, $P = 0.02$. B) Spike partitioning index versus leaf sheath partitioning index – $R^2 = 0.005$, $P = 0.4$. C) Spike partitioning index versus stem partitioning index - $R^2 = 0.367$, $P = <.001$. D). Lamina partitioning index x Stem partitioning index - $R^2 = 0.536$, $P = <.001$. Values represent means of 2017-18 and 2018-19.78

Figure 4.8. Linear Regressions between Stem DM shoot-1 (g) and stem internode length (cm) : Ped, $R^2 = 0.155$, $P = 0.051$. Int 2: $R^2 = 0.01$, $p=0.977$. Int 3: $R^2 = 0.05$, $P=0.266$ for the 27-line subset of the KWS association panel, cross year means for 2017/18 and 2018/19. 1

Figure 4.9. Linear relationships between True stem partitioning indices and spike partitioning index for the 27-line subset of the KWS association panel (Subset 1). A) Spike partitioning index x Peduncle partitioning index. $R^2 = 0.07$, $P = 0.09$. B) Spike partitioning index x Internode 2 partitioning index $R^2 = 0.1302$, $P = 0.03$. C) Spike

partitioning index x Internode 3 partitioning index, $R^2 = 0.04$ $P = 0.37$.

..... 1

Figure 4.10. Comparison of NDVI grand means for 2017/18 and 2018/19 Field Trials at comparable developmental time points. Error bars show Least significant difference of the mean. Initial measurements were taken in the middle of March, and final measurements at the end of July. Vertical coloured lines represent date of anthesis for representative year. 1

Figure 5.1. Distribution of significant marker- trait associations ($-\log_{10} < 3$) among 137 genotypes for the of the KWS winter wheat panel in 2017/18 by a A) genome and B) chromosome, and in 2018/19 field trial by c C) genome, and d D) chromosome. 1

Figure 5.2. Principal Component Analysis showing population structure of the KWS association panel. 1

Figure 5.3. A) Manhattan plot for GWAS on the trait Grain Yield (g m^{-2}) in 2018 with $-\log_{10}$ p thresholds of 3, and 5 plotted against chromosome position and B) QQ plot with $-\log_{10}$ transformed p-values using the mixed linear model..... 1

Figure 5.4. A) Manhattan plot for GWAS on the trait Grain Yield (g m^{-2}) in 2019 with $-\log_{10}$ p thresholds of 3, and 5 plotted against

chromosome position and B) QQ plot with $-\log_{10}$ transformed p-values using the mixed linear model..... 1

Figure 5.5. Manhattan plot of GWAS MTAs for the above-ground DM (g m⁻²) (AGDM) with $-\log_{10}$ p thresholds of 3, and 5 plotted against chromosome position and for 2017/18 and 2018/19. 1

Figure 5.6. Manhattan plot of GWAS marker trait associations for Fruiting efficiency with $-\log_{10}$ p thresholds of 3, and 5 plotted against chromosome position for 2017/18 and 2018/19. 1

Figure 5.7. Manhattan plot of GWAS marker trait associations for Harvest Index for 2017/18 with $-\log_{10}$ p thresholds of 3, and 5 plotted against chromosome position for 2017/18 and 2018/19. 1

Figure 5.8. Manhattan plot of GWAS marker trait associations for Thousand grain weight (g) with $-\log_{10}$ p thresholds of 3, and 5 plotted against chromosome position for 2018/18 and 2018/19. 1

Figure 5.9. Phenogram of MTA locations by chromosome and genome for the field trials of the KWS association panel. 2018 results are shown as blue lines, 2019 results as green lines..... 1

List of Tables

Table 1.1. Highest and lowest wheat average on-farm yields by country in tonnes per hectare as of 2014. Data from FAOSTAT (statistics division of the Food and agriculture organisation of the United Nations, <http://www.faostat.fao.org/>24

Table 2.1 Summary of genome-wide association studies.....52

Table 4.1. Line substitutions for the 2018/19 field trial.65

Table 4.2. Rainfall data from the Cambridge NIAB weather station at 543500E 260600N , Lat 52.245 Lon 0.102 for the months of March – July in 2018 and 2019. Values shown are in mm. 'Average' is the average rainfall data at this station between 1981-201065

Table 4.3.1 Means, ranges and significance of grain yield and harvest traits from the 137 lines in the KWS association panel, combined means across 2017/18 and 2018/19 field trials. Grain yield, Fruiting efficiency (Calculated from anthesis spike DM), fruiting efficiency (calculated from chaff DM), above-ground dry matter(AGDM) g m-2, thousand grain weight and harvest index.70
.....

Table 4.4 Range, mean average, and significance for dry-matter partitioning indices, plant component dry matter per shoot, and plant component dry matter per m-2 for the for the 137 lines in the KWS association panel, combined across 2017/18 and 2018/19 field trials. 77

Table 4.5 Cross-year genetic ranges, means, and significance values of 25 lines from the KWS association panel (Subset 1) for Stem-internode length, stem-internode partitioning indices and internode specific weights. All values are for true stem only. Significance values are for Genotype (G), Year (Y), and Genotype x year (GxY). Values presented are cross-year means (2018/19, 2019/20).80

Table 4.6. Pearson’s correlation coefficient between stem-internode traits and grain yield and yield components for the 25-line subset of the KWS association panel (Subset 1). Values presented are cross-year means (2018/19 and 2019/20). PI = Partitioning index, SPW = Specific weight. † p<0.1, *p<0.05, **P<0.01) 1

Table 4.7. Cross- year means, significance and ranges for NDVI senescence parameters. Stay-green score shows the NDVI value at onset of senescence (20%) and end of senescence (80%) for 138 genotypes in KWS panel.. 1

Table 4.8. Cross-year means, significance and ranges for leaf SPAD and leaf chlorophyll fluorescence parameters for 138 genotypes in KWS panel in 2018-19. Phi2 is a measure of the Quantum Yield of Photosystem II. PhiNPQ shows the ratio of absorbed light used in the non-photochemical quenching response. PhiNO shows ratio of absorbed light lost via other miscellaneous processes. 1

Table 4.9. Linear relationships between canopy and leaf photosynthetic traits and grain partitioning and yield traits for the 25-line subset of the KWS association panel 2018/19 (subset 1). Senescence parameters show data for the full panel of 138 lines. Values shown are R². 1

Table 5.1. Summary of GWAS results obtained using a threshold of -log₁₀ <3 for two different models using both individual year means and combined means. GLM: General linear model; MLM: Mixed linear Model; PC: Principal component; K: kinship matrix; Ave: Average. 1

Table 5.2. Summary of MTA's obtained from the GWAS on the KWS winter wheat association panel, by trait, year and location at chromosome and genome level. * indicates the marker co-located for multiple traits within a year. 1

Table 5.3. List of potential genes from marker trait associations obtained from GWAS with the KWS association panel using KnetMiner, separated by year for the two individual year GWAS performed. Combined mean candidate genes can be found in the appendix 1

List of abbreviations

%	Percentage
°C	Degree centigrade
AGDM	Above-Ground Dry Matter
AM	Association Mapping
ANOVA	Analysis of Variance
Aw	Awn
BLUE	Best Linear Unbiased Estimator
BT	Booting
bp	Base pair
CGR	Crop dry matter accumulation
	International Maize and Wheat Improvement
CIMMYT	Center
chr	Chromosome
cM	centimorgan
cm	centimetre
DAE	Days after emergence
DM	Dry Matter
DNA	Deoxyribonucleic acid
Ds	Duration of spike growth
DTA	Days to anthesis
DTM	Days to maturity

DW	Dry Weight
FAO	Food and Agriculture Organization
FE	Fruiting Efficiency
F _s	Fraction of this dry matter partitioned to the spike averaged over the spike growth period
FW	Fresh Weight
g	Grams
G	Genotype
GA	Green Area
GAI	Green Area Index
GLM	General Linear Model
Glu	Glume
GN	Grain Number
GS	Growth Stage
GS65	Anthesis (Zadok's growth scale)
GS65+7d	Seven days after anthesis (Zadok's growth scale)
GS87	Physiological Maturity (Zadok's growth scale)
GW	Grain Weight
GWAS	Genome-Wide Association Study
GY	Grain Yield
h	Hours
H ²	Broad-sense heritability

ha	Hectare
HI	Harvest Index
Int	Internode
Int4+	Internode 4 and rest
kg	Kilogram
L	Litre
Lam	Lamina
LamPI	Lamina Partitioning Index
LD	Linkage Disequilibrium
Le	Lemma
Ln	Length
LOD	Logarithm of Odds
LS	Leaf Sheath
m	Meters
MAF	Minor Allele Frequency
Max	Maximum
MAS	Marker Assisted Selection
Mean	Average
mg	Milligrams
Min	Minimum
MJ	MegaJoule
MLM	Mixed Linear Model

mm	Millimetre
MTA	Marker Trait Association
NGS	Next-Generation Sequencing
NIL	Near-Isogenic Lines
Pa	Palea
PAR	Photosynthetically Active Radiation
PCA	Principal Component Analysis
Ppd	Photoperiod
PGR	Plant Growth Regulator
PH	Plant Height
PI	Partitioning Index
PM	Physiological Maturity
PT	Physiological Trait Breeding
QTL	Quantitative Trait Loci
Ra	Rachis
Rht	Reduced Height
RIL	Recombinant Inbred Line
Rubisco	Ribulose-1,5-bisphosphate carboxylase/oxygenase
RUE	Radiation Use Efficiency
SDWa	Dry weight of spikes at anthesis
SE	Stem Elongation
SG	Stay Green

SNP	Single Nucleotide Polymorphism
SPI	Spike Partitioning Index
Spk	Spike
Spk/spk	Spikelets per spike
StePI	Stem Partitioning Index
SW	Specific Weight
TGW	Thousand-Grain Weight
Tin	Tiller inhibition
t	Tonne
TS	True Stem
UK	United Kingdom
Vrn	Vernalization
WSC	Water Soluble Carbohydrates
Yr	Year

Chapter 1. General Introduction

1.1 Global wheat production

As one of the most widely consumed cereal crops globally, ensuring production of wheat meets demand in the future is of paramount importance for food security. The three major cereal crops comprise 70% of human calorie intake (Melrose et al., 2015, Braun et al., 2010). In order for demand to keep pace with population growth, it has been suggested that crop yields will need to double by 2050 (FAO, 2017). For wheat specifically, a total yield of 1 billion tonnes per annum has been predicted as necessary to meet demand (Bruinsma, 2009), with current annual production at approximately 771 million tonnes (FAO, 2019). Wheat yield has been increasing linearly at approximately 1% per annum, however it has been projected that this must increase to 2-3% in order to meet projected demand (Hawkesford et al., 2013). Annual yield increases of wheat have been increasing at the slowest rate of all three major cereals (fig 1.1). Furthermore, these yield increases must come primarily from higher yields per hectare, rather than simply increasing the amount of land used for arable agriculture, due to lack of currently available unused land. Total global area cultivated for wheat has not significantly changed in the last 50 years and has in fact been declining slightly since its peak of 267 million hectares in 1981, compared to 242 million hectares in 2020 (fig 1.2).

The problem of wheat yields meeting projected demand is further compounded by potential environmental effects due to climate change, which will alter temperatures and rainfall distribution and cause significant changes to the productivity of agricultural land (Berry et al., 2006; Olesen & Bindi, 2002). Changes

to rainfall distribution and temperature in particular are expected to have a significant impact on agriculture globally, mainly due to the impact of drought and temperature and flooding stresses. Increased global temperatures alter precipitation patterns and atmospheric moisture through changes in atmospheric water circulation and increases to water holding capacity in the atmosphere (Dore, 2005). In general, mid and high latitude areas such as the U.S, Canada and Northern Europe appear to be experiencing increases in precipitation (Hanssen-bauer & Førland, 2000; Karl et al., 1998; Nikulin et al., 2011). Average precipitation frequency is expected to decrease in China (Piao et al., 2010; Zhai et al., 2005) and Mediterranean regions such as Southern Europe, as well as the Southwest United states, leading to drought stress. However, the frequency of extreme precipitation events in these places is also expected to increase, leading to an increased frequency of both drought and flooding events (Gao et al., 2006; Meehl et al., 2005). Finally, North Africa and India are likely to experience increased temperatures above the global average, and higher incidence of droughts, which are predicted severely to impact agricultural productivity in these regions (Mall et al., 2006; Radhouane, 2013).

The predicted changes in climate would have a significant impact on cereal yields. One study examining Chinese wheat cultivars found that an increase of 1°C decreased yields of winter wheat by between 3-10%, and that increased temperatures had accounted for a 4.5% decline in wheat yields over the past twenty years; yield increases recorded over that period were a result of increased physical inputs (You et al., 2009) Globally, climate-driven changes to yield are estimated at per- annum losses of 88.2 kg/ha for wheat, 10.5 kg/ha for rice, and 12.5 kg/ha for maize (Lobell et al., 2011; Lobell & Field, 2007). Even regions that experience an average increase in precipitation could be subject to drought

stresses due to longer periods between rainfalls, broken by extreme weather events more likely to lead to flooding (Lehner et al., 2006).

Another factor to be considered is how changes to rainfall distribution and temperatures may affect the area of arable land available for crop production. One study by (Zhang and Cai, 2011) suggests that under scenario A1B (IPCC, 2007) where CO₂ emissions reach 850ppmv, total global arable land area could decrease by as 0.8 to 1.7%. However, under scenario b1, where CO₂ emissions reach 600ppmv, total arable land may increase between 2 and 4.4%. Under both scenarios however, total arable land is lost in Europe, Africa and South America, whereas in the higher latitude regions of Russia, China and the U.S total arable land is gained. Russia in particular could gain as much as an additional 67% of its current arable land. Another study by (King et al., 2018) predicts that by 2099, 76% of the Boreal region will be agriculturally viable to some degree, compared to 32% currently, and that the northern edge of feasible growing degree days will shift north by 1200km. Exploiting this newly available arable land with varieties bred specifically for these climates could be a valuable way of increasing total global crop yields.

Changes to dietary habits associated with growing incomes will lead to an increased consumption of meat and dairy products (Delgado, 2003) further pressuring agricultural land responsible for growing grain feed. Although in certain areas of the world there will be an opportunity to increase total cultivated land area (Rejesus et al., 1999) expansion of agricultural land area is largely non-viable, due to increasing urbanisation and competition for available land (Lambin & Meyfroidt, 2011; Smith et al., 2010). Global yield increases must therefore come from the intensification of current land by improving yields per hectare, by the genetic improvement of wheat. As of 2018, the average global wheat yield is 3.5

t/ha, although global variation is significant, with yields as high as 5.8 t/ha in the European Union, and as low as 2.95 t/ha in the U.S.A (Fig 1.2). Average on-farm yields as high as 10 t ha⁻¹ are present in Ireland, and as low 0.39 t ha⁻¹ in Somalia (Table 1.1.). This variation is the result of differences in agronomic practice, environment such as temperature, rainfall, photoperiod and soil type, and genetic differences, such as vernalization or photoperiod sensitivity affecting length of growing season. The relationship between temperature, photoperiod sensitivity and crop growth and development will be discussed in more depth in section 1.2.

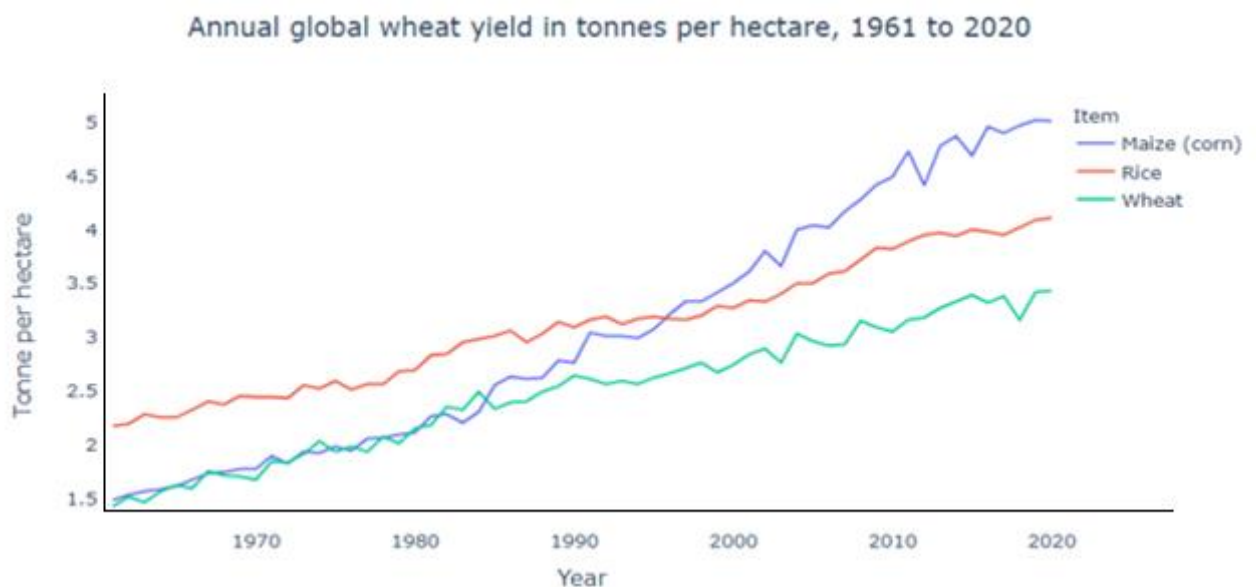


Figure 1.1. Annual Global wheat yield average in tonnes per hectare 1961 – 2020. Data from FAOSTAT (statistics division of the Food and agriculture organisation of the United Nations. (<http://www.faostat.fao.org/>))

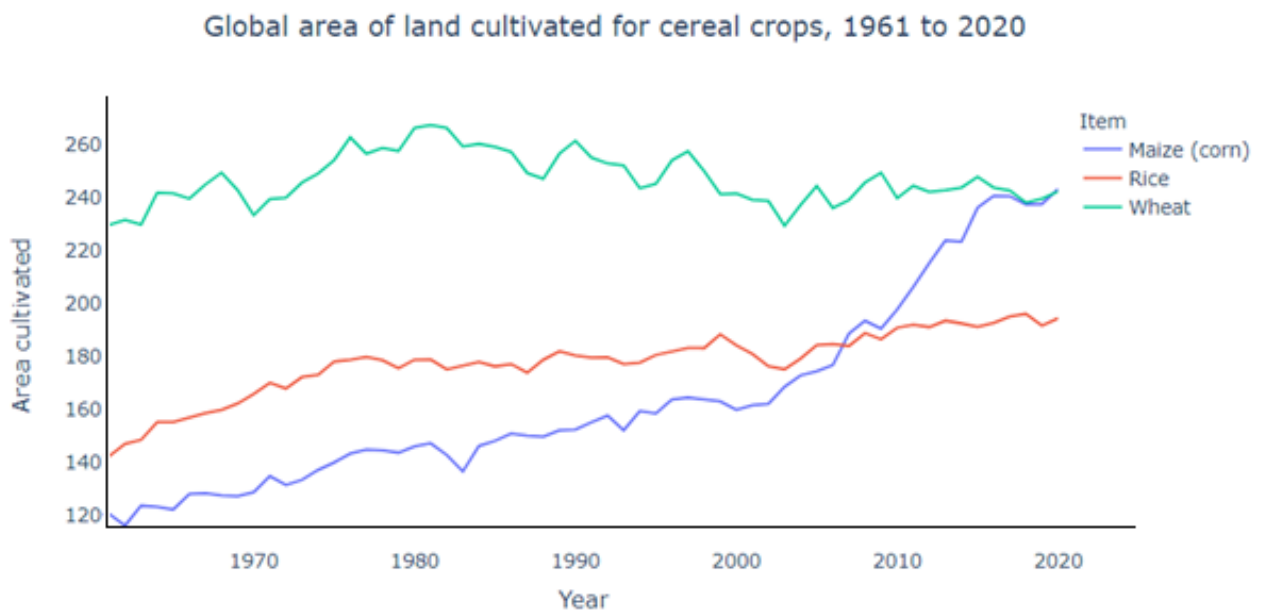


Figure 1.2. Global area cultivated for cereal crops by year in million hectares, 1961 – 2020. Data from FAOSTAT (statistics division of the Food and agriculture organisation of the United Nations).

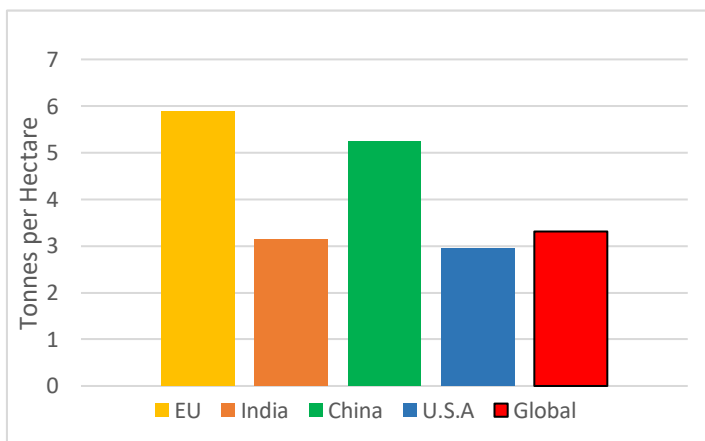


Figure 1.3. Average wheat yields for different regions by tonne per hectare as of 2018. Data from FAOSTAT (statistics division of the Food and agriculture organisation of the United Nations,

<http://www.faostat.fao.org/>

1.2 Wheat demand and usage

Highest and lowest wheat yields by Country	
Country	T/ha
Highest 5	
Ireland	10.01
Belgium	9.41
Netherlands	9.16
Germany	8.62
New Zealand	8.62
Lowest 5	
Somalia	0.39
Honduras	0.52
Burundi	0.57
Cyprus	0.72
Libya	0.77

Table 1.1. Highest and Lowest wheat average on-farm yields by country in tonnes per hectare as of 2014. Data from FAOSTAT (statistics division of the Food and agriculture organisation of the United Nations, <http://www.faostat.fao.org/>)

Wheat comprises approximately 20% of the daily protein and calorific requirements of the global population (Shiferaw et al., 2013). Wheat cultivars fall into two categories, spring or winter. Wheat cultivars referred to as 'spring' or 'winter' are usually *Triticum aestivum* L., bread wheats; however, durum wheat, *Triticum turgidum* var. *durum* Desf. which is used to make pasta, can also be of winter or spring varieties. Spring varieties are sown in spring and harvested in autumn, whereas winter wheats are sown in autumn and harvested in the summer of the following year. They remain in the vegetative phase throughout the winter and enter the reproductive stage in the early spring, after a period of exposure to

low vernalizing temperatures (0-6°C) that is essential for triggering the transition to flowering (Streck et al., 2003; Yan et al., 2003). Winter varieties have a higher yield potential than spring varieties due to the longer growing season. Both can be used in bread making, provided they meet the 13% grain protein requirement. The grain protein percentage relates to the nitrogen input, and bread-making varieties usually require high N applications to meet necessary grain protein content (Barraclough et al., 2014). Wheats with a higher concentration of the protein glutenin and a 'hard' endosperm texture are used for bread making, and those with a low glutenin concentration and 'soft' endosperm texture for making biscuits or cakes. Glutenin affects the viscoelasticity of the dough and allows for the dough to rise and firmer loaf crumb structure. Soft wheats that are low in Glutenin produce a lighter, more crumbly texture suitable for cakes (Payne et al., 1987) Another distinction in wheat is between red wheats and white wheats, determined by seed coat colour. The reddish hues found in red wheats are primarily controlled by three loci with partial dominance, each residing on a different chromosome (Sears, 1944) However, grain colour expression is also influenced by several minor genes (Reitan, 1980) White wheats are usually preferred over red wheats in most markets, primarily due to differences in flavour (Wu et al., 1999)

As well as direct use of wheat grain in breads, pasta and biscuits, wheat is also a key component of animal feeds. Feed wheat can account for 70% of calorific energy and 40% of the protein requirements of broiler chickens (Hew et al., 1998) and is a major component of cattle feed (Gibb et al., 2008). Finally, wheat is produced as a biofuel crop in the European union and Scandinavian countries, specifically Italy, Spain, Denmark, Sweden and Norway where wheat straw is used for the production of bioethanol, and pilot bio-refineries have been established

running on wheat straw in China and Slovakia (Gregg et al., 2017)Wheat has also been used in the Southern Canadian region of Saskatchewan as a biofuel crop (H. Wang et al., 2012)

1.3 Evolution of bread wheat

Bread wheats are the dominant wheat grown globally, accounting for more than 90% of global wheat production (Lantican et al., 2005) In total, 220 M Ha are cultivated globally (FAO, 2017), 70% of which are spring wheat. Cultivated wheat is thought to have originated in the Fertile Crescent region (modern day Southwest Turkey and Northern Syria), approximately 8000 to 10000 years ago(Gill & Friebe, 2002; Lev-Yadun, 2000) and has been a staple crop of importance across Europe, Western Asia and North Africa ever since (Curtis, 2002). Modern hexaploid bread wheat is the result of interspecific hybridisation involving three diploid donor species(Kimber & Riley, 1963; Zohary et al., 2012). The initial event would have been a hybridisation of a progenitor closely related to *Triticum urartu* providing the AA genome, and a close relative of *Aegilops Speltoides*, providing the BB genome (Feuillet et al., 2008). This produced Emmer wheat, *T. Turgidum*, a fertile tetraploid wheat (AABB) that was domesticated approximately 12,000 years ago to become Durum wheat (Luo et al., 2007)A second hybridisation event seems to have taken place about 10,000 years ago, between the Emmer wheat *T. Turgidum* and *Ae. Tauschii*, a wild grass relative which provided the D genome (Feuillet, Langridge and Waugh, 2008). Although this would usually result in the production of a sterile hybrid (ABD), chromosome doubling in progeny resulted in the fertile hexaploid with the AABBDD genome (Zohary et al., 2012)(Fig. 1.3.).

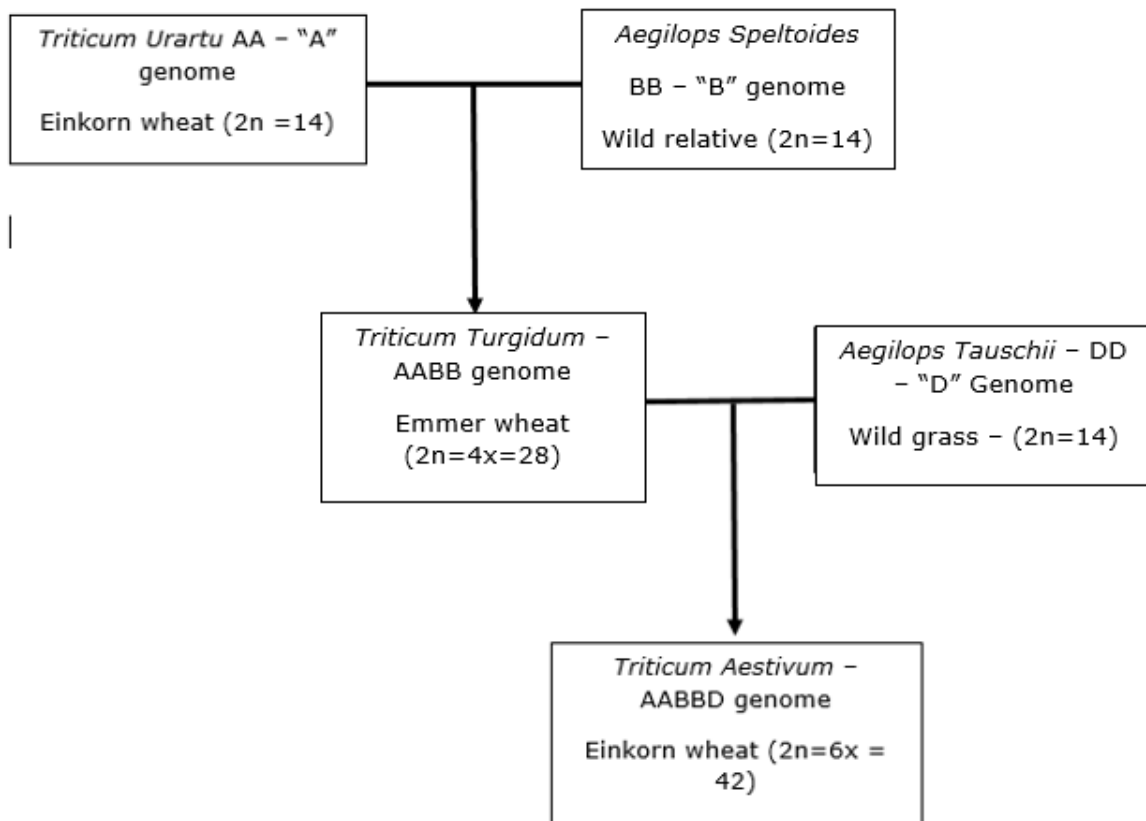


Figure 1.4. Phylogeny of hexaploid wheat *Triticum aestivum* L, adapted from Feullet et al. (2008)

A similar process occurs in the production of synthetic hexaploid wheat, where tetraploid *Triticum turgidum* and the diploid grass ancestor *Aegilops Tauschii* are crossed to replicate the hybridisation event that created modern hexaploid wheat. Primarily this is done in order to introgress novel genes from *T. turgidum* and *Ae. tauschii* accessions that could be used for the improvement of modern wheat (van Ginkel & Ogonnaya, 2007). The D genome of modern *Aegilops tauschii* contains greater genetic variation than the D genome of modern *Triticum aestivum* (Gianibelli et al., 2002). These genes can then be included in breeding programs for the creation of new synthetic-derived cultivars, e.g., as with the successful Chinese cultivar Chuanmai-42 (Yang et al., 2009). CIMMYT have produced over

100 synthetic hexaploid wheat lines, and introgressed key biotic/abiotic stress resistance genes into elite germplasm (Dreisigacker et al., 2008) and CIMMYT synthetic-derived wheats have displayed higher photosynthetic rates than recurrent parents (Blanco *et al.*, 2000). The primary synthetic wheats are a key source of genes to improve traits such as drought resistance, salt tolerance and pest and disease resistance (Schachtman et al., 1992; van Ginkel & Ogonnaya, 2007; YuMin et al., 2012).

1.4. Previous genetic gains in wheat yield potential

It is important to define yield potential when discussing the physiological basis of wheat yield in wheat. Yield potential is the maximum possible yield under ideal environmental conditions and agricultural practices, assuming that no inputs are limited and the plant is free of diseases, pests and has minimal risk of lodging (Evans, 1997) It is a function of the light intercepted (LI) and radiation-use efficiency (above-ground biomass per unit radiation interception; RUE) which results in the above-ground biomass produced, and the harvest index (HI), the proportion of above-ground biomass partitioned to the grain, or

$$YP = LI \times RUE \times HI \text{ (Reynolds et al., 2009)}$$

The global average wheat yield per hectare has tripled since the green revolution 50 years ago, with a 30% increase in land area cultivated. The majority of increase in total wheat yield production has been largely due to the improvements in yield per hectare. (Wik et al., 2008). Although improved agricultural practices are partially responsible for the yield increases, genetic improvement of yield potential is a significant source of higher yield. A major step increase in yield potential came from the creation of shorter, 'semi-dwarf' varieties of wheat, through the introgression of *Rht* (reduced-height) genes, which cause an insensitivity to the

plant hormone Gibberellin (Peng *et al.*, 1999). This increases grain yield by increasing partitioning of assimilate to the grain as a result of decreased straw biomass, as well as improving resistance to lodging (Rajkumara, 2008). Another source of genetic yield potential improvement is the translocation of the short arm of the 1R chromosome from Rye (*Secale cereale*), and the long arm of the 1B chromosome from wheat. The 1B/1R translocation is a frequently used alien introgression for breeding programs globally (Rabinovich, 1998; Schlegel & Korzun, 1997) and is present in many modern cultivars (Sukumaran *et al.*, 2014). 1B/1R lines show an increased resistance to several stem and stripe rusts, as well as powdery mildew. 1B/1R lines have been shown to exhibit significant improvement in yield-related traits such as thousand-grain weight, aboveground biomass and number of spikes per m² (Villareal *et al.*, 1991). The 1B/1R translocation, however, has a negative impact on bread-making quality due to the expression of ω -secalin in place of glutenin, a protein from the 1R chromosome which causes poor dough stickiness and mixing tolerance (CHAI *et al.*, 2016).

Most linear yield potential progress in the first 25 years post green revolution was as a result of selecting for yield empirically rather than specific physiological traits (Loss & Siddique, 1994). As rate of yield gain appears to have been decreasing over the last two decades (R. A. Fischer, 2007), yields may be further increased through improving yield potential by targeting specific physiological traits in breeding programs that affect yield, such as photosynthetic capacity (Reynolds *et al.*, 2011), spike partitioning index (Foulkes *et al.*, 2011) or fruiting efficiency (G. A. Slafer *et al.*, 2015). The approach of targeting specific physiological traits, known as physiological trait breeding (PT) can be successful. CIMMYT have achieved genetic gains in yield potential by performing crosses based on spike

fertility traits and high radiation-use efficiency (Reynolds et al., 2009; Reynolds & Langridge, 2016).

There is significant evidence that grain sink strength is one of the key yield-limiting factors in wheat (Abbate et al., 1995; Borrás et al., 2004; Miralles & Slafer, 2007) even in high-yielding conditions. Improving sink strength through the avenue of increasing grain number, or grains m^{-2} would be a key step in improving yield potential of wheat (Shearman et al., 2005). Target traits for improving grain number include spike-partitioning index (SPI) and fruiting efficiency (Reynolds et al., 2012). Spike partitioning index refers to how much assimilate is partitioned to the spike of the wheat prior to anthesis, where the grains form. One possibility for increasing SPI could be reducing assimilate partitioning to competing sinks, such as the stem or leaves (Foulkes *et al.*, 2011). Fruiting efficiency, also known as spike fertility index, is the number of grains set per unit spike dry weight at anthesis and is another major determinant of grain number. Fruiting efficiency could possibly be improved through an increased partitioning of assimilates to the florets during spike growth prior to anthesis, or a reduction in structural components of the spike such as the rachis or glume (Ferrante et al., 2017; G. A. Slafer et al., 2015)

1.5. Genetic analysis of wheat yield potential traits

Advancements in molecular biology have had a significant impact on wheat breeding over the last 15 years, allowing for the development of marker-assisted selection in breeding programs. Marker-assisted selection (MAS) involves using

the presence or absence of specific DNA markers that are tightly linked to genes or QTLs of interest in the place of phenotypic selection when breeding and can be more efficient and reliable than conventional breeding techniques (Collard et al., 2005). A large number of qualitative traits in wheat have already been characterised using molecular markers, particularly grain quality and disease-resistance traits (Hoisington et al., 2007). One key advantage of MAS is that it allows for selection for sets of traits that have low heritability, but are advantageous for other reasons, such as disease resistance or bread-making quality (William et al., 2007).

Genome wide association studies (GWAS) are a useful method of identifying the genetic architecture of complex physiological traits, such as yield components, by examining associations between single nucleotide polymorphisms and the phenotype of numerous individuals (Korte & Farlow, 2013), which can then be used as markers for breeding programs. This approach has been used to identify loci responsible for variation in grain yield in wheat (Sukumaran et al., 2014; W Tadesse, 2015). GWAS has been used extensively by CIMMYT to target bread quality and increase grain protein content. In the GWAS study by (Battenfield et al., (2018), 6 of 7 identified QTL's were adopted into the CIMMYT bread wheat breeding program. Advances in phenotyping techniques facilitate the high-throughput methods that are necessary to score large numbers of individuals. Remote sensing is a non-intrusive method of measuring traits such as canopy temperature or vegetation index using visible/near infrared cameras to measure reflected or transmitted radiation from the crop (Araus & Cairns, 2014). This can be done proximally by handheld devices, or even by Unmanned Aerial Vehicles (UAVs) and satellite imagery, provided resolution is high enough. UAV-based cameras are particularly effective, as they can measure many plots in a relatively

short amount of time for high resolution thermal and multispectral imagery (Tattaris et al., 2016).

1.6 Overall Objectives

- To identify mechanisms underlying spike partitioning index and fruiting efficiency in order to improve grains m^{-2} and harvest index in high biomass backgrounds.
- To develop molecular markers for SPI/FE traits for improved grain partitioning and grain yield in high biomass backgrounds.

Chapter 2. Literature review

2.1 Genetic progress in grain yield potential

In addition to the potential yield, there is also the attainable yield, the yield reached by using the best available technology, which is close to the potential yield ceiling. Farm yields usually reach 60-80% of the attainable yield (Foulkes *et al.*, 2011). Yield potential is well expressed across different environments (Calderini & Slafer, 1998; G. Slafer & Araus, 2007), and is therefore an important target for improving yields even in suboptimal environments.

Work on CIMMYT spring wheat lines in NW Mexico by (Waddington *et al.*, 1986) showed yield increases of 59 kg/ha/yr, about 1.1% per year, between 1950 and 1982, with increases attributable to grains per m². Similarly, work by (Sayre *et al.*, 1997) on CIMMYT spring wheat in NW Mexico found increases of 67 kg/ha/yr (0.88% per year) for releases between 1962 and 1988 related to grains per m². Argentinian wheats between 1985 and 1995 showed genetic yield gains of 0.92% between 1985 and 1995 (Calderini *et al.*, 1995). In winter wheat in the UK, slightly higher increases in genetic grain yield potential have been observed (Shearman *et al.*, 2005) of 100 kg/ha/yr (1.2% per year) for cultivars released between 1972 and 1995, associated with an increase of 217 grains /m²/yr. Genetic gains in CIMMYT spring bread wheat advanced lines showed a mean annual gain of 0.65% per year, over 15 year and across 919 environments (Sharma *et al.*, 2012). Furthermore, genetic yield gains of 1% per year of low and high yielding CIMMYT lines in semi-arid environments between 1994-2010 were reported by ((Manès *et al.*, 2012). (Aisawi *et al.*, 2015) found yield potential increases of 30 kg/ha/yr in CIMMYT lines between 1966 and 2009, whilst (Lopes, Reynolds, Jalal-Kamali, *et al.*, 2012) found increases of 0.7% per year between 1977 and 2008 in 26 CIMMYT

spring wheat lines in Mexico, across a range of environments. Genetic progress of Brazilian spring wheat lines between 1940 and 2009 has been reported of 0.92% per year, or 29 kg/ha/yr (Beche *et al.*, 2014), whilst south Australian wheat varieties between 1958 and 2007 showed genetic yield progress of close to 0.5% per year, or 25 kg/ha/yr (Sadras & Lawson, 2011).

There is some evidence to suggest that the recent rate of genetic gains in wheat yield potential is decreasing in some regions and countries. An analysis of North American winter wheat yields between 1959 and 2008 found that grain yields of Great Plains hard winter wheat may have peaked in the early to mid-1990's and genetic progress has reached a plateau (Graybosch & Peterson, 2010). Analysis of CIMMYT spring wheat lines by (Beche *et al.*, 2014) found similar results for ten modern cultivars of Brazilian spring wheat, reporting that no significant increases in genetic gain have occurred between 1999 and 2009. Elsewhere, plateau's for genetic yield progress in both winter and spring wheats have been observed in Mexico, the United Kingdom, and Spain during a similar period (Acreche *et al.*, 2008; R. A. Fischer & Edmeades, 2010). Interestingly, a study of cereal yields in France reported that the recent rate of genetic gain has not declined, but yields have been impacted by drought stress during stem elongation, leading to the decline in yield gains observed (Brisson *et al.*, 2010). A study by (PJ *et al.*, n.d.) examined genetic progress of bread wheat cultivars in Argentina between 1918 and 2011. They found that between 1940 and 1999, genetic yield progress was highest at 1.17% per year but between 1999 and 2011, gains have decreased to 0.17% per year. Similarly, yield potential progress of CIMMYT bread wheat varieties between 1996 and 2005 has declined to approximately 0.5% per year (Fischer, 2007). Finally, (Acreche *et al.*, 2008) examined genetic yield progress of Mediterranean bread wheat yields in Spain and found that yield progress between 1998 and 2008

for moderate and low yielding environmental conditions was not significantly different from zero, but that in high yielding conditions genetic gains in yield potential were present for modern cultivars. Conversely, some studies have reported recent gains in genetic yield progress. (Sadras & Lawson, 2011) in Australia reported that the rate of genetic yield improvement for spring wheat varieties had been increasing linearly from 1958 to 2007. Likewise, (Peltonen-Sainio et al., 2009) reported that the rate of genetic gain in Finnish winter and spring wheats was also increasing steadily. In Spain, a study of 28 Spring bread-wheat cultivars that were mostly widely cultivated during the 20th century also reported that rate of genetic yield was stable at 0.88% per year (SANCHEZ-GARCIA et al., 2013).

2.2 Physiological basis of genetic gains in grain yield potential

Most previous increases in yield and grains per m⁻² have been associated with increases to the harvest index (HI), the percentage of above-ground biomass as grain yield (Waddington *et al.*, 1986; Slafer, Andrade and Satorre, 1990; Sayre, Rajaram and Fischer, 1997; Calderini and Slafer, 1998). Modern high-yielding cultivars of spring wheat are estimated to have a HI of about 0.50 (Sayre, Rajaram and Fischer, 1997; Reynolds, Rajaram and Sayre, 1999; Fischer and Edmeades, 2010) and winter wheat has reached as high as 0.55 (Shearman *et al.*, 2005). The theoretical limit for HI in winter wheat is estimated at between 0.62 (Austin, 1982) and 0.64 (Foulkes *et al.*, 2011). Large increases in HI were achieved in green revolution cultivars through the introgression of the *RhT* alleles, *Rht-B1* and *Rht-D1* (Ehdaie & Waines, 1996; Peng et al., 1999) which cause semi-dwarfing in wheat plants and reduce height by ~20% and partitioning of dry matter to the stem. The *Rht* alleles encode DELLA proteins that repress gibberellin responsive growth. The mutant versions *Rht-B1* and *Rht-D1* are thought to be more active forms that confer GA-insensitive dwarfism (Pearce *et al.*, 2011). Post Green Revolution

increases in yield have also been associated with improvements to HI and grains per m². An investigation into yield progress of six CIMMYT spring bread wheat semi-dwarf cultivars grown in North-west Mexico by (Sayre, Rajaram and Fischer, 1997) found that yield progress was associated solely with increases to HI and grains m⁻², with no significant increase to AGDM or grain weight. In France, yield increases of 14 winter wheat cultivars between 1946 and 1992 were associated with reduced height and improved HI, along with increased grains m⁻² (Brancourt-Hulmel et al., 2003). Argentine bread wheat between 1918 and 2011 showed a 63% increase in grains m⁻², accounting for yield increases, but no significant change in a grain weight of 30 mg grain⁻¹ (Lo Valvo, Miralles and Serrago, 2017).

Increases to genetic grain yield potential have been associated with improved fruiting efficiency, the ratio between grain number and spike dry weight at anthesis, representing the reproductive efficiency of the spikes. For example, (Abbate *et al.*, 1998a) found that increases in grains m⁻² in six Argentinian wheat cultivars were associated with FE, rather than increased spike DM partitioning at anthesis. Similarly, (Terrile et al., 2017) found that grains in grains m⁻² were strongly related to FE in spring wheat, but that trade-off's with spike dry weight at anthesis and grain weight may place limits on increases to grain yield potential, which was also observed by (Slafer *et al.*, 2015). Finally, the genetic yield gains observed by (Acreche *et al.*, 2008) in Mediterranean wheat cultivars in Spain were associated with increased grains per spike and higher fruiting efficiency.

Photosynthetic traits have also been associated with yield gains in wheat. Increases to yield in eight spring wheat cultivars released between 1962 and 1988 in Mexico were positively correlated with increased flag-leaf stomatal conductance, maximum photosynthetic rate, and canopy temperature depression, with the greatest increase attributable to stomatal conductance (g_s) (R. A. Fischer et al.,

1998) Similar results were obtained by (Reynolds et al., 1994) in a study of sixteen diverse spring wheat cultivars grown in hot, irrigated conditions across 6 different countries. Furthermore, (Gaju et al., 2016) examined relationships between leaf photosynthesis and grain yield, for a variety of wheat lines, including wheat landraces, synthetic-derived wheats and modern winter wheat cultivars. They found that pre-anthesis flag-leaf photosynthetic rate was strongly associated with AGDM and grain yield for all lines, and that flag-leaf photosynthetic capacity was associated with flag-leaf chlorophyll content at anthesis.

Several recent studies, however, have found increases in yield to be associated with increased AGDM and grain weight rather than grains m⁻². (Aisawi et al., 2015) examining a set of historic CIMMYT spring wheat semi-dwarf cultivars found that yield progress between 1966 and 2009 was associated with AGDM at harvest and higher individual grain weight. However, increases were attributable partly to increases in plant height that can lead to a trade-off between AGDM and HI. A similar result was reported by (Lopes, Reynolds, Manes, et al., 2012) for 26 advanced CIMMYT spring wheat lines released between 1977 and 2008, with increases resulting from higher grain weight and cooler canopy temperature. Increases to HI in CIMMYT spring wheat have shown no significant improvement since the 1990's (Sayre, Rajaram and Fischer, 1997; Reynolds, Rajaram and Sayre, 1999), and increases in AGDM in more modern cultivars correlated negatively with HI (Fischer, 2007), due to suboptimal partitioning of dry matter.

2.3 Crop development

The developmental stages of wheat are defined by the differentiation of the plant organs, and are usually referred to as germination, leaf emergence, tillering, floral initiation, terminal spikelet, beginning of stem elongation, booting, spike heading,

anthesis and maturity (Acevedo, E., Silva, P., Silva, 2002; Waddington et al., 1986). Several systems have been designed to designate numerically the different developmental stages of wheat. The most commonly used is the BBCH (Biologische Bundesanstalt, Bundessortenamt und Chemische Industrie) scale, a decimal based system that is based on the Zadoks scale (Hess et al. 2008, Zadoks et al., 1974). The lesser used Feekes scale (Large, 1954) that preceded it is still used somewhat in the United States. The Zadoks scale defines 10 key developmental stages as "growth stages (GS). GS0 (germination), GS10, (Seedling growth), GS20 (Tillering), GS30 (Stem elongation), GS40 (booting), GS50 (Heading), GS60 (Anthesis), GS70, (Grain milk development), GS80 (Grain dough development), GS90 (Ripening and Maturity).

Between GS0 and GS10, the seedling germinates, and the seminal roots and coleoptile grow. At GS10 the first leaf has grown, and unfolds at GS11 (Acevedo, E., Silva, P., Silva, 2002). By GS20, at least three leaves are unfolded, and a fourth is usually emerging on the main shoot. The first tiller emerges at GS21, (Kirby, 2002), until the cessation of tiller production at GS30, coinciding with the terminal spikelet phase. GS30-GS40 comprises the stem elongation stage. By GS40 the first, second and third detectable nodes are present, and the blade of the flag leaf is visible. The stem-elongation phase introduces a new sink for photo assimilate (Kirby et al., 1994). GS40 to GS50 is the booting stage, during which the developing ear within the flag leaf becomes enlarged by GS43, and the flag leaf sheath opens by GS47. At GS51, ear emergence begins, and the first spikelet emerges. By the conclusion of heading at GS59, the ear is completely formed, and pollen grains and carpel are fully developed. At GS60 to GS69 is anthesis, during which the florets open and pollination occurs (Acevedo, E., Silva, P., Silva, 2015). At this stage, the final grain number of the wheat is fixed, (G. A. Slafer & Andrade,

1993) and grain filling occurs from GS70-GS90, during which milk and dough development, respectively, take place. GS89 is physiological maturity, and ripening is complete by GS93 at which point grain water concentration is below 37% (Calderini et al., 2000).

2.3.1 Major genes for flowering time

Variation in photoperiod sensitivity and vernalisation response are both sources of genetic variation in duration of the stem elongation period (Whitechurch et al., 2007). Vernalisation is the period of sustained low temperatures required by some plants, including winter wheats, to initialise flowering. It is governed by the genes: *VRN1* and *VRN2*. *VRN1* promotes flowering after the period of vernalisation and is downstream of *VRN2* (Yan et al., 2003). *VRN2* is a flowering repressor that is down-regulated by vernalisation and is key to the winter growth habit of wheat. Loss of function mutants in *VRN2* lead to the spring growth habit (Yan et al., 2004). Vernalisation has been observed to reduce the period in thermal time between sowing and terminal spikelet, without altering the duration of the stem elongation phase in some cultivars (Rodrigues et al., 2014), whereas (González et al., 2003) reported the opposite; they also noted that a longer vernalisation period increased photoperiod sensitivity for certain cultivars. In cultivars that possess photoperiod sensitivity, several studies have explored the relationship between photoperiod and duration of the stem elongation phase.

2.3.2 Key developmental phases related to grain number

Grain number per m² is a major component of grain yield. Events during certain developmental windows are key when determining final grain number. As previously stated, final grain number is fixed at anthesis. The key period is the

stem elongation phase, between the terminal spikelet and anthesis (G. Slafer & Rawson, 1994). A comparison of "modern" and older wheat cultivars by (Siddique et al., 1989) observed that differences in grain number and yield were attributable to a higher ear: stem dry matter ratio at anthesis, as competition for dry matter from the stem was reduced. In the modern lines with the improved partitioning during this stage, a greater number of florets were initiated, and survived to anthesis. Furthermore, the final number of florets has been shown to be dependent on spike dry matter for up to 25 days prior to anthesis (Slafer and Andrade, 1993), during the heading stage. (González, Miralles and Slafer, 2011) reported that onset of floret death was related to the beginning of rapid spike growth, and that lower spike DM at anthesis correlated with a higher degree of floret mortality in a study of both semi-dwarf and tall winter and spring wheat lines subjected to variation in photoperiod and growth conditions. Floret initiation begins with terminal spikelet and is concluded by anthesis. During the development of florets, the competition for assimilate between stem and spike is a major factor in determining floret survival, especially during the key period of booting through to anthesis (Bindraban et al., 1998; Stockman et al., 1983).

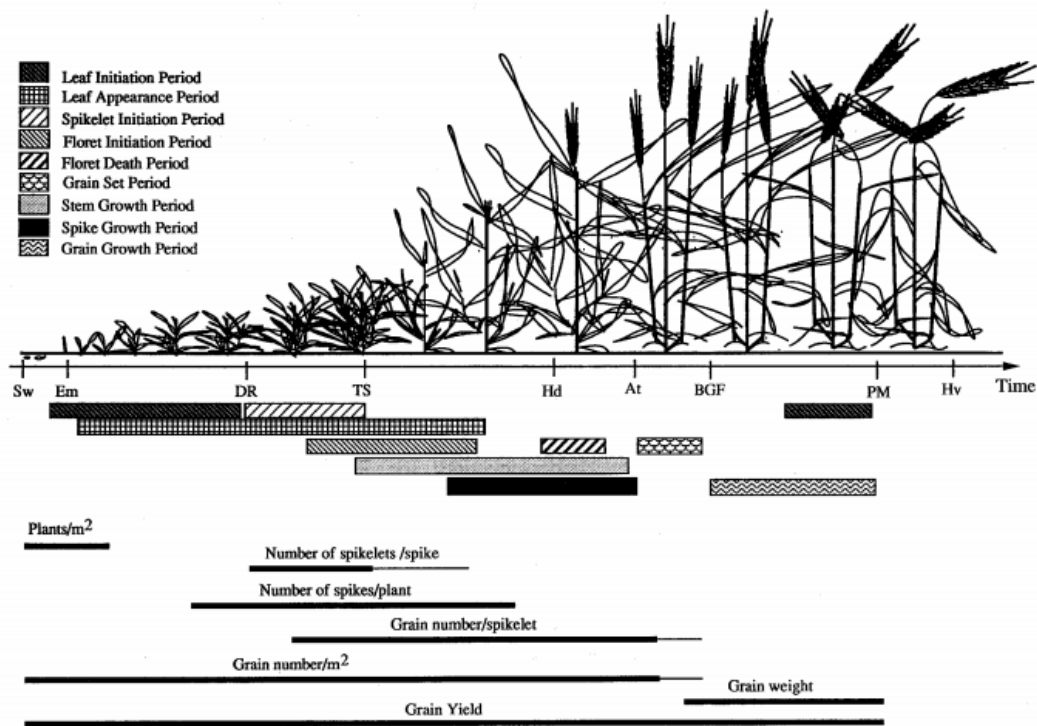


Figure 2.1. Diagram of wheat developmental stages and their relation to yield components. Taken from

The duration of the stem-elongation phase is an important factor in final grain number, with an extended phase leading to a higher quantity of spike DM per unit area (Miralles, Richards and Slafer, 2000). The duration of stem elongation can be modified by both vernalisation and photoperiod. The mechanism behind increased spikelet fertility as a result is not fully understood, but evidence appears to support that it is linked to an increased assimilate supply to the spike, leading to higher floret survival (Rodrigues et al., 2014). (Miralles, Richards and Slafer, 2000) examined the photoperiod-sensitive spring wheat cultivar UQ189 and observed that a shorter photoperiod reduces the rate of floret development, but also increases the duration of the stem-elongation phase, leading to higher spike

fertility. A follow-up study found that the increased duration of the stem-elongation phase only resulted in higher spike fertility if the duration of the stem elongation period was being modified by the current photoperiod. A reduced photoperiod earlier in the plants development, or historic photoperiod effect, may increase duration of the stem-elongation phase without increasing spike fertility (MIRALLES et al., 2003). Similar results were obtained by (Serrago, Miralles and Slafer, 2008), who noted that although spike fertility was increased as a result of the elongation of the stem-elongation phase, the number of fertile florets per spike was reduced. In their experiment, they trimmed the spike at booting in 2/3 cultivars analysed and observed that number of fertile florets per spike returned to normal. They concluded that increasing the supply of photoassimilate to the spike by modifying source-sink balance, in conjunction with an increase to stem elongation period could be useful for improving yield. Furthermore, a possible target for plant breeding would be increasing the period between initiation of stem elongation at GS31 and anthesis at GS61 as a proportion of thermal time from sowing to anthesis.

Tiller development is another key determinant of grains m^{-2} , as it determines the number of shoots, and subsequently the number of spikes. When tiller growth becomes limited by resources, tillers die beginning with youngest tiller and working back towards to the oldest. Tiller number stabilises immediately prior to anthesis when the number of spikes is fixed (Gallagher & Biscoe, 1978). Variation in tillers produced, number of reproductive tillers and tiller mortality are all factors in final grain number. (Sharma, 1995) reported significant variation in tiller mortality in 20 lines of spring wheat of between 7% and 30%; as well as finding positive correlation between number of reproductive tillers and grain number. He also reported a significant negative correlation between higher tiller mortality and

grain yield. Another study looking at UK winter wheat observed similar results and found variation of 32% to 63% for tiller mortality. They concluded that tillers that do not survive will reduce yield potential through competition for assimilate with developing ears in fertile shoots, and that negative effects on yield will be most evident in drought conditions (Berry et al., 2003). Furthermore, the end of tiller production coincides with the initiation of the terminal spikelet phase, linked to changes in the received ratio of R:FR light (CASAL, 1988; EVERS et al., 2006)

2.4 Grain number model

The grain number model was first proposed by (R. A. Fischer, 1983) as a method of explaining final grains m^{-2} . AGDM at anthesis alone does not fully explain variation in grain number, even in near optimal environments (R. A. Fischer, 2008; G. A. Slafer et al., 1990). Furthermore, final grain number is highly dependent on the final period of rapid spike growth during the last 20 or 30 days to anthesis, during which 95% of spike growth occurs, along with natural variations in radiation and temperature (R. A. Fischer, 1985; Sinclair & Jamieson, 2008). However, (Sinclair & Jamieson, 2008) disputed the importance of dry matter accumulation in yield determination, suggesting instead that acquisition of nitrogen was equally or more important. (Fischer, 2008) argued that under potential conditions grain number is not related to spike N, and that even under limiting conditions, spike dry weight is more directly related to grain number, and that variation in fruiting efficiency is not associated with spike N concentration. The importance of spike dry weight accumulation at anthesis is now widely accepted and supports the model below (Fischer, 2007; Slafer, 2007; Matthew Reynolds *et al.*, 2009).

Eqn. 2.1

$$\mathbf{Grains\ m^{-2} = SDWa\ (g\ m^{-2})\ x\ FE}$$

Where SDWa represents spike dry matter at anthesis, and FE represents fruiting efficiency, the number of grains per gram of spike DM at anthesis. The model is expanded by (Fischer, 2008) to show how SDWa is determined.

Eqn. 2.2

$$\mathbf{SDWa = Ds \times CGR \times SPI}$$

Where Ds represents days from emergence to anthesis, CGR is the crop growth rate in terms of accumulation of dry matter, and SPI the spike partitioning index, the proportion of AGDM dry matter partitioned to the spike averaged over the spike growth period, as discussed in the previous section.

Several studies have produced evidence supporting the idea that genetic variation in grains m^{-2} appears to be closely related to spike DM at anthesis. (Slafer, Andrade and Satorre, 1990) examined physiological traits pre-anthesis of six Argentinian spring bread-wheat cultivars and found that SPI was closely associated with grains m^{-2} and HI. Field trials conducted by (Abbate et al., 1997) examined two spring bread-wheat cultivars and found that variation in grains m^{-2} was linked to variation in spike dry weight measured 7 days post anthesis. Differences in radiation caused more variation in spike dry weight than grains g^{-1} spike. An analysis of grain number in Norin-10 derived dwarf wheats by (R. Fischer & Stockman, 1986) concluded that increased grain number was due to increased DM partitioning to the spike, which was in turn a result of reduced competition from growing stems. Finally, an analysis of the physiological basis of yield gain in Mediterranean bread wheats grown in Spain concluded that increases in grains m^{-2} were associated with SDWa, along with grains per unit SDWa, or fruiting efficiency (Acreche *et al.*, 2008). Variation in fruiting efficiency is a key

component, and recent studies have suggested that GN is determined more from FE than from SDWA (G. A. Slafer et al., 2015).

2.4.1 Crop growth rate

Crop growth rate (CGR) is the amount of above-ground dry matter produced per unit area per day and when the canopy PAR interception is close to 100% genotype differences in CGR will relate to the efficiency with which intercepted PAR is converted to dry matter. It is influenced heavily by environmental factors such as levels of photosynthetically active radiation and water availability and is strongly correlated with the spike growth rate (Lazaro & Abbate, 2011). CGR for wheat should have a maximum limit of around 71 g m⁻² per day given sufficient available PAR and relatively low respiration loss (Loomis and Williams, 1963) but growth rates in the field are much lower at around 26 g m⁻² per day (Abbate *et al.*, 1998a). (Slafer, Andrade and Satorre, 1990), who examined different Mediterranean spring-wheat cultivars released between 1912 and 1980, found no differences in PAR intercepted at anthesis, or the efficiency of its conversion to dry matter. However, genetic variation in RUE would be expected to produce variation in CGR provided LAI was high enough to ensure sufficient light interception.

2.4.2 Spike partitioning index

The spike-partitioning index represents the spike DM as a proportion of AGDM at anthesis. Variation in SPI between cultivars appears to be mostly independent of radiation intercepted, instead having a basis of variation between cultivars, with SPI being highest in shorter cultivars (Fischer, 1983). As SDWa is such an important indicator of final grain number, which in turn is the major determinant of grain yield, higher SPI values are desirable for the improvement of wheat grain

yields. There is numerous evidence that differences in SPI between cultivars have a genetic basis, through variation of phenology or partitioning, allowing for its selection in trait-based breeding programs. Genetic variance in spike dry matter as a proportion of overall AGDM has been observed to vary from 0.12 to 0.21 in UK wheat winter-wheat (Shearman *et al.*, 2005), whilst (Pask, 2009) reported variation of 0.15-0.20. For spring wheat, SPI has been shown to range between 0.24 and 0.28 for 12 CIMMYT cultivars released between 1966 and 2009, with a mean of 0.256 (Aisawi *et al.*, 2015). A similar study of Mexican cultivars, both semi-dwarf and non-dwarf, by (Fischer, 1983) found SPI ranged from 0.11 to 0.19. (Abbate *et al.*, 1998a) reported SPI ranged from 0.19 to 0.21 in six semi-dwarf Argentinian cultivars. (Slafer, Andrade and Satorre, 1990) found that higher SPI at anthesis, along with SDWa, was closely associated with the improved HI and grains m⁻² observed in the higher yielding modern cultivars compared to older ones. A study of 26 CIMMYT spring-wheat cultivars found a strong association between SPI and HI, along with an association between reduced true-stem structural DM partitioning and increased SPI, suggesting that reducing partitioning of structural DM to the stem as a competing sink for the spike could increase yields (Rivera-Amada *et al.*, 2016). Competition for structural DM with the stem is particularly prevalent for internodes 2 and 3 (Rivera-Amado, 2015). As well as structural DM, stem dry matter consists of water-soluble components (stem WSC's). These are chiefly fructan sugars, but also include glucose, fructose, and sucrose (Dreccer *et al.*, 2014). They begin accumulating in the stem approximately 20 days prior to anthesis (Gebbing & Schnyder, 1999), and can act as storage pools for later relocation to grain when photosynthetic rate is suboptimal (Slewinski, 2012). Stem WSC appears to compete with structural DM during periods of drought, and positive association between WSC and grain yield

under drought conditions has been reported (Foulkes, Sylvester-Bradley, et al., 2007). It is possible that by optimising for increased spike partitioning pre-anthesis, sink strength for stem WSC reserves may be reduced, impacting the ability of the plant to translocate assimilate to the grain during water limited periods.

A study by (Gaju et al., 2009) reported that increased SPI at anthesis was present in large-spike phenotype lines compared to other lines resulting in greater spike dry matter per unit area. Grain number was reduced however due to a lower fruiting efficiency, but they concluded that large-spike phenotype lines might be useful in breeding programs aimed at increasing grain size. (Gaju et al., 2014) also compared large-spike phenotype spring-wheat lines possessing the tillering inhibition gene *Tin1* with UK winter wheat lines of normal spike phenotype that lacked the gene. They found the presence of the gene increased SPI due to reduced competition from extraneous tillers, and this increased grain number, albeit not significantly. Finally, (Abbate *et al.*, 1998a) reported that SDWa was closely associated with SPI, and that variation between cultivars in DM partitioning to the spike was between 28%-34%. The genetic variation in grain number between cultivars however was explained by increased fruiting efficiency. Regarding breeding to reduce competition from other sinks to the benefit of the spike, a careful balance must be found to avoid hindering the development of the plant. As previously discussed the stem, between stem-internodes 2 and 3 especially, is a significant competitor for spike DM. Too much of a decrease of stem partitioning however may increase the risk of lodging, negating any benefits gained from the increased partitioning to the spike (Piñera-Chavez et al., 2016). Furthermore, decreasing DM partitioning to leaf sheath or leaf lamina may reduce post-anthesis source capacity, impeding grain filling. However, at present

defoliation experiments performed on modern cultivars at anthesis do not appear to affect grain weight, grain number or grain protein content in Mediterranean environments (Ahmadi et al., 2009; Cartelle et al., 2006).

2.4.3 Fruiting efficiency

Fruiting efficiency (FE; number of grains set per unit of spike dry weight at anthesis), represents the efficiency of resources allocated to the spike that are used for grain setting, and is key determinant of yield (Fischer, 1983). Evidence for genetic variation in FE for wheat is abundant in the literature; along with its importance in determining final grain number (Abbate et al., 1998; Ferrante et al., 2017; Guo et al., 2016; G. A. Slafer & Andrade, 1993; Terrile et al., 2017). For example, spring bread wheat grown in Spain to compare yield traits between modern and older cultivars, showed significant differences in yields with a linear association between yield and grains per m², associated with fruiting efficiency (Acreche et al., 2008). (Slafer et al., 2015) found a variation of between 110-170 grains per g spike without a reduction in grain size. Differences in yield between cultivars were largely a result of higher grain numbers associated with fruiting efficiency. One other recent study by (Terrile, Miralles and González, 2017b) examined the Genotype x Environment interactions on fruiting efficiency for 3 cultivars with contrasting FE genotypes, varying nitrogen availability, shading the canopy during stem elongation and altering sowing date. G x E interactions were observed, but high FE genotype cultivars still showed higher grain number across the range of environments. They also reported a negative correlation between higher FE and SDWa. Similar results of a trade-off between FE and SDWa have been reported elsewhere (Abbate et al., 1998b; Lazaro and Abbate, 2011). (González et al.,

2014) examined yield potential in 39 modern spring wheat cultivars with variation in FE under different potential conditions in order to study source limitation during grain filling. Increased source had a minor effect on grain weight, and no negative relationship between grain weight and fruiting efficiency was observed (Slafer *et al.*, 2015).

The use of fruiting efficiency as a target trait to improve grain number is well supported by the literature. A study by (García *et al.*, 2014) observed positive transgressive segregation (DH lines exceeding values of parent phenotypes) in a doubled-haploid population grown in two different environments for grain number traits. These included CGR, partitioning of biomass to spike, duration of stem elongation phase, and fruiting efficiency. Fruiting efficiency however was the most relevant physiological trait for improving grain number and therefore grain yield.

2.5 Genetic variation in wheat

Hexaploid bread wheat (AABBDD) domestication occurred through the natural outcrossing of *Triticum urartu* (AA) and *Aegliops speltoides* (BB) to produce emmer wheat (AABB) 0.5 million years ago, and then 8,000 years ago a second hybridisation event occurred between emmer wheat and *Ae. tauschii* (DD), which led to modern bread wheat *Triticum aestivum* (Haas *et al.*, 2019). Methods for genetic analysis and mapping of the natural variation in crops were developed a few decades ago (Alonso-Blanco *et al.*, 2009), and this was initially mainly carried out through quantitative trait loci (QTL) linkage mapping and then more recently through genome-wide association studies (GWAS). Identification of these molecular markers for grain number traits is important so they can be incorporated into elite wheat varieties through marker-assisted selection (MAS).

While QTL mapping is useful for identifying genetic loci for traits, the precision with which the QTL are identified depends on the genetic variation covered by a mapping population as well as the size of a mapping population (Sehgal et al., 2016). Therefore, it is now considered the 'classical approach'. In comparison, Genome Wide Association Study (GWAS) can survey a larger gene pool and bypass the need for crossing cycles to generate populations (Neumann et al., 2011)

2.6 Genome Wide Association Studies in wheat

With recent advances in DNA sequencing such as genotyping-by-sequencing thousands of single nucleotide polymorphisms (SNPs) have been generated that cover most of the wheat genome, e.g., (Walkowiak et al., 2020). The genome-wide association study was a statistical tool developed to identify SNPs that relate to important phenotypic traits.

In order to perform a GWAS, a large group of genotypes must be selected that have a wide range of genetic diversity, the larger the population size, the more power the GWAS will have (Kumar et al., 2012). Then, the phenotypic characteristics on the panel must be measured before genotyping the panel with molecular markers. Using the molecular marker data, the extent of linkage disequilibrium (LD) of a population (an indicator to detect the distance between loci) must be quantified and the population structure and kinship assessed and used to test the association between the phenotypic and genotypic data (Sehgal et al, 2016). It is important to remove SNPs that have a low minor allele frequency (MAF) as they may lead to a lack of resolution and power (Soto-Cerda & Cloutier, n.d.). However, rare alleles have been shown to have a relatively large effect on complex traits (Youssef et al, 2017). GWAS based on SNPs also relies on the genetic reference that was used for sequencing and mapping the individuals, this

can lead to missing information and GWAS cannot detect rare mutations of complex traits (Alqudah et al., 2020).

There are different statistical models that can be used to conduct a GWAS. The general linear model (GLM) does not take population structure into account, and has widely been replaced by the mixed linear model (MLM), which does consider population structure in its model (Alqudah et al, 2020). Several methods have been developed to increase the efficiency of the MLM, and these are documented in (Cortes., 2021). To date, several GWAS studies have been performed in wheat on grain yield-related traits, which are listed in Table 2.1.

Table 2.1. Summary of genome-wide association studies with the range of traits and their associated genomic regions

Trait	Traits	Chromosomes	Germplasm	Environment	Genotyping	Papers
Yield traits	Yield	2A, 2B, 3D, 4A, 5A, 5B, 6A, 6B, 7B	179 spring bread wheat cultivars	Field trial	20K Illumina iSelect SNP array	Amalova et al. (2021)
	Grain number per spike	1A, 1B, 1D, 2A, 2B, 2D, 3B, 4A, 4B, 5A, 5B, 6A, 6B, 7A, 7D				
	Thousand grain weight	1B, 1D, 2A, 2B, 4B, 5A, 5D, 6A, 6B, 7A, 7B, 7D				
	Plant height	1B, 2B, 3A, 3D, 5A, 5B, 6A, 7A				
	Peduncle length	1A, 1B, 1D, 2B, 3B, 4B, 5A, 6A, 6B, 7A				
	Yield	2A, 4B, 5A, 7A		Field trials	15K Infinium	

Yield traits	Harvest index	2B, 2D	96 cultivars with high diversity in yield traits		SNP array	Alqudah et al. (2020a)
	Thousand grain weight	1B, 4B, 6A				
	Grain weight per spike	2B, 5B, 6A				
	Grain number per spike	1A, 2B, 2D, 3B				
	Peduncle length	2B, 3B, 4D, 5D, 6A, 7A				

Target trait	Traits	Chromosomes	Germplasm	Environment	Genotyping	Papers
Grain yield	Grain yield	1B, 2B, 4A, 5B, 6B, 7B	6,461 spring bread wheat cultivars	Field trial	192-plexing on Illumina HiSeq2000	Sehgal et al. (2020)
Yield traits	Spike weight at anthesis Grain number per spike	2B, 7A, 1A, 2B, 2D	96 cultivars including	Field trial	15K Infinium SNP array	

	Thousand grain weight Grain weight per spike FE anthesis DW	1B, 2A, 2A, 2B, 7A, 2A, 2D, 4D, 5A	founder genotypes globally			Gerard et al. (2019)
Yield traits	Thousand grain weight Plant height	1A, 2A, 2B, 2D, 4A, 4B, 5B, 6A, 7A, 7B, 7D 1A, 1B, 1D, 2A, 2B, 2D, 3B, 4A, 4B, 4D, 5A, 5B, 5D, 6A, 6B, 6D, 7A, 7B, 7D	192 bread wheat cultivars including 25 SHW, 80 landraces	Field trial	90 K Illumina iSelect SNP Array	Liu et al. (2018)
Target trait	Traits	Chromosomes	Germplasm	Environment	Genotyping	Papers
Yield traits	Grain yield	1A, 2A, 2B, 3B, 4A, 4B, 5A, 7A		Field trial		

	Grain number per spike	1A, 2B, 2D, 3A, 3B, 4B, 5A, 5B, 6A, 7A, 7B	239 cultivars of soft red winter wheat		Illumina 9K iSelect assay	Lozada et al. (2017)
	Grain weight per spike	3A, 4A, 4B, 4D, 5A, 6B,7D				
	Peduncle length	1A,2A,2D, 3A, 3B, 7A				
Floret fertility	Apical grain number per MS	1A, 1D, 3A, 3D, 7A, 7D	210 German hexaploid winter wheat cultivars	Glasshouse	90K Illumina iSelect SNP Array	Guo et al. (2017)
	Central grain number per MS	6A, 6D				
	Basal grain number per MS	6A, 6D				
	Grain number	2D, 3B				
	Grain weight	1B, 7A				

	Fruiting efficiency (FE chaff)	2B, 5B, 6B				
--	-----------------------------------	------------	--	--	--	--

2.7 Project objectives and hypotheses

The overall aim of the project is to determine how dry matter partitioning traits are influencing grain number and grain yield, using a modern winter wheat KWS association panel, and to understand the genetic regulation of the grain number traits

The specific objectives of the thesis were:

1. To quantify genetic variation in physiological traits that determine grain number and yield in a panel of 138 winter wheat bread wheat cultivars and advanced lines in field experiments in Cambridgeshire, UK, and perform detailed analysis on a subset of 8 genotypes in glasshouse experiments at The University of Nottingham, UK
2. Develop breeder-friendly molecular markers for grain partitioning and grain number traits through a genome-wide association study

The specific hypotheses of the thesis were:

1. Genetic variation in grain yield in the KWS panel is correlated with both harvest index and above-ground dry matter at maturity.
2. Grain number is positively associated with spike partitioning index and fruiting efficiency among genotypes in the KWS panel.
3. A trade-off is observed between spike partitioning index and fruiting efficiency among the KWS panel genotypes.

4. Competition observed between spike growth and stem internodes 2 and 3 is stronger than between spike growth and the peduncle or other internodes.
5. Genetic variation in fruiting efficiency is associated with grains m^{-2} among genotypes in the KWS panel.
6. In the glasshouse, a positive association is observed in flag leaf photosynthesis rate pre-anthesis and spike biomass and grain number per spike in the KWS panel subset
7. Field and glasshouse expression of grain number traits are positively correlated among the KWS panel genotypes
8. Marker-trait associations can be identified for the key grain partitioning traits, fruiting efficiency and grain number per m^2
9. Co-locating markers will be identified for fruiting efficiency and grains m^{-2}
10. Candidate genes for the key SNPs associating with grain partitioning and grain number traits will be identified and confirmed with reference to previous literature

Chapter 3. General Materials and Methods

Two field experiments were conducted at KWS UK Ltd sites in Cambridgeshire near Thriplow, during the seasons 2017-18 and 2018-19. Two glasshouse experiments were conducted at Sutton Bonington Campus, Nottingham, United Kingdom in 2018 and 2020.

3.1 Field experiments

3.1.1 Experimental design and treatments and crop management

An association panel of 138 UK winter wheat elite doubled-haploid lines from the KWS breeding program was studied in two field experiments at KWS UK Ltd Thriplow. The panel contains established released cultivars and doubled-haploid advanced lines from the KWS breeding program. The 2017/18 experiment was sown on 1 October 2017. In 2018/19 the experiment was sown on 9 November 2018. The experimental design was a randomised block design of three replicates in both years. The plot size was 2 m x 5 m. The plots were managed with standard farm practice for application of N, P and K fertilizers, herbicides, fungicides, and pesticides and PGRs to ensure ample supply of nutrients and minimize the effects of weeds, diseases, and pests. The crops were first wheats in each season following oil seed rape. The soil type was a sandy clay loam.



Fig 3.1 – Image of plots for the 2017/18 field trial, 28th June 2018.



Fig 3.2 Image of plots for the 2018/19 Field trial in January 2019.

3.1.2. Crop measurements

The crop measurements in each field experiment are described in Chapter 4.

3.2 Glasshouse experiment experimental treatments and design

Two glasshouse experiments were conducted, one in each of two years (2018 and 2020) at Sutton Bonington Campus, University of Nottingham, UK campus. The seeds were sown in a controlled-environment room at 20°C in John Innes 2 soil medium. Eight genotypes from the KWS panel were used in the glasshouse

experiment in 2018 and eight genotypes in 2020 (ST13_24200, Santiago, St13_24090, TC16_128, TC16_417, TC16_97, W309, Zyatt). The plants were grown in 2 L pots (1 plant per pot). A randomised complete block design was used and there were three replicates

3.2.1. Plant measurements

Full details are given in Chapter 6. In brief, in the experiment in 2018, gas-exchange photosynthesis was measured for each plant on the flag leaf of the main shoot using a LI-COR 6400 XT Portable Photosynthesis System (Li-Cor Biosciences, NE, USA). Light-saturated photosynthetic rate (A_{max}) and stomatal conductance (g_s) were measured on the flag-leaf.

In the experiment in 2020, at physiological maturity, plants were sampled by cutting at ground level to estimate grain yield per plant, above-ground biomass per plant, harvest index and yield components including grain number per plant and grain weight. The number of fertile and infertile shoots per plant was counted. The plant was separated into stem and leaf sheath, spike, and leaf-lamina for the: i) main shoot and ii) other fertile shoots and dry-weights recorded separately for each component after drying for 48 h at 80°C. The total dry weight for the infertile shoots was recorded after drying for 48 h at 80°C.

3.3 Statistical analysis

ANOVA and generation of best linear unbiased estimates was performed using META-R (Alvarado *et al.*, 2020) with genotype as a fixed effect and replicate and environment as random effects. Linear regressions were carried out with python 3.10.4 using the of least squares method with Python packages 'Statsmodels' (Seabold, S. & Perktold, J., 2010), 'Numpy', (Harris *et al.*, 2020), 'itertools' (Van

Rossum, G., 2020) and 'scikit-learn' (Pedregosa *et al.*, 2011). Scatter graphs were created using the python package 'plotly' (Plotly technologies Inc. 2015). The genotype 'ST12_18471' from the 2017/18 field trial was excluded from all analysis.

For Glasshouse data all summary statistics, linear regressions and ANOVA was carried out using Statsmodels, Numpy and Pandas using Python 3.10.4. Correlation matrices were generated using the Seaborn package in Python 3.10.4

Chapter 4. Dry matter partitioning and associations with grain number and yield in an elite doubled-haploid winter wheat panel.

4.1. Introduction

Cereal crops are a cornerstone of human diets, with wheat being the most widely cultivated of the three main food crops on a global scale (Shewry, 2009). Ensuring production of wheat meets demand in the future is of paramount importance for food security. As the foundation of 70% of human calories, annual production of all three major cereal crops, maize, wheat, and rice, must increase by 0.9 billion tonnes to meet the food requirements of a population of 9 billion by 2050 (Melrose, Perroy and Careas, 2015). Annual yield increases have reduced from 3.2% per year in 1960 to 1.5% in 2000 (FAO, 2009), with wheat, which contributes ca. 20% of human calories, showing the lowest rate of increase at ca. 0.5-1.0% per year. Although at present global wheat yield production is meeting demand, with an estimated 732.8 million tonnes utilised in 2016/2017, (FAO, 2017) it must increase by 60% to continue to match it in 2050, when demand is estimated to reach 900 million tonnes. This will require an annual yield increase of 1.6%, up from the current annual increase of approximately 0.5-1.0% (Lucas, 2012).

Current rates of genetic gains in yield in optimal environments at about 0.5-1.0% p.a. are not, however, enough to satisfy projected future demand (Gonzalez-Navarro et al., 2016) The majority of linear yield potential progress in wheat for the last 60 years has been a result of selecting for yield empirically and has been largely due to increases in harvest index (Gonzalez-Navarro *et al.*, 2016). There is evidence that, although grain yield may be co-limited by source and sink in high yielding environments, the greater limiting factor on yield is still grain sink

strength (Gonzalez-Navarro *et al.*, 2016), and that increasing grain sink strength through increased grains m^{-2} in high biomass varieties would be an avenue towards improved yield (Gonzalez-Navarro *et al.*, 2016), as genetic variation in grain yield is more strongly associated with grain number than grain weight. In order to increase the grain sink strength (assuming no increase in anthesis above-ground dry matter), one avenue is to reallocate dry matter from other plant organs to the spike pre-anthesis. There is evidence in spring wheat that structural dry matter partitioning to the stem is a stronger competitor with the spike for dry matter than other alternative plant organs, particularly stem internodes 2 and 3 (Rivera-Amado *et al.*, 2019), making the identification of markers for lower true-stem partitioning a viable avenue for selection for increased grain sink strength. The complementary trait to spike partitioning and spike growth to enhance grain number and HI is the fruiting efficiency (FE, number of grains per unit spike dry-matter at anthesis or chaff dry-matter at harvest). Wide genetic variation has been reported among modern wheat cultivars (Gonzalez-Navarro *et al.*, 2016), as well as a strong association between improved fruiting efficiency and grain number (García *et al.*, 2014).

Chapter hypotheses

- Overall genetic variation in grain yield in the KWS panel will be associated with HI and grains per m^2
- Overall genetic variation in HI and grains per m^2 will be associated with FE and SPI.
- Stem-internode 2 and 3 will be stronger competitors for spike dry matter during stem elongation than other plant components; and stem internode 2 and 3 partitioning index are more closely correlated with SPI than peduncle PI

- Grain yield will be more closely associated with grain partitioning traits than with photosynthetic source traits.

4.2. Materials and Methods

4.2.1 Plant materials and experimental design

An association panel of 138 UK winter wheat elite cultivars and doubled-haploid lines from the KWS breeding program (Appendix table 4.1) selected by stratified sampling, was studied in two field experiments at KWS UK Ltd Thriplow to explore genetic diversity in grain partitioning traits and associations with grain number and grain yield. The panel contains a number of genotypes that are established released cultivars alongside a number of doubled-haploid advanced lines from the KWS breeding program. Further measurements were performed on a subset of 27 lines (Subset 1) to explore more detailed partitioning traits. The subset was selected based on high and low lines contrasting for fruiting efficiency, grains m⁻² and overall grain yield. The panel was phenotyped for key traits relating to yield potential, harvest index and dry matter partitioning. In 2017/18 the experiment was located near Fowlmere, Cambridgeshire (52°05'18.0"N 0°03'49.6"E) and in 2018/19 at a field site 3 miles away near Newton, Cambridgeshire (52°07'40.9"N 0°06'18.2"E). Genotypes were grown in plots of 2 m x 5 m, in a randomised block design of three replicates in both years. The seed rate was 300 seed per m². The 2017/18 trial was sown on 1 October 2017. In 2018/19 the experiment was sown on 9 November 2018. Seven genotypes were removed from the panel after the first field trial in 2017/18 for reasons of relatedness or admixture. Seven additional lines were added to the trial (Table 4.1).

Table 4.1. Line substitutions for the 2018/19 field trial.

REMOVED		
LINE	REASON	REPLACEMENT LINE
St15_36404	- Relatedness	Spotlight
St15_36062	- Relatedness	Graham
St15_35747	- Relatedness	Gleam
St15_35191	- Relatedness	Skyscapper
St15_35098	- Relatedness	Kerrin
St15_34898	- Relatedness	Silverstone
St12_18471	- Admixture	W346

Table 4.2. Rainfall data from the Cambridge NIAB weather station (543500E 260600N , Lat 52.245 Lon 0.102) for months of March – July in 2018 and 2019. Values shown are in mm. 'Average' is the average rainfall data at this station between 1981-2010.

	2018 (mm)	2019 (mm)	Average (mm)
March	64.2	37.4	38.3
April	64.6	10.8	41.2
May	43.8	41.4	46
June	0.8	79.2	51.5
July	12.4	43.4	47.5

The field trials were not irrigated and suffered from some drought stress in 2018, just prior to and after anthesis. Rainfall in June (0.8mm) and July of 2018 (12.4mm) was significantly lower than the averages of 51.5 mm and 47.5 mm,

respectively (Table 4.2). The median date for GS61 in both years field trials was 2 June 2018. In 2019 there was no significant drought stress during stem extension, anthesis or grain filling.

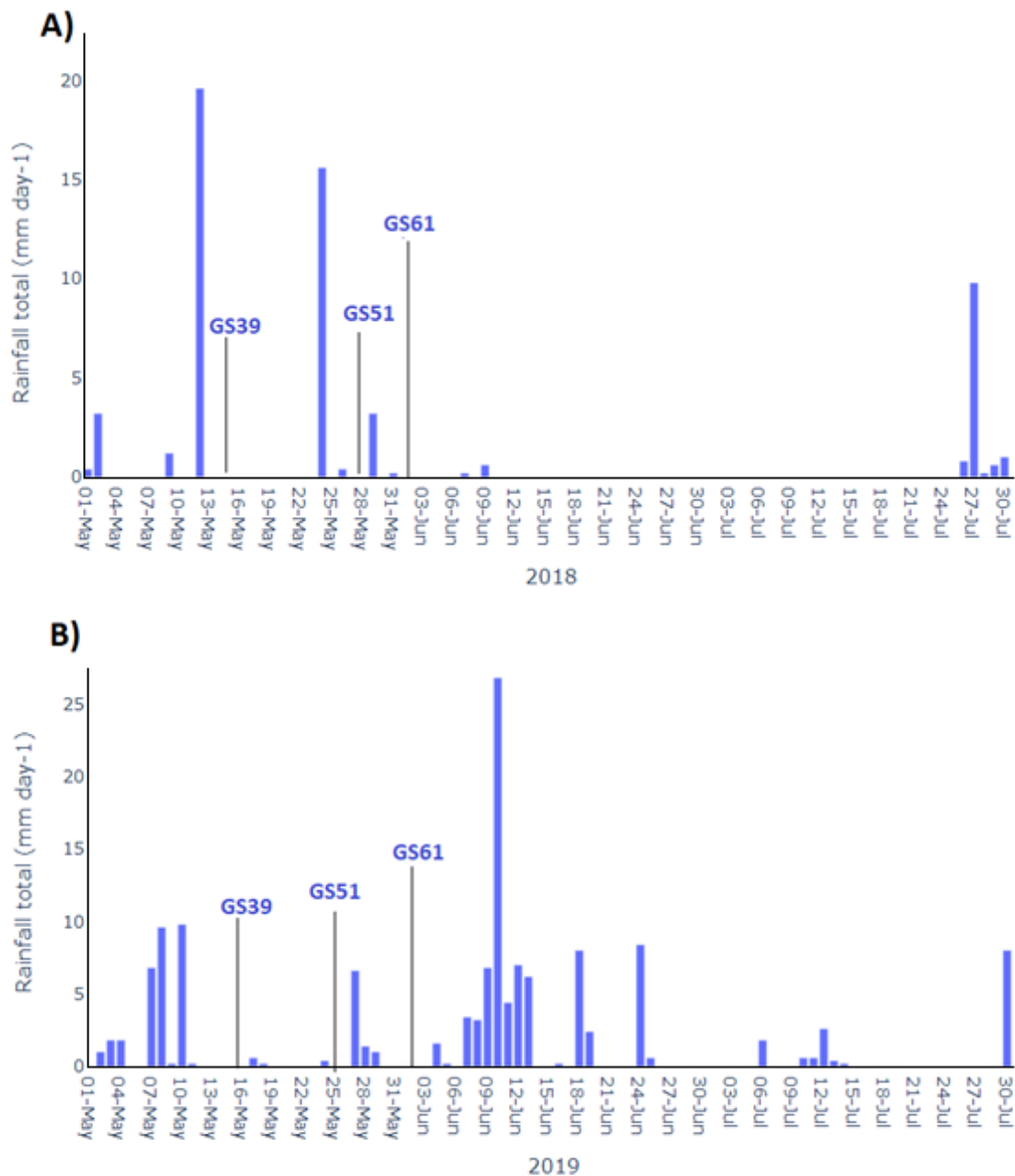


Fig 4.1 – Daily rainfall between 1st May and 30th July in 2018 (A) and 2019 (B), with dates of average developmental growth stages for flag-leaf emergence (GS39), onset of ear emergence (GS51) and anthesis (GS61) in the KWS

association panel in the 2017-182018 and 2018-192019 field trials. Meteorological data from Cambridge NIAB Met office Location: 52.245, 0.103

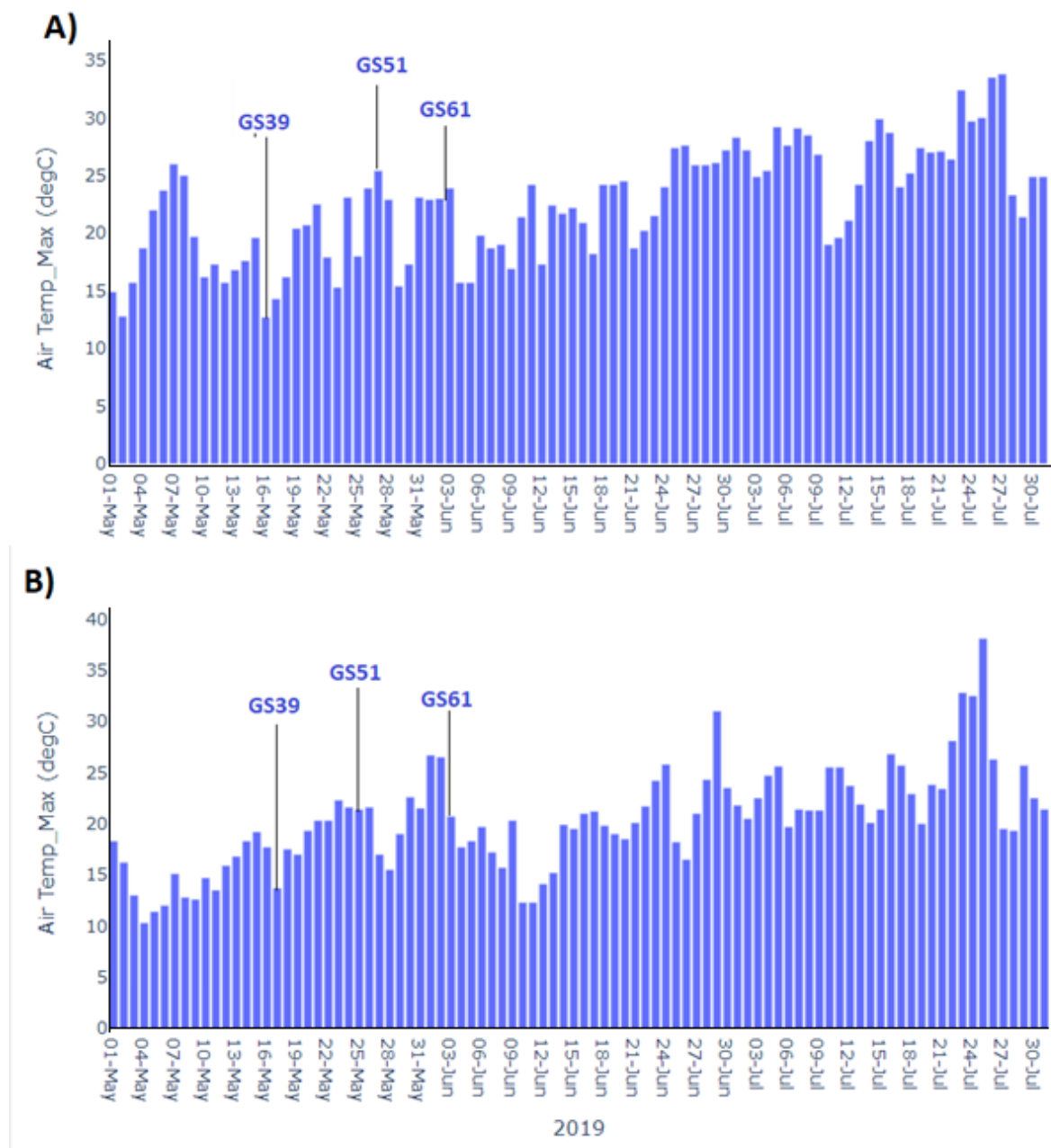


Fig 4.2 Max air temperature between 1st May and 30th July in 2018 (A) and 2019 (B), with dates of average developmental growth stages for flag-leaf emergence (GS39), onset of ear emergence (GS51) and anthesis (GS61) in the KWS association panel in the 2017- 2018 and 2018-2019 field trials. Meteorological data from Cambridge NIAB Met office Location: 52.245, 0.103

In the 2018 trial, median growth stage of 39 was recorded on the 15th of May, compared to 16th of May in 2019. Median growth stage of GS 51 was reached on 28th May in 2018, compared to 25th May in 2019. Median growth stage of 61, anthesis, was reached on the 2nd of June in both years (Fig 4.1). One key difference between years is rain fall during the grain filling period post anthesis. In 2018, there was less than 1mm of rain during the 30 days post anthesis, whereas in 2019 several days experienced daily rainfall exceeding 5 mm, with a total of 86 mm observed in the following 30 days post anthesis.

4.2.2 Crop measurements

Sampling

Samples were collected at anthesis (GS65) and at physiological maturity (peduncle fully senesced, GS87-90) (Zadoks, Chang and Konzak, 1974). Growth stage was defined as 50% of shoots in the plot being at the relevant growth stage. For samples taken at anthesis, 12 main shoots were selected, representative of the plot as a whole. Main shoots were identified during early stem extension and marked with wire tags. For samples taken at maturity a grab sample method was used where two 30 cm row-lengths were taken and plant pulled up from at least 50 cm from the edge of the plot, and approximately 30 cm from the end of the plot.

Biomass and dry matter partitioning at GS65

At GS65 for three replicates, sampling was carried out on the 138 genotypes. Twelve representative fertile shoots (those with an ear) were selected from the plot, at least 50 cm from the edges of the plots. Fresh weight of the samples was recorded. For dry-matter partitioning analysis, each shoot from the sample was divided into ear, leaf lamina, leaf sheath and true stem, then dried for 48 hours at 80°C and the dry weight of each component was recorded. Furthermore, stem-internode lengths were recorded for the peduncle, stem-internode 2 and stem-internode 3 with a ruler. For 25 genotypes (subset 1), each internode of the true-stem was separated (peduncle, internode 2, internode 3, and internode 4+) and the dry weights recorded after 48 hours of drying at 80°C. Internodes were defined from the top down, with internode 2 being below the peduncle. The partitioning index (PI) for each plant component was calculated as the plant component DM / aboveground DM.

Grain yield and yield components at physiological maturity

For both field experiments, at physiological maturity grab samples were taken for three replicates of the 138 genotypes as described above. The roots were removed with secateurs at the root-shoot interface and separated into the spikes and stems (leaf lamina, true stem, and leaf sheath). Ear number and weight was recorded then samples were dried for 48 hours at 80°C. Dry weights of both components were then recorded. The ears were then threshed to collect the grains. Grain samples were counted in a digital seed counter and dry weights recorded after 48 hours drying at 80°C. Chaff weight was calculated by the difference between grain weight and ear weight. Grain yield per plot was recorded by machine harvesting the plot and values were further adjusted to moisture percentage measured in each plot. From the data obtained ears m⁻², grains m⁻², harvest index, above-

ground biomass m^{-2} and fruiting efficiency were calculated. A further direct estimate of ears m^{-2} was measured by stubble count post-harvest.

NDVI and leaf chlorophyll fluorescence measurements

NDVI (normalised difference vegetation index) was recorded between GS21 and GS89. Measurements were taken on all 138 genotypes in the experiment for both 2017/18 and 2018/19 using a Trimble green seeker handheld crop sensor. Measurements were taken by a continuous scan up the centre of the plot, then down again and an average calculated. Flag-leaf fluorescence parameters (PSII QY, PhiNPQ, PhiNO and SPAD) were also taken for the 2018/19 experiment using a PhotosynQ MultispeQ v.2 handheld device. The MultispeQ measures SPAD relative chlorophyll content by a series of transmission measurements over a range of light intensities, and over a larger area (1cm^2) compared to the commonly used Minolta 502 SPAD meter (Kuhlgert *et al.*, 2016). Measurements with the MultispeQ are averages of a single measurement in the centre of the main shoot flag leaf, on 3 individual plants per plot spaced evenly apart and 20 cm from the edge of the plots.

The recorded NDVI data for each plot was fitted against days from GS 61, fitting an S-shaped logistic curve using Genstat 21st edition. From this, four parameters B, M, C, and A were estimated and then the onset of senescence and end of senescence.

The logistic regression equation was fitted using GenStat 21st edition as:

$$Y = A + C / (1 + \exp(-B \times (X - M)))$$

Where Y is the NDVI; X is days from GS61; A is the upper asymptote; M is the time for the point of inflection; B is the slope at the point of inflection; and A+C is

the lower asymptote. The onset of NDVI senescence was taken as the time post-GS61 at NDVI 80% of value at GS55 and end of NDVI senescence as time at NDVI 20% of value at GS61. Senescence rate was estimated as B. Values were calculated for each sub-plot and the fitted values subjected to ANOVA.

4.2.3 Statistical analysis

ANOVA and generation of best linear unbiased estimates was performed using META-R (Alvarado *et al.*, 2020) with genotype as a fixed effect and replicate and environment as random effects. Linear regressions were carried out with python using the of least squares method with Python packages 'Statsmodels' (Seabold, S. & Perktold, J., 2010), 'Numpy', (Harris *et al.*, 2020), 'itertools' (Van Rossum, G., 2020) and 'scikit-learn'(Pedregosa *et al.*, 2011). Scatter graphs were created using the python package 'plotly' (Plotly technologies Inc. 2015). The genotype 'ST12_18471' from the 2017/18 field trial was excluded from all analysis due to being a significant outlier in biomass and grain yield. All three plots in the trial showed significant chlorosis and wilting, as well as a far below average number of tillers per plant.

4.3. Results

The combined data from the field trials in 2017/18 and 2018/19 shows a significant genetic variation for grain yield, HI, above-ground biomass, and most yield components, despite considerable differences in environmental conditions between years (Table 4.3.2, 4.3.3). For these harvest traits, the year and

genotype effects were always significant, whereas the G x Y effect was not consistent for all traits, though most traits showed significant variation.

4.3.1 Grain yield and yield components traits in the KWS panel

For grain yield traits for the combined analysis across years, the year effect was a significant source of variation in harvest index ($p = 0.02$), as well as above-ground dry matter per m^2 (AGDM), TGW and grain yield ($P = <0.001$). It was not a significant effect for grains m^{-2} or fruiting efficiency calculated from chaff (grains per unit chaff DM). The genotype effect was significant for all traits (Fruiting efficiency - $P = 0.04$, AGDM $g\ m^{-2}$ - $P = 0.02$, all other traits - $P = <0.001$). At the G x Y level, harvest index, grains m^{-2} , fruiting efficiency and fruiting efficiency from chaff were highly significant (Table 4.3.1, $P = <.001$). However, overall above ground biomass and thousand grain weight (TGW) did not show a significant G x Y interaction. Overall biomass showed a range of 1744 to 2385 m^{-2} , grain yield 879 $g\ m^{-2}$ to 1143 $g\ m^{-2}$, and harvest index 0.44 to 0.54. (Table 4.3.1). Individual year data are presented to highlight differences in trait expression between years. In the 2017/18 trial the genotype effect for all traits was highly significant (Table 4.3.2, $P = <.001$). Overall biomass showed a range of 1549 to 3203.7 m^{-2} , grain yield was from 708.5 and 1080.3 $g\ m^{-2}$, and harvest index from 0.30 to 0.57. In the 2018/19 trial all traits were highly significant ($P = <0.001$ except for AGDM at $P = 0.013$, Table 4.3.3). Above-ground biomass showed a range of 1763 to 2825 m^{-2} , grain yield 772 to 1346 m^{-2} , and harvest index of 0.41 to 0.60 (Table 4.3.3). From the cross-year analysis, grain yield showed a year effect ($P = <0.001$, Table 4.3.1); and was lower in 2017/18 at 914 $g\ m^{-2}$ than in 2018/19 at 1148 $g\ m^{-2}$. Biomass also showed a year effect ($P = <0.001$, Table 4.3.3) and was lower in 2017/18 at 1941 $g\ m^{-2}$ than in 2018/19 at 2277 $g\ m^{-2}$. Grains per m^2 did not show a significant year effect. Thousand grain weight showed a year

effect ($p = <0.001$) being lower in 2017/18 at 32.9g than in 2018/19 at 41.0 g (Table 4.3.3). Fruiting efficiency was also decreased in 2017/18 at 96.6 grains per gram of spike dry matter at anthesis compared to 2018/19 at 121.5. For Fruiting efficiency calculated using chaff, there was no significant year effect (Table 4.3.1).

Table 4.3.1 Means, genotype ranges and year, genotype, and year \times genotype significance for grain yield and harvest traits for the 137 lines in the KWS association panel, combined means across 2017/18 and 2018/19 field trials. Grain yield, fruiting efficiency (calculated from anthesis spike DM), fruiting efficiency (calculated from chaff DM), above-ground dry matter (AGDM) g m^{-2} , thousand grain weight and harvest index.

	Min	Max	Average	F.Pr (Year)	F.Pr (genotype)	F.pr (genotype \times year)	LSD (genotype 5%)
AGDM g m^{-2}	1743.99	2384.86	2100.21	<0.001	0.02	0.12	254.69
TGW g	28.72	47.23	37.07	<0.001	<0.001	0.11	4.96
Grain yield (g m^{-2})	879.11	1143.06	1032.92	<0.001	<0.001	0.02	81.1
Harvest Index	0.44	0.54	0.49	0.02	<0.001	<0.001	0.04
Grains m^{-2}	20364.05	35260.73	28257.2	1	<0.001	<0.001	4668.63
Fruiting efficiency grains g^{-1}	75.47	137.07	109.06	<0.001	0.04	<0.001	32.01
Fruiting efficiency (Chaff) grains g^{-1}	76.38	151.04	120	0.55	<0.001	<0.001	22.01

Table 4.3.2 Means, ranges and significance of grain yield and harvest traits for the 137 lines in the KWS association panel for the 2017/18 field trial. Grain yield, fruiting efficiency (calculated from anthesis spike DM), fruiting efficiency (calculated from chaff DM), above-ground dry matter (AGDM) g m⁻², thousand grain weight and harvest index.

	Min	Max	Average	F.Pr (genotype)	LSD 5%
AGDM g m ⁻²	1550	3203.47	1941	<0.001	292.89
TGW g	14.65	58.21	32.83	<0.001	5.80
Grain yield (g m ⁻²)	708.5	1080.27	913.5	<0.001	78.07
Harvest Index	0.301	0.57	0.473	<0.001	0.06
Grains m ⁻²	15499	61383.67	28284	<0.001	5293.25
Fruiting efficiency grains g ⁻¹	48.07	160.02	96.63	<0.001	36.84
Fruiting efficiency (Chaff) grains g ⁻¹	70.98	175.77	121.5	<0.001	28.09

Table 4.3.3 Means, ranges and significance of grain yield and harvest traits for the 137 lines in the KWS association panel for the 2018/19 field trial. Grain yield, fruiting efficiency (calculated from anthesis spike DM), fruiting efficiency (calculated from chaff DM), above-ground dry matter (AGDM) g m⁻², thousand grain weight and harvest index.

	Min	Max	Average	F.Pr (genotype)	LSD 5%
AGDM g m ⁻²	1763	2824.82	2277	0.013	411.65
TGW g	31.2	80.77	40.98	<0.001	5.98
Grain yield (g m ⁻²)	772	1345.91	114	<0.001	104.52
Harvest Index	0.41	0.60	0.506	<0.001	0.05
Grains m ⁻²	12590	38260.91	28323	<0.001	5013.04
Fruiting efficiency grains g ⁻¹	46.93	196.34	123.2	<0.001	35.10
Fruiting efficiency (Chaff) grains g ⁻¹	65.98	172.82	118.5	<0.001	23.68

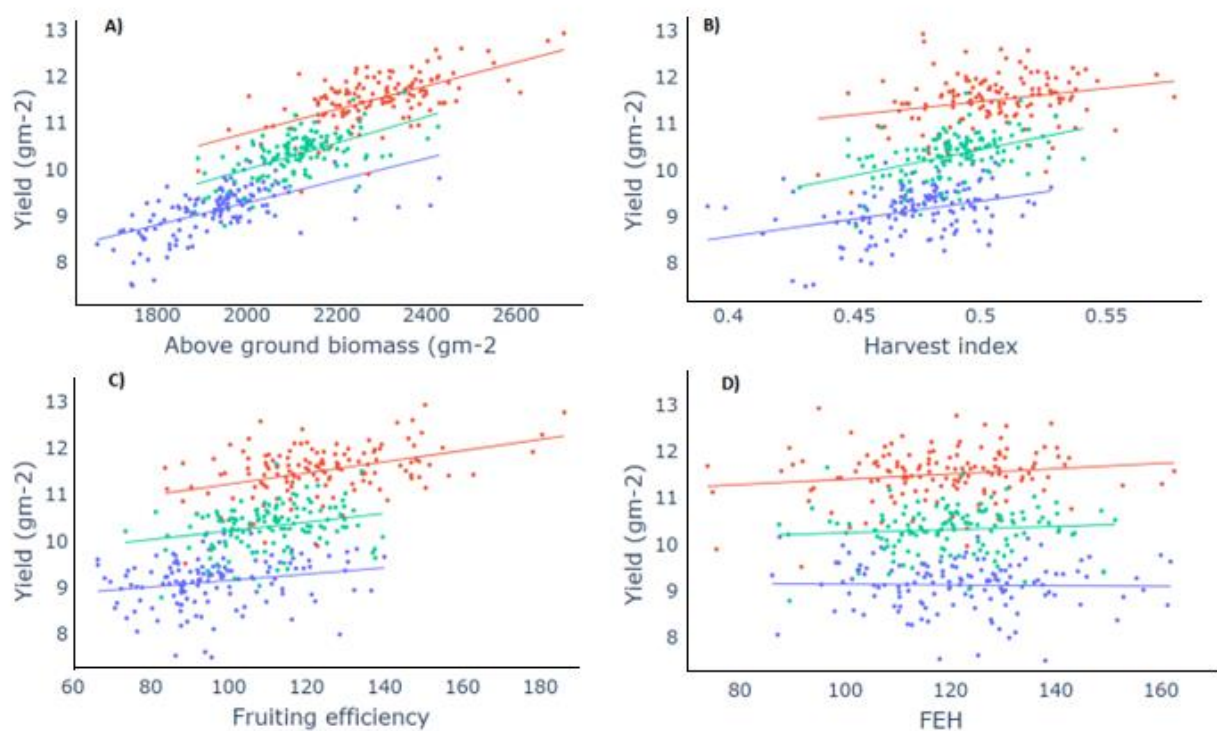
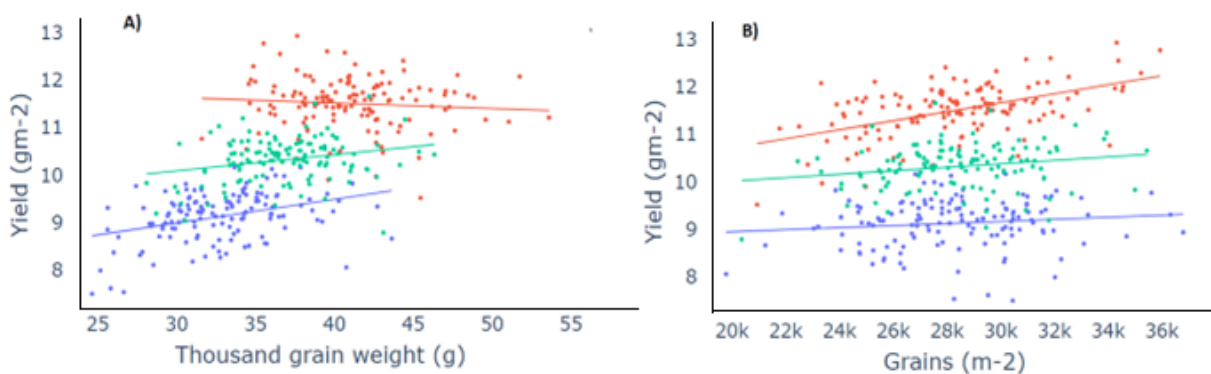


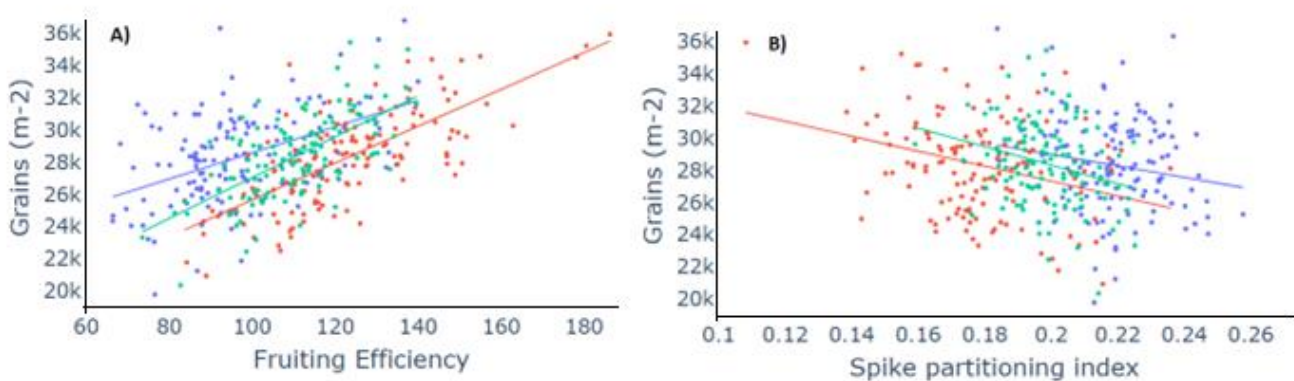
Fig 4.3. Cross-year means and individual year means Linear regressions of grain yield with biomass and yield components in the KWS association panel for 2017/18 and 2018/19 field trials and cross-year means. Blue = 2017/18 individual year, red = 2018/19 individual year, and green = combined year means. For 2017/18

- A) Yield versus above-ground dry matter g per m⁻²(AGDM) - R² = 0.354, P = <.001. B) Yield versus Harvest index R² = 0.125, P = <.001 C) Yield g m⁻² x fruiting efficiency (Anthesis; grains g⁻¹) - R² = 0.046, P = 0.006. D) Yield g m⁻² x fruiting efficiency (chaff; grains g⁻¹) - R² = 0.09, P = 0.06). For 2018/19 - A) Yield versus above ground dry matter g per m⁻²(AGDM) - R² = 0.383, P = <0.<.001. B) Yield versus Harvest index R² = 0.062, P = 0.003 C) Yield g m⁻² versus fruiting efficiency (Anthesis; grains g⁻¹) - R² = 0.171, P = <0.<.001. D) Yield g m⁻² versus Fruiting efficiency (FEH, chaff; grains g⁻¹) - R² = 0.026, P = 0.06). For combined year means, A) Yield versus above-ground dry matter g per m⁻²(AGDM) - R² = 0.287, P = <.001. B) Yield versus harvest index R² = 0.142, P = <.001 C) Yield g m⁻² versus fruiting efficiency (Anthesis; grains g⁻¹) - R² = 0.057, P = 0.003. D) Yield g m⁻² x fruiting efficiency (chaff; grains g⁻¹) - R² = 0.01, P = 0.7).



Grain yield showed the strongest positive linear association with above-ground biomass (*Fig. 4.1A*, R² = 0.287, P <.001). However, harvest index was also associated with yield (*Fig. 4.1b*, R² = 0.142, P <.001). Neither fruiting efficiency calculated from anthesis dry matter nor chaff dry weight were associated significantly with grain yield (*Fig 4.1c*, *Fig 4.1D*).

Fig. 4.4 Individual year and cross – year mean Linear regressions of yield with grains m^{-2} and thousand grain weight traits. Blue = 2017/18, red = 2018/19, and green = combined means. For 2017/18, A) Yield versus Thousand grain weight $R^2 = 0.128$, $P = <.001$. B) Yield $g\ m^{-2}$ x grains m^{-2} - $R^2 = 0.015$, $P = 0.15$. For 2018/19, A) Yield versus Thousand grain weight $R^2 = 0.07$, $P = 0.336$. B) Yield $g\ m^{-2}$ x grains m^{-2} - $R^2 = 0.267$, $P = <.001$. For combined means, A) Yield versus thousand grain weight $R^2 = 0.054$, $P = 0.005$. B) Yield $g\ m^{-2}$ x grains m^{-2} - $R^2 = 0.0320$, $P = 0.03$.



For grain traits, neither grains m^{-2} or thousand grain weight were significantly associated with yield (*Fig 4.2a*, *Fig 4.2b*) in the combined years. However, for individual years, yield showed a weak positive linear association with thousand grain weight (*Fig. 4.3a*, $R^2 = 0.127$, $P = <.001$) in 2017/18, as well as a positive association with grains m^{-2} in 2018/19 (*Fig. 4.3b*, $R^2 = 0.1487$, $P = <.001$).

Fig. 4.5. A) Fruiting efficiency vs Grains m^{-2} for the KWS association panel for individual years and combined means. For 2017/18 - $R^2 = 0.203$, $P = <.001$. For 2018/19 - $R^2 = 0.523$, $P = <.001$, for combined means - $R^2 = 0.332$, $P = <.001$
B) Spike partitioning index vs Grains m^{-2} for the KWS association panel. 2017/18 - $R^2 = 0.028$, $P = <.001$, 2018/19 - $R^2 = 0.094$, $P = <0.01$, combined means. $R^2 = 0.053$, $P = 0.005$.

Fruiting efficiency showed a significant positive association with grains m^{-2} (Fig. 4.3a, $R^2 = 0.332$, $P = <.001$), which was associated with yield in the 2018/19 trial. Spike partitioning index showed a weak, but significant negative association with grains m^{-2} (Fig. 4.4b, $R^2 = 0.053$, $P = 0.005$).

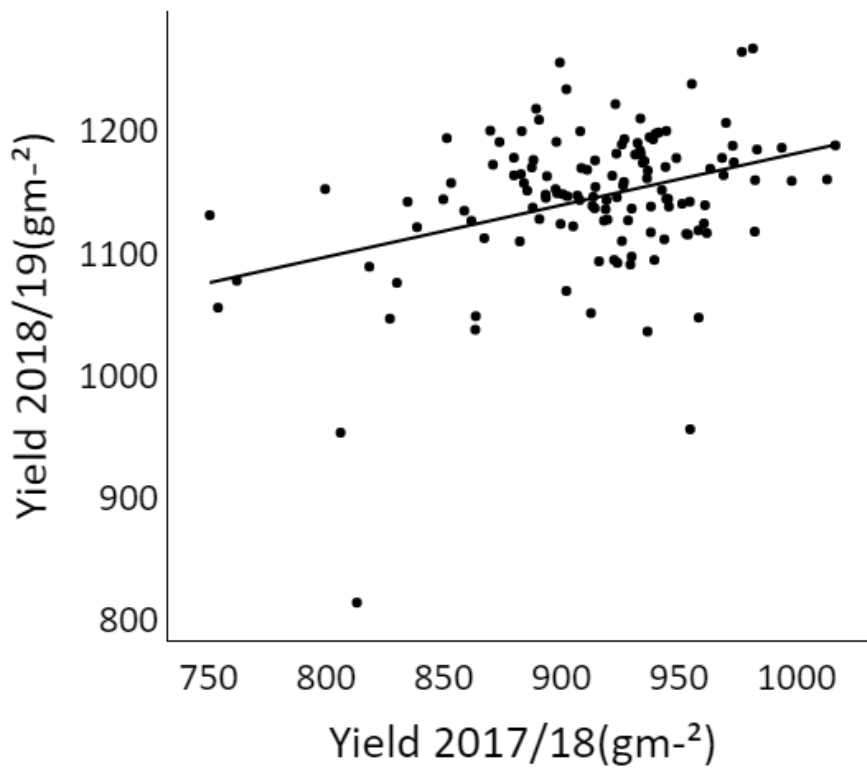


Fig 4.6. Yield 2017/18 g m⁻² x grain Yield 2018/19 g m⁻² for the KWS association panel. $R^2 = 0.1228$, $P = <.001$

Genetic variation in grain yield between years showed a weak positive linear correlation ($R^2 = 0.1231$, $P = <.001$, Fig. 4.5). Overall grain yield was significantly lower in the 2017/18 field trial compared with the 2018/19 trial.

	Ped AVG	Int 2 AVG	Int 3 AVG	Spike DM g/m ²	Lamina DW m ⁻²	LS dw m ⁻²	Stem dw m ⁻²	SPI	LPI	LsPI	StPI	AGDM g m ⁻²	TGW	Yield(g m ²)	Harvest Index	GM m ⁻²	Fruiting efficiency (A)	Fruiting efficiency Harvest	
Ped AVG																			
Int 2 AVG	-0.13																		
Int 3 AVG	-0.33	0.69																	
Spike DM g/m ²	0.24	-0.31	-0.48																
Lamina DW m ⁻²	0.23	-0.31	-0.51	0.76															
LS dw m ⁻²	-0.08	0.00	0.06	0.47	0.48														
Stem dw m ⁻²	-0.16	0.09	0.22	0.33	0.25	0.72													
SPI	0.33	-0.32	-0.56	0.59	0.28	-0.32	-0.49												
LPI	0.31	-0.32	-0.60	0.31	0.68	-0.18	-0.47	0.48											
LsPI	-0.17	0.19	0.33	-0.27	-0.20	0.51	-0.00	-0.41	-0.28										
StPI	-0.33	0.32	0.59	-0.44	-0.53	0.09	0.61	-0.74	-0.83	-0.01									
AGDM g m ⁻²	-0.34	0.36	0.62	-0.33	-0.31	0.23	0.30	-0.52	-0.48	0.35	0.48								
TGW	-0.29	0.34	0.58	-0.43	-0.45	-0.08	0.02	-0.35	-0.40	0.23	0.37	0.41							
Yield(g m ²)	-0.39	0.45	0.77	-0.45	-0.45	0.15	0.26	-0.59	-0.57	0.37	0.57	0.83	0.59						
Harvest Index	-0.16	0.26	0.40	-0.32	-0.34	-0.09	-0.01	-0.24	-0.28	0.14	0.27	-0.05	0.44	0.51					
GM m ⁻²	-0.04	0.05	0.07	0.09	0.11	0.25	0.23	-0.13	-0.08	0.10	0.09	0.30	-0.60	0.24	-0.04				
Fruiting efficiency (A)	-0.22	0.27	0.45	-0.82	-0.58	-0.26	-0.14	-0.62	-0.30	0.28	0.45	0.46	0.11	0.53	0.27	0.39			
Fruiting efficiency Harvest	0.06	-0.01	-0.06	0.11	0.13	0.07	0.06	0.03	0.08	-0.04	-0.05	-0.21	-0.40	-0.04	0.26	0.45	0.15		

Fig 4.7. Pearson's correlation matrix of key grain partitioning and plant component partitioning indices, yield, and other traits. Internode lengths (cm), Anthesis components dw m⁻², anthesis component partitioning indices, Above ground dry matter g m⁻², TGW, Yield g m⁻², Harvest index, grains m⁻², fruiting efficiency calculated with anthesis biomass, fruiting efficiency with chaff at harvest. Values shown are for the combined field trials in 2017/18 and 2018/19. LPI = lamina partitioning index, LsPI = leaf sheath partitioning index; St PI = stem partitioning index. Ped = peduncle length, Int2 = stem-internode 2 length; Int3 = stem-internode 3 length.

4.3.2 DM partitioning traits at anthesis in KWS Panel

Partitioning traits for the combined means of the KWS association panel showed a highly significant year effect for all traits ($P = <.001$). Although no significant variation was seen at the genotype level for any plant component partitioning

index, Genotype x Year showed a trend for significance for the spike partitioning index ($P = 0.091$); the genotypes ranged from 0.174 to 0.220. The component with the largest proportion of dry matter partitioned to it was the true stem, mean 0.429 and ranging from 0.36 to 0.485. Following the true-stem was the spike with a mean 0.198, ranging from 0.174 to 0.22. Lamina and leaf sheath PI were extremely close: the Leaf sheath showed a slightly higher average of 0.190 compared to an average of 0.182 for lamina. Leaf sheath PI ranged from 0.161 to 0.218, whereas Lamina PI ranged from 0.153 to 0.221 (Table 4.4). Internode lengths were all highly significant at the year level ($P = <.001$) and the Genotype x Year level ($P = <.001$), but none showed significant variation at the genotype level. Peduncle length ranged from 18.1cm to 23.7 cm, stem-internode 2 from 12.2 cm to 16 cm, and stem-internode 3 from 8.9 cm to 13.3 cm (Table 4.4).

Table 4.4.1 Range, mean average, and significance for dry-matter partitioning indices, plant component dry matter per shoot, and plant component dry matter per m^{-2} for the for the 137 lines in the KWS association panel, combined across 2017/18 and 2018/19 field trials.

Trait	Min	Max	Average	F.pr (Year)	F.pr (Genotype)	F.pr	
						(Gen Year)	X LSD 5%
Spike PI	0.174	0.220	0.198	<.001	0.978	0.091	0.033
Lamina PI	0.153	0.221	0.182	<.001	0.194	1.000	0.032
Leaf sheath PI	0.161	0.218	0.190	<.001	0.770	0.481	0.028
True stem PI	0.369	0.485	0.429	<.001	0.435	0.163	0.053
AGDM per shoot g	1.872	2.477	2.134	1.000	0.932	0.277	0.383
Ear DW per shoot g	0.350	0.505	0.423	0.004	0.935	0.050	0.106
Lamina DW per shoot g	0.313	0.470	0.389	0.001	0.918	0.175	0.100
Leaf sheath DW per shoot g	0.332	0.503	0.405	0.005	0.797	1.000	0.085
True stem DW per shoot g	0.777	1.122	0.918	<.001	0.649	0.783	0.200
Spike DM g m ⁻²	209.583	342.853	270.355	<.001	0.285	0.274	75.101
Lamina DM g m ⁻²	190.718	380.308	249.588	<.001	0.003	1.000	70.737
Leaf sheath DM g m ⁻²	188.807	347.945	260.105	0.217	<.001	0.759	71.054
True stem DM g m ⁻²	412.594	783.116	589.209	0.020	0.001	0.118	178.084
Total AGDM g m ⁻²	1061.710	1768.886	1369.149	0.126	<.001	0.533	324.724
Peduncle length (cm)	18.102	23.772	20.761	<.001	0.108	<.001	2.734
Internode 2 length (cm)	12.258	16.012	13.727	<.001	0.519	<.001	1.528
Internode 3 length (cm)	8.975	13.370	10.312	<.001	0.459	<.001	1.503

Table 4.4.2 Genetic Range, mean average, and significance for above-ground dry matter (AGDM) per shoot, dry-matter partitioning indices, plant component dry matter per shoot, and plant component dry matter per m⁻² at anthesis (GS61) for the for the 137 lines in the KWS association panel for 2017/18

Trait	Min	Max	Average	F.pr (Genotype)
Spike PI	0.141	0.288	0.219	0.382
Lamina PI	0.101	0.308	0.207	0.686
Leaf sheath PI	0.104	0.280	0.207	0.666
True stem PI	0.298	0.505	0.394	0.375
AGDM per shoot g	1.204	2.895	2.120	0.589
Ear DW per shoot g	0.238	0.713	0.464	0.741
Lamina DMDW per shoot g	0.180	0.698	0.438	0.747
Leaf sheath DMDW per shoot g	0.193	0.748	0.382	0.459
True stem DMDW per shoot g	0.418	1.207	0.836	0.346
Spike DM g m⁻²	165.0164.997	591.8786	305.843	0.130
Lamina DM g m⁻²	121.4364	594.110	290.030	0.101
Leaf sheath DM g m⁻²	112.633	487.3296	253.101	0.055
True stem DM g m⁻²	165.0164.997	591.8786	305.843	0.047
Total AGDM g m⁻²	1549.931	2894.8766	1931.01930.976	<.001
Peduncle length (cm)	15.40400	27.500	21.630	0.686
Internode 2 length (cm)	7.57567	16.03025	13.102	0.256
Internode 3 length (cm)	5.43425	13.61609	8.393	<.001

Table 4.4.3 Genetic Range, mean average, and significance for above-ground dry matter (AGDM) per shoot, dry-matter partitioning indices, plant component dry matter per shoot, and plant component dry matter per m⁻² for the at anthesis (GS61) for the 137 lines in the KWS association panel for 2018/19.

Trait	Min	Max	Average	F.pr (Year)
Spike PI	0.108	0.287	0.178	0.214
Lamina PI	0.084	0.251	0.159	0.278
Leaf sheath PI	0.102	0.274	0.200	0.229
True stem PI	0.339	0.628	0.464	0.035
AGDM per shoot g	1.350	3.079	2.149	0.307
Ear DW per shoot g	0.200	0.708	0.381	0.007
Lamina DW per shoot g	0.142	0.553	0.341	0.044
Leaf sheath DW per shoot g	0.208	0.617	0.428	0.899
True stem DW per shoot g	0.575	1.643	0.998	0.582
Spike DM g m⁻²	125.831	372.248	233.5462	0.093
Lamina DM g m⁻²	105.315	427.1066	210.5496	0.125
Leaf sheath DM g m⁻²	120.7657	504.205	267.519	0.014
True stem DM g m⁻²	301.8763	1459.4371	626.1083	0.000
Total AGDM g m⁻²	1763.109	2850.2171	2277.7683	0.501
Peduncle length (cm)	14.74738	23.63625	19.76758	8.113
Internode 2 length (cm)	11.84838	17.68675	14.30299	0.729
Internode 3 length (cm)	8.900	15.48475	12.154	0.697

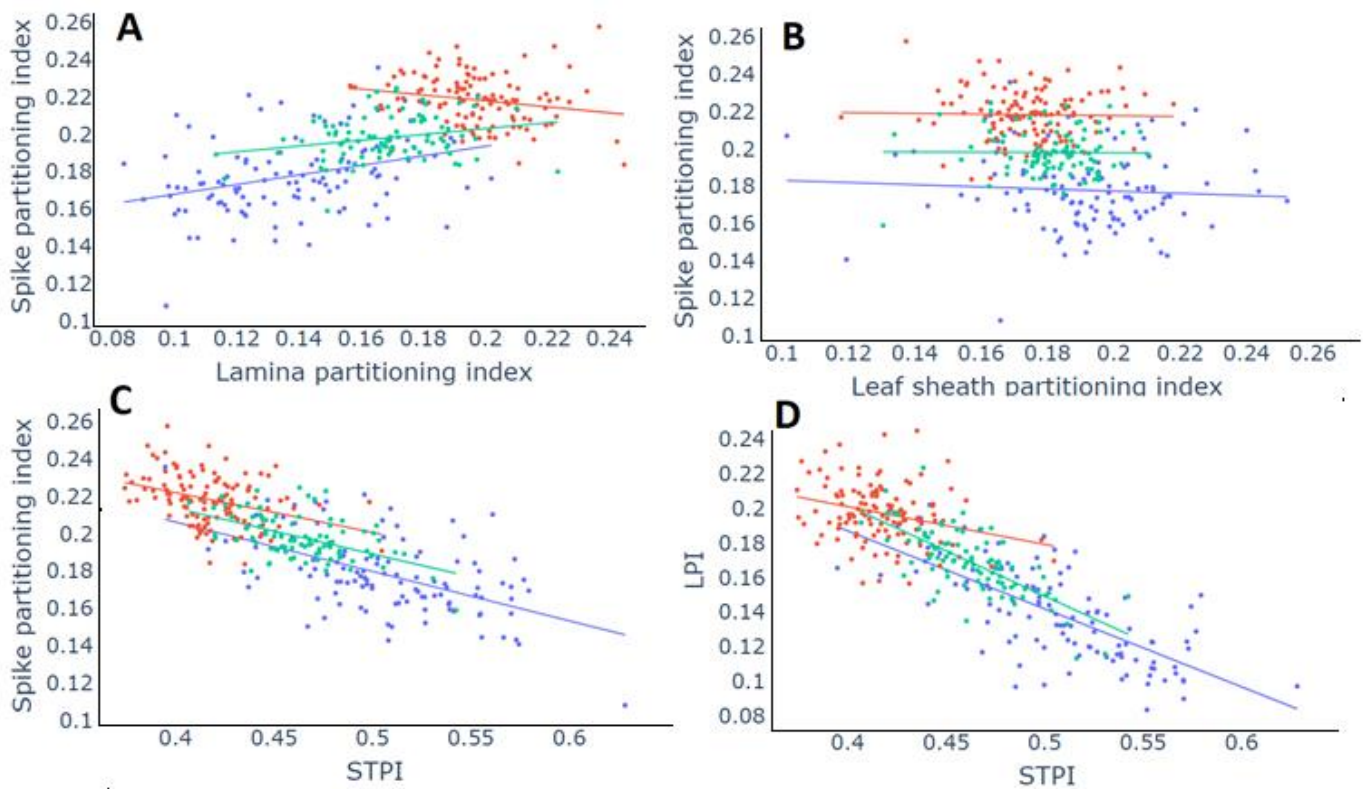


Fig. 4.8 Linear relationships between dry matter partitioning indices for 2017/18 (Red), 2018/19 (Blue) and combined means (Green). A) Spike partitioning index versus Lamina partitioning index. For 2017/18, $R^2 = 0.042$, $P = 0.02$. For 2018/19, $R^2 = 0.109$, $P = <.001$. Combined = $R^2 = 0.035$, $P = 0.02$. B) Spike partitioning index versus leaf sheath partitioning index. For 2017/18, $R^2 = 0.001$, $P = 0.793$. For 2018/19, $R^2 = 0.05$, $P = 0.49$. Combined = $R^2 = 0.005$, $P = 0.4$. C) Spike partitioning index versus stem partitioning index. For 2017/18/19, $R^2 = 0.129$, $P = <.001$. For 2018/19, $R^2 = 0.282$, $P = <.001$. Combined = $R^2 = 0.367$, $P = <.001$. D) Lamina partitioning index x Stem partitioning index. For 2017/18 $R^2 = 0.082$, $P = 0.001$. For 2018/19 $R^2 = 0.489$, $P = <.001$. Combined = $R^2 = 0.536$, $P = <.001$.

Linear relationships between spike PI at anthesis and other plant component PI at anthesis show that the most significant competitor for spike dry matter was the stem ($R^2 = 0.367$, Fig. 4.7). Neither leaf lamina nor leaf sheath partitioning indices showed any significant association amongst genotypes with the spike partitioning index. Stem partitioning index also showed a strong negative linear association with the leaf lamina partitioning index ($R^2 = 0.536$, Fig. 4.7).

4.3.3 True Stem Internode DM partitioning at anthesis for subset 1

Key stem-internode partitioning traits at anthesis are presented in Table 4.5 for the 25 genotypes (Subset 1). Averaging across years, peduncle length ($p=0.026$), ranging from 19.1 cm to 23.1 cm and stem-internode 3 length ($P= 0.03$) ranging from 8.7 cm to 12.6 cm showed significant variation. Internode 2 length ranged from 12.2 cm to 14.7cm and did not differ significantly amongst the genotypes ($P=0.217$). For stem-internode partitioning indices, all three internodes showed significant GxY level effect ($P=0.03$, $P=0.02$, $p=0.04$, for ped, int 2, int 3 respectively). The genetic ranges for Int 2 PI (0.20-0.24) and Int 3 PI (0.19-0.23) were similar. Variation in stem-internode specific weight, determined as dry matter per unit length of the internode (g cm^{-1}), was significant for the peduncle and internode 2 and there was a GxY interaction ($P=0.033$, $P=0.022$) but not for stem-internode 3 ($P=0.938$). Internode specific weight decreased with each internode from the spike down, with ped SPW being lowest, and internode 3 SPW highest.

Table 4.5. Cross-year genetic ranges, means, and significance values of 25 lines from the KWS association panel (Subset 1) for Stem-internode length, stem-internode partitioning indices and internode specific weights. All values are for true stem only. Significance values are for Genotype (G), Year (Y), and Genotype x year (GxY). Values presented are cross-year means (2018/19, 2019/20).

True stem internode traits						
Trait	Min	Max	Mean	F. PR (G)	F. Pr (Y)	F. PR (GxY)
Ped cm	19.101	23.101	20.899	0.001	<.001	0.026
Int 2 cm	12.266	14.721	13.434	0.234	<.001	0.217
Int 3 cm	8.78	12.666	10.105	<.001	<.001	0.03
Ped PI	0.06	0.13	0.08	0.01	<.001	0.023
Int 2 PI	0.09	0.14	0.11	0.008	<.001	0.047
Int 3 PI	0.09	0.15	0.11	<.001	0.197	0.012
Ped SPW g cm ⁻¹	0.07	0.124	0.098	0.023	0.381	0.033
Int 2 SPW g cm ⁻¹	0.013	0.021	0.017	0.006	0.006	0.022
Int 3 SPW g cm ⁻¹	0.02	0.145	0.07	0.004	<.001	0.938

A weak positive linear relationship was observed between true-stem (TS) internode dry matter per shoot and TS internode length for the peduncle ($R^2 = 0.16$, $P = 0.05$) in the subset 1 (Fig. 4.8). Stem-internodes 2 and 3 did not exhibit a significant relationship for the equivalent linear relationships (Fig. 4.8). There was no significant linear relationship between TS internode length and TS

internode specific weight for any of the three internodes measured. However, a very strong and significant positive linear relationship between TS internode DM (g shoot^{-1}) and stem specific weight was observed for all three internodes.

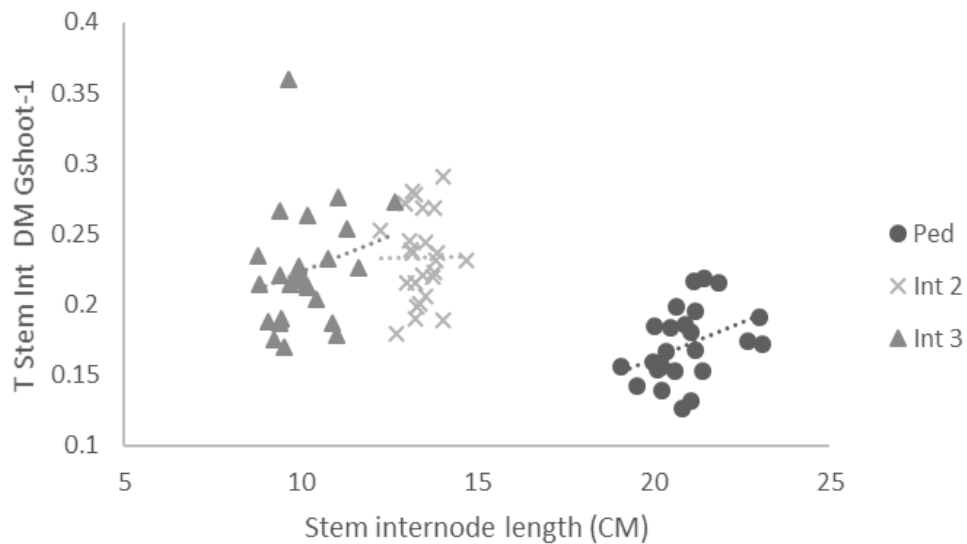


Figure 4.9. Linear regressions between true-stem DM shoot^{-1} (g) and true-stem internode length (cm) : Ped, $R^2 = 0.155$, $P = 0.051$. Int 2: $R^2 = 0.01$, $p=0.977$. Int 3: $R^2 = 0.05$, $P=0.266$ for the 25-line subset of the KWS association panel, cross year means for 2017/18 and 2018/19.

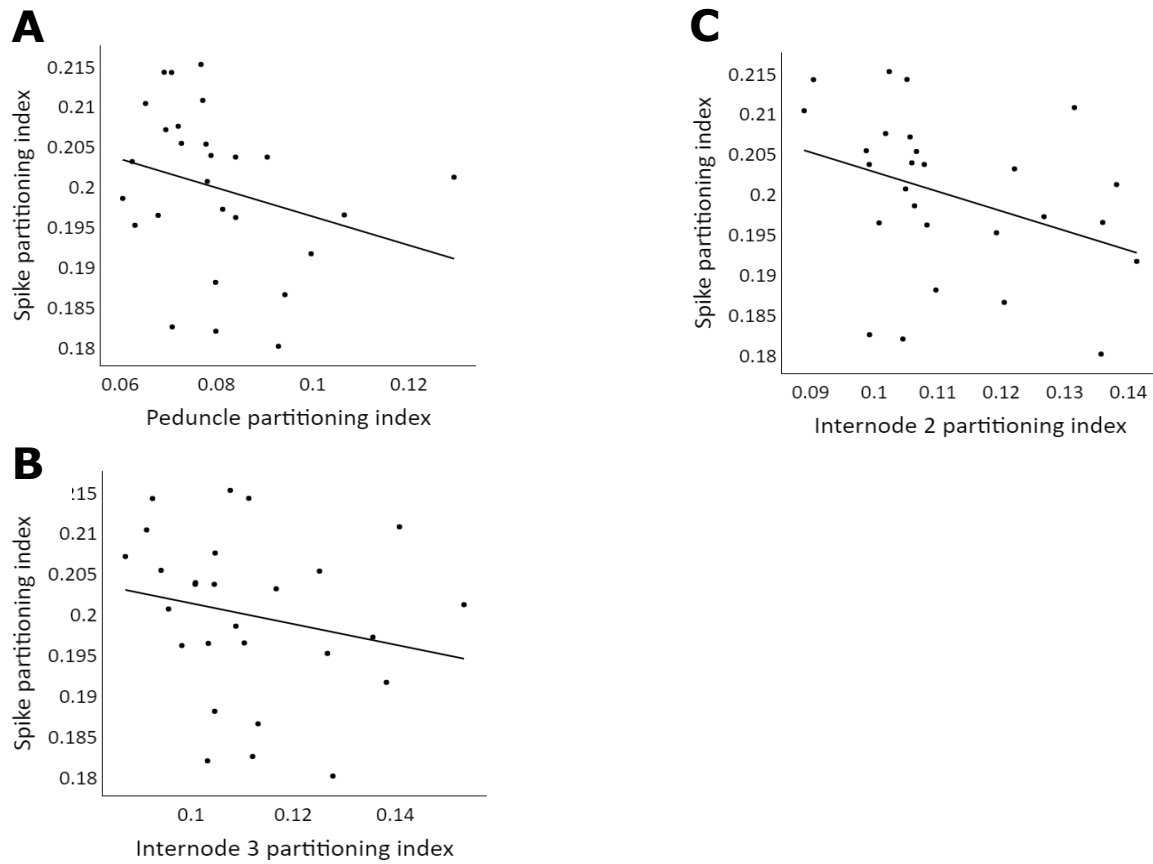


Fig. 4.10 Linear relationships between True stem partitioning indices and spike partitioning index for the 25-line subset of the KWS association panel (Subset 1). A) Spike partitioning index x Peduncle partitioning index. $R^2 = 0.07$, $P = 0.09$. B) Spike partitioning index x Internode 2 partitioning index $R^2 = 0.1302$, $P = 0.03$. C) Spike partitioning index x Internode 3 partitioning index, $R^2 = 0.04$ $P = 0.37$.

A significant negative association was found amongst genotypes between the spike partitioning index and true-stem internode 2 partitioning index for subset 1 of the KWS association panel (Fig. 4.9, $R^2 = 0.1302$, $P = 0.03$). No significant trend was observed between either of the other true-stem internode partitioning indices and spike partitioning index.

Table 4.6 Pearson's correlation coefficient between true-stem-internode traits and grain yield and yield components for the 25-line subset of the KWS association panel (Subset 1). Values presented are cross-year means (2018/19 and 2019/20). PI = Partitioning index, SPW = Specific weight.

† $p < 0.1$, * $p < 0.05$, ** $P < 0.01$,

	Ped_PI	Int_2_PI	Int_3_PI	PED_SPW	Int_2_SPW	Int_3_SPW	SPI	HI	GM2	GY
Ped_PI	-									
Int_2_PI	0.5053	-								
Int_3_PI	-0.127	0.1017	-							
PED_SPW	0.5121	0.1281	-0.0246	-						
Int_2_SPW	0.2862	0.4053	0.2794	0.7696	-					
Int_3_SPW	-0.2971	0.0087	0.4213	-0.3445	-0.0255	-				
SPI	0.1313	-0.0311	-0.2382	-0.1577	-0.2231	0.0912				
HI	-0.0131	0.3556	0.2155	0.2198	0.3919	-0.0594	0.1375	-		
GM2	0.2431	-0.0127	-0.1298	-0.263	-0.3706	0.0253	0.0728	-0.1354	-	
GY	-0.2526	-0.2414	0.222	-0.0029	-0.0189	-0.0091	0.2211	0.4287	0.2732	-

Linear correlations between true-stem-internode traits, harvest index, grain yield, grains per m⁻², spike dry matter at anthesis and thousand grain weight are shown in Table 4.6. Spike partitioning index showed negative correlations with TS Ped PI ($r = 0.1313$) and TS Ped SPW ($r = -0.1577$). SPI also showed negative relationships with TS Int 3 PI ($r = -0.2382$) and Int 2 TSSPW ($r = -0.2231$). Harvest index showed several relatively strong positive associations with internode traits, including TS int 2 PI and int 2 TSSPW ($r = 0.3556$, $r = 0.3919$, respectively), and TS int 3 PI ($r = 0.2155$). Harvest index also showed a weak negative relationship with SPI ($r = -0.1375$). Grains m⁻² showed a positive association with Ped PI ($r = 0.2431$), and a negative association with Int 3 PI ($r = -0.1298$). Grains m⁻² also showed a negative association with Ped SPW and int 2 SPW ($r = -0.263$, $r = -0.3706$, respectively) and HI ($r = 0.1354$). Grain yield was negatively associated with Ped PI ($r = -0.2526$) and Int 2 PI ($r = -0.2414$), but positively associated with Int 3 PI ($r = 0.222$). Grain yield also showed a weak negative association with SPI (-0.2211), and positive associations with HI ($r = 0.4287$) and grains m⁻² ($r = 0.2732$, $P < 0.01$).

4.3.4 NDVI senescence and leaf chlorophyll fluorescence traits

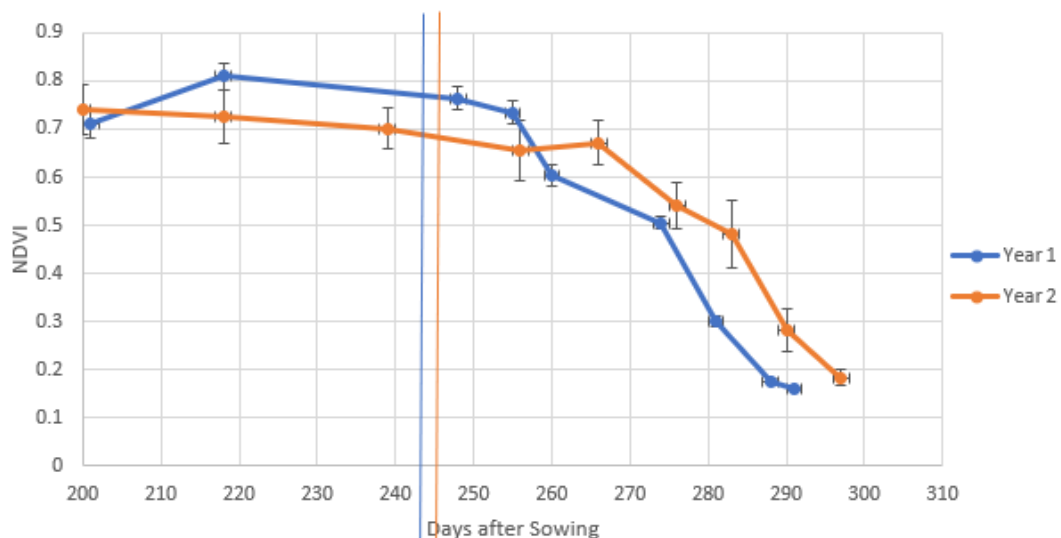


Fig 4.10. Comparison of NDVI grand means for 2017/18 and 2018/19 at comparable developmental time points. Error bars show Least significant difference of means. Initial measurements were taken in the middle of March, and final measurements at the end of July. Vertical coloured lines represent date of anthesis for representative year.

Comparison of NDVI by year shows some significant differences in the grain filling stage post anthesis. The most significant deviation between years took place between 260 and 290 days after sowing, where the NDVI in 2018 declined more rapidly than in 2019.

4.3.4.1 Leaf photosynthesis and canopy senescence parameters

Table 4.7. Cross-year means, significance, and ranges for NDVI senescence parameters. Stay-green score shows the NDVI value at onset of senescence (20%) and end of senescence (80%) for 138 genotypes in KWS panel.

	Year	Min	MAX	AVG	Genotype	G x Y	Year
Onset Sen. 20%	2017/18	50.99	71.72	59.42	<0.001	-	-
End Sen. 80%	2017/18	12.75	17.93	14.857	<0.001	-	-

Onset Sen.								
20%	2018/19		59.39	78.78	65.405	<0.001	-	-
End Sen.								
80%	2018/19		14.85	19.69	16.35	<0.001	-	-
Onset Sen.	2017/18	+						
20%	2018/19		59.39	78.78	65.364	<0.001	<.001	<.001
End Sen.	2017/18	+						
80%	2018/19		14.85	19.69	16.343	<0.001	<.001	<.001

Genetic variation in NDVI senescence timing parameters was highly significant in both 2017/18 and 2018/19 at both onset and end of senescence, ($P = <0.001$, $P = <0.001$, Table 4.7). Cross-year means were also highly significant at both the genotype ($P = <0.001$, $P = <0.001$) and GxY level for both onset and end of senescence ($P = <0.001$, $P = <0.001$). There was also a year effect for both NDVI senescence traits ($P = <0.001$, $P = <0.001$). In 2018-19, genetic variation in leaf SPAD was highly significant early in development on March 12th at around late tillering, approximately GS 25 ($P = <0.001$), but the genotypes did not differ on 14 May at around booting ($P = 0.849$).

Table. 4.8 Cross-year means, significance, and ranges for leaf SPAD and leaf chlorophyll fluorescence parameters for 138 genotypes in KWS panel in 2018-19. Phi2 is a measure of the Quantum Yield of Photosystem II. PhiNPQ shows the ratio of absorbed light used in the Non-photochemical quenching response. PhiNO shows ratio of absorbed light lost via other miscellaneous processes.

Trait	Min	MAX	AVG	Genotype
Phi2 Mar 12	0.178	0.307	0.252	<.001
PhiNPQ Mar 12	0.491	0.654	0.574	<.001
PhiNO Mar 12	0.142	0.238	0.173	<.001
SPAD 12/04	29.97	36.69	33.517	<.001
Phi2 14/05	0.017	0.157	0.074	<.001
PhiNPQ 14/05	0.648	0.786	0.713	<.001
PhiNO 14/05	0.188	0.235	0.212	0.229
SPAD 14/05	30.31	36.46	33.696	0.849

Values for Flag-leaf fluorescence parameters are presented only for 2018/19, and all show highly significant genotype variation ($P = <0.001$), except for PhiNO at 14/05, ($P = 0.229$, Table 4.8).

4.3.4.2 Correlations between leaf photosynthetic and senescence traits

Linear relationships between flag-leaf photosynthetic and NDVI senescence parameters and key yield traits are presented in Table 4.9. NDVI onset of senescence showed a negative linear relationship with harvest index ($R^2 = -0.206$, $p=0.022$) for combined year means.

For leaf photosynthetic activity traits measured on 12 March in 2018/19, a trend for a positive association between increased Photosystem II activity (Phi2 Mar 12) and spike partitioning index at anthesis was observed ($R^2 = 0.117$, $P = 0.09$). However, a stronger negative association was observed between the leaf NPQ

value (PhiNPQ Mar 12) and SPI ($R^2 = -0.165$, $P=0.04$). No relationships were observed between leaf PhiNO (sum of energy not used in PSII or NPQ response) and any other trait at this timepoint. The same parameters measured at the 14 May timepoint (Growth stages ranging from 41-49) showed similar relationships. PSII activity was positively and linearly associated with SPI ($R^2 = 0.18$, $p=0.03$), and NPQ activity showed a negative linear relationship with SPI ($R^2 = 0.23$, $P = 0.01$). Leaf PSII activity showed a weakly significant positive association with fruiting efficiency at anthesis ($R^2 = 0.140$, $P = 0.07$), whereas NPQ showed a negative linear relationship with fruiting efficiency ($R^2 = -0.184$, $P = 0.03$). Leaf SPAD readings taken at this timepoint showed a trend for positive association with harvest index ($R^2 = 0.123$, $P = 0.09$), and a positive linear association with spike dry matter per m^2 at anthesis ($R^2 = 0.172$, $P = 0.04$), but no relationships with other grain or partitioning traits.

Table 4.9. Linear relationships between canopy and leaf photosynthetic traits and grain partitioning and yield traits for the 25-line subset of the KWS association panel 2018/19 (subset 1). Senescence parameters show data for the full panel of 138 lines. Values shown are R²

		SPI	HI	GY	GM2	SpkDM A	FE
NDVI	Staygreen						
20%	2017/19 + 2018/19	0.0646	-0.206*	0.0018	0.110	0.010	0.010
NDVI	Staygreen						
80%	2017/19 + 2018/19	0.0107	0.0695	0.0018	0.05	0.040	0.002
NDVI	Staygreen						
20%	2017/18	0.0226	0.0423	0.0104	0.0735	0.0067	0.0625
NDVI	Staygreen						
80%	2017/18	0.0226	0.0423	0.0103	0.0735	0.0067	0.0625
NDVI	Staygreen						
20%	2018/19	0.043	0.1411*	0.0001	0.0755	0.002	0.025

NDVI Staygreen					-		
80%	2018/19	0.043	0.1411*	0.0161	0.1679*	0.042	0.031
Phi2 12/04	2018/19	0.117†	0.03	0.02	0.101	0.108	0.004
	2018/19	-					
PhiNPQ 12/04		0.165*	0.03	0.002	0.08	0.060	0.003
PhiNO 12/04	2018/19	0.0124	0	0	0.07	0.022	0.005
SPAD 12/04	2018/19	0.0210	0	0.004	0.022	0.000	0.003
Phi2 14/05	2018/19	0.180*	0.09	0.003	0	0.108	0.140†
	2018/19						-
PhiNPQ 14/05		-0.23*	-0.04	0.004	0	0.106	0.184*
PhiNO 14/05	2018/19	0.0048	0.04	0	0	0.010	0.001
SPAD 14/05	2018/19	0.0545	0.123†	0.173	0.05	0.172*	0.005

4.4 Discussion

4.4.1 Grain yield, biomass, and harvest index associations.

Grain yield in the 2019 trial was significantly higher than in 2018. In the 2018 field trial, grain yield was associated with and partly explained by thousand grain weight but showed no significant relationship with grain number. The inverse was true in the 2019 trial. Grain yield in 2018 was affected by a period of high temperature and drought unusual to the UK. Rainfall from two weeks prior to anthesis to the conclusion of the grain filling period was significantly lower than the long-term mean. In 2018, there was 0.8mm rainfall for the 21 days following anthesis, compared to 86mm in 2019. Water deficit prior to anthesis can significantly limit yield potential by reducing the number of fertile florets per spike, and therefore reducing the sink capacity for assimilate. During the grain filling stage, water deficit can cause a reduction in photosynthetic activity, leading to less photo assimilate to be partitioning to the grains (Rajala et al., 2009). The stress was likely not significant enough pre anthesis to cause an increase in floret abortion, leading to a high number of grains competing for reduced assimilate. Grain number between years did not vary significantly, but thousand grain weight was significantly higher in the 2019 trial compared to 2018, along with overall grain yield. One key difference between the UK Winter wheat material from the KWS association panels and lines used in similar work, such as the CIMMYT HiBAP, is the lack of awns in the UK material. Awns have previously been shown to increase water use efficiency and grain yield in severe drought conditions, but do not appear to have an adverse effect on grain number in more favourable conditions (Evans et al., 2008). In the present study, there was moderate drought during the grain filling stage in the summer of 2018. Previous work has shown that awns do not give significant advantages to tolerance under more moderate

drought conditions, such as those in the UK (Foulkes et al., 2008). In the present study, Skyfall, one of the awned varieties was the third highest yielding variety at 997.9 g m⁻² in the year with drought, 2018, but only 62nd with 1157.4 g m⁻² in the 2019 trial. A more detailed study of awned vs non awned varieties of UK winter wheat under drought conditions would need to be undertaken to fully explore the efficacy of awns as a drought resistance trait in UK wheat.

Genetic gains to yield potential have previously been attributable primarily to increases of harvest index, a greater proportion of the above ground biomass being partitioned to the grains (Aisawi et al., 2015; Ferrante et al., 2017). This was largely due to the introgression of Rht alleles during the green revolution (R. Fischer et al., 2014; Hedden, 2003), but subsequent post green revolution gains to yield have continued to be associated with improved harvest index, albeit at a slower rate of improvement (Waddington et al., 1986; Calderini, Dreccer and Slafer, 1995; Lopes et al., 2015). Harvest index has not shown significant progress from peak values of 0.45 to 0.55 since the mid 1980's (Aisawi et al., 2015; Whitest & Wilson, 2006), despite a theoretical limit of 0.62 (Austin et al., 1980; Foulkes et al., 2011) and increases to yield potential in recent decades have been associated instead with increases to biomass in both CIMMYT spring wheat varieties and UK winter wheat varieties (Shearman et al., 2005; Aisawi et al., 2015; Reynolds et al., 2017).

This pattern was also observed in the UK winter wheat lines of the KWS association panel, where grain yield was strongly associated with and better explained by above-ground dry matter than it was by harvest index, which showed a slightly weaker association. However, no trade-off was observed between AGDM and

harvest index in the KWS association panel, whereas in previous work on CIMMYT spring wheat varieties (Rivera-Amado, Trujillo-Negrellos, Gemma Molero, *et al.*, 2019; Sierra-Gonzalez, 2019) an association was reported. The results in spring wheat support the strategy of improving harvest index in modern high biomass cultivars as a means to significantly improve grain yield (Foulkes, Snape, *et al.*, 2007; Giunta *et al.*, 2009). In the KWS association panel a significant trade off was observed between grain number and grain weight, likely due to an increased number of smaller average grains in high grain number varieties, where those with a greater number of surviving fertile florets at anthesis set more grain, which in turn compete for assimilate, leading to small overall grains (Calderini *et al.*, 2001; Acreche *et al.*, 2008). One possible target trait for the improvement of Harvest index is to increase grain number via improved fruiting efficiency, which represents the efficiency with which dry matter allocated to the spike is converted to grains (Gustavo A. Slafer *et al.*, 2015; Terrile, Miralles and González, 2017b), which in this panel showed a weak but significant association with yield and harvest index, and an association with grain number, which was in turn associated with yield in the 2019 field trial.

4.4.2 Anthesis partitioning and fruiting efficiency

A similar relationship between Fruiting efficiency and grain number has been reported in a number of other studies on spring wheats (Elía *et al.*, 2016; Rivera-Amada *et al.*, 2016), but not previously in UK winter wheats. In this panel, spike partitioning index was approaching significance and showed strong a strong negative relationship with fruiting efficiency, along with spike dm m², as also reported in two high Fruiting efficiency cultivars by (Terrile *et al.*, 2017). The existence of a trade-off between Fruiting efficiency and spike dry matter implies that dry matter to the spike is being allocated disproportionately to other spike

components than grain, or a source limitation is preventing allocation of dry matter to developing grains that are not prioritised over structural spike components. (González et al., 2011) reported that the trade-off was most significant in genotypes with high spike dry matter weight, suggesting that dry matter is not efficiently translated into grain in high SPI varieties. (Sierra-Gonzalez et al., 2021) reported increased FE was associated with a reduction in lemma and awn partitioning indices. The vast majority of lines in the KWS association panel do not possess awns, however future work would examine the relationship of spike dry matter components both to each other and fruiting efficiency for the KWS UK winter wheat association panel. As expected, due to the difference in environmental conditions between years, the year effect for all partitioning indices was highly significant. However, there was no significant variation observed for any individual plant component index at the genotype or genotype x year level, possibly due to the relatively low level of genetic diversity in the panel compared to other association panels such as the CIMMYT HIBAP (high biomass association panel) (Sierra-Gonzalez et al., 2019)..

4.4.3 NDVI and chlorophyll fluorescence parameters

Exploration of Fluorescence parameters in the 2019 field trial of the KWS association panel was performed at 2 time points. The first set was taken during tillering in mid-March, the second during early boot in mid-May, during the period of rapid spike growth between booting and anthesis. The key findings were that Spike partitioning index is associated positively with PSII activity, and negatively with NPQ activity at both measurement points; fruiting efficiency is associated with higher PSII activity/ lower NPQ activity during the later measurement at

booting. Higher flag leaf photosynthesis can be associated with an increased supply of assimilate, leading to higher fertile floret number and grains per spike, and greater partitioning of assimilate to the spike during its growth. (Dreccer et al., 2014; G. A. Slafer & Andrade, 1993). Reduced PSII activity leads to lower available assimilate, potentially reducing the available assimilate supply available that could be partitioned to the spike. There is also an association with overall spike DM /m² and PSII activity, though not significant.

An additional possibility is differences in the NPQ response affecting PSII activity and the supply of assimilate. The non-photochemical quenching response is a photoprotective mechanism used by plants to safely shed energy from excess light absorption. (Demmig-Adams et al., 2012; Horton et al., 2000; Verrotte et al., 1979). Although the NPQ response can prevent cellular damage caused by high light, increasing crop yields (Hubbart et al., 2018), the mechanism can also be over tuned, potentially decreasing grain yields via reduced PSII quantum yield due to the persistence of the response during fluctuating conditions, such as a cloud passing across the sky (Kromdijk et al., 2016). The association seen in this panel could be partially explained by differences in sensitivity to, or recovery rate from, the NPQ response.

NDVI at onset and conclusion of senescence showed a positive relationship with harvest index for 2019. The 2017/18 values of NDVI and any relationships with grain traits may have been skewed by the drought experienced in that season. A higher NDVI at conclusion of senescence was also negatively associated with lower grains per m². NDVI is extensively used as a crop monitoring tool by agronomists and has been used for creating models of yield estimation (Boken & Shaykewich,

2010; Huang et al., 2014; Meng et al., 2013; Mkhabela et al., 2011). Higher NDVI scores during grain filling have also shown strong associations with grain yield and biomass in spring wheat varieties (Hassan et al., 2019).

4.4.4. Detailed stem internode partitioning

The detailed stem internode partitioning performed on subset 1 revealed internode 3 partitioning index to be negatively associated with spike partitioning index, along with internode 2 specific weight. This is similar to results reported by (Rivera-Amado, Trujillo-Negrellos, G. Molero, *et al.*, 2019; Sierra-Gonzalez *et al.*, 2021) in CIMMYT spring wheats, suggesting that internodes 2 and 3 are also significant competitors for spike dry matter in UK winter wheat.

4.7. Appendix

Appendix Table 4.1 KWS Panel genotypes and parental backgrounds

Subset 1 of 25 Genotypes

St12_19379	St13_25110
W344	St16_41954

Lili	TC16_175
TC16_622	St16_41372
W309	W279
Santiago	Leeds
TC16_128	Zyatt
TC16_97	Crusoe
St15_35489	St13_24200
W310	TC16_479
Tempo	St15_35050
St12_18726	TC16_407
TC16_466	Cordiale
St16_41754	

Chapter 5. Genetic analysis of physiological traits to improve grain partitioning and yield in an elite UK winter wheat association panel

5.1. Introduction

As one of the three most cultivated cereal crops, it is important that wheat yields keep pace with the increasing consumption of a growing global population. At present, yield genetic increases are not sufficient, increasing only 1% per year (Lucas, 2012; Reynolds *et al.*, 2012a), compared to a target of 2.4% necessary to maintain food security (Crain *et al.*, 2018). Furthermore, yields are likely to be negatively impacted by urbanisation and by changes to climate such as increases to temperature. Wheat yields could be reduced by 6% for each 1°C increase in temperature, and winter wheat specifically by 3 – 10% (Voss-Fels *et al.*, 2019; You *et al.*, 2009) This provides significant challenges to breeders to increase gains to genetic yield potential beyond just those required for growing demand, but also to account for the destabilising effects of climate change on environmental conditions. During the Green Revolution period, higher values of grain yield and harvest index were achieved due to the introduction of semi-dwarf (*Rht*: Reduced Height) cultivars which had shorter stems able to support heavier spikes due to increased fertile florets and grains per unit area (GN) (Hedden, 2003). However, in the last decades CIMMYT spring wheat yield gains have progressed at a slower rate, associated mainly with increases in biomass (Lopes *et al.*, 2015; Brisson *et al.*, 2010; Lynch *et al.* 2017; Rivera-Amado *et al.* 2019). Additionally, selection for fruiting efficiency - FE: grain number per unit spike dry weight at anthesis (Terrile *et al.*, 2017) has been suggested as an avenue to increase grain number

in wheat. However, its trade-off with spike dry weight at anthesis and grain weight may affect its usefulness (Slafer et al., 2015).

Wheat breeding programs focus mainly on the development of two types of species: *T. aestivum* ssp. *aestivum* and *T. turgidum* ssp. *Durum*. The use of existing data and multidisciplinary platforms needs to be integrated for the identification of ideal parents that will contribute to yield progress. The incorporation of high-throughput phenotypic data and improvements in next-generation sequencing (NGS) have improved understanding of genetic basis the regulation/function of specific traits (Friesner et al., 2017).

Association mapping (AM) relies on identifying genomic regions associated with a particular phenotypic trait (Milner et al., 2016). In wheat, association mapping exploring linkage disequilibrium has improved in the last decade as the International Wheat Genome Sequencing Consortium (IWGSC) revealed an annotated reference sequence of the Chinese spring wheat variety, covering 94% of the genome containing 107,891 high-confidence gene models (IWGSC, 2018). Identifying marker-trait associations (MTAs) for complex polygenic traits, such as grain number per m² is a challenging research area as these traits are highly influenced by the environment (Wu, Chang, and Jing, 2012). In GWAS the implementation of population structure can increase the power of statistical associations, which may be due to local adaptation and breeding history and unequal relatedness among genotypes (Yu et al., 2011; Yue et al., 2006). These methodologies estimate the proportion of genes identical by descent between any pair of individuals excluding closely related individuals (Schork et al., 2013). Additionally, principal component analysis (PCA) was recently proposed as a fast and effective way to summarise variation observed across all markers into a smaller number of underlying component variables (Wang et al., 2009). The

loadings of each individual on each principal component describe the population membership or the ancestry of each individual (Zhu et al., 2008)).

Previous GWAS studies have been published focusing on grain quality traits (Kristensen *et al.*, 2018; Liu *et al.*, 2018) and disease resistances (Gao *et al.*, 2016; Li *et al.*, 2016; Juliana *et al.*, 2018) but relatively limited research has been done to date in yield-related traits. Using a spring wheat HIBAP population, Sierra-Gonzalez *et al.* (2021) reported > 20 novel MTAs, including MTA for grain yield and FE, explaining from 1-14% of phenotypic variance. Guo *et al.* (2018) genotyped 215 wheat cultivars and reported 117 significant associations for spikelets per spike, grains per spike and thousand-grain weight under irrigated environments where the phenotypic variation explained ranged from 2–13%. Using a high biomass spring wheat panel Molero *et al.* (2019) identified 94 SNPs significantly associated with yield, including phenology-related traits and RUE and biomass at various growth stages, which explained 7–17% of phenotypic variation. Development of molecular markers for spike fertility and grain partitioning in wheat will facilitate the selection process in breeding programs. In the present study using the Breeders 35K Axiom® array, which contains 35,143 SNPs and phenotypic data from a KWS winter wheat panel which was collected over two field seasons under rain-fed conditions in the UK, a GWAS analysis was carried out to identify marker trait associations and associated molecular markers and candidate genes for grain partitioning traits.

Chapter hypotheses:

- Novel MTAs, including co-located MTAs, can be identified for HI, GN, FE and associated grain partitioning traits in a winter wheat panel using SNP markers.

- Candidate genes for HI, GN, FE and grain partitioning traits can be identified from SNP markers associated with MTAs.

5.2. Materials and methods

5.2.1 Plant Material and experimental design

The field experiments were carried out over two seasons (Y1 2017-18 and Y2 2018-19) in field trials using a randomised complete block design of three replicates in each season. The field trial sites were located in Cambridgeshire UK, Y1 near Fowlmere, Cambridgeshire (52°05'18.0"N 0°03'49.6"E, and Y2 near Newton, Cambridgeshire (52°07'40.9"N 0°06'18.2"E). An association panel of high biomass UK winter wheat varieties and advanced lines, comprising 138 doubled- haploid genotypes (137 used for genetic analysis) was used (see Chapter 4 for details).

5.2.2 Crop measurements

Full field methods for the crop measurements can be found in the materials and methods section of Chapter 4. In brief, samples were collected at anthesis (GS65) and at physiological maturity (GS87-90). Anthesis samples comprised 12 fertile shoots cut a ground level, of which the dry weights of lamina, leaf sheath, spike and true stem components were recorded separately. Stem-internode lengths were also recorded. Maturity samples (grab samples from two 30 cm row lengths) were separated into spikes and straw (lamina, true stem, and leaf sheath), and the dry weight of the components was recorded after drying for 48 h at 70 °C prior to threshing of the ears. After threshing, grain number using a seed counter and grain weight after drying for 48 h at 70 °C were recorded. Plot yield was determined by machine harvesting each plot. Spikes m⁻², grains m⁻², Harvest

index, above-ground biomass per m⁻² and fruiting efficiency were calculated from the collected data (see Chapter 4.2 for further details).

5.2.3 DNA extraction and genotyping

DNA extraction was performed on leaf samples by KWS UK Ltd. SNP markers were generated using the Affymetrix 35k Wheat breeders' array.

5.2.4 Marker-trait analysis

Adjusted means (BLUEs) for traits were obtained using META-R for both individual years (Y1 + Y2), and the cross- year mean. These were used as phenotype input for Genome Wide Association Study (GWAS) mapping analysis, both for individual years and combined years, using both a GLM and an MLM model to determine marker- trait associations. GWAS mapping was carried out using TASSEL (V5.2.75) (Bradbury *et al.*, 2007). 35,143 single nucleotide polymorphisms were anchored to the reference wheat genome sequence. Markers with low allele frequency (MAF) of 5% were removed resulting in 7794 SNP markers for analysis, of which 2449 were genome A, 2889 genome B, and 2455 genome D.

The first model applied was a General linear model using population structure derived from using 5 principal components as covariates. The second model applied was a mixed linear model, in which population structure derived from PCA, and a K matrix of familial relatedness were used as covariates. Principal component analysis was performed using TASSEL (v5.2.75).

Candidate gene analysis was accomplished using the bioscience gene discovery platform KnetMiner, which integrates known agronomic data and scientific literature information to generate links between traits and genes and gene networks (Hassani-Pak *et al.*, 2021). Potential candidate genes were identified by

using the most prominent marker trait associations found in the GWAS as input, using the location of the MTA on the genome as the midpoint, with the start and end positions 500,000BP before and after the positions marked as the start and end of the MTA.

5.3. Results

5.3.1 Distribution of significant markers

For the phenotypic data from the 2017-8 field experiment, marker-trait associations were detected on all chromosomes except 2A, 2B, 4A, 6B and 6D. For 2018-9, MTAs were detected for all chromosomes except 3B, 4B and 4D. For the combined means marker-trait associations were detected on all chromosomes except 1D, 3A, 4A and 7A. In 2018, most significant markers detected were on chromosome 1, whereas in 2019 the most were on chromosome 5 (Fig 5.1). For genomes, most associations were detected on genome B in 2018, and genome D in 2019 (Fig 5.1). Candidate genes will be investigated, taking into account the location of the marker-trait associations found for different models and across different years to advance understanding of the genetic basis of key physiological traits.

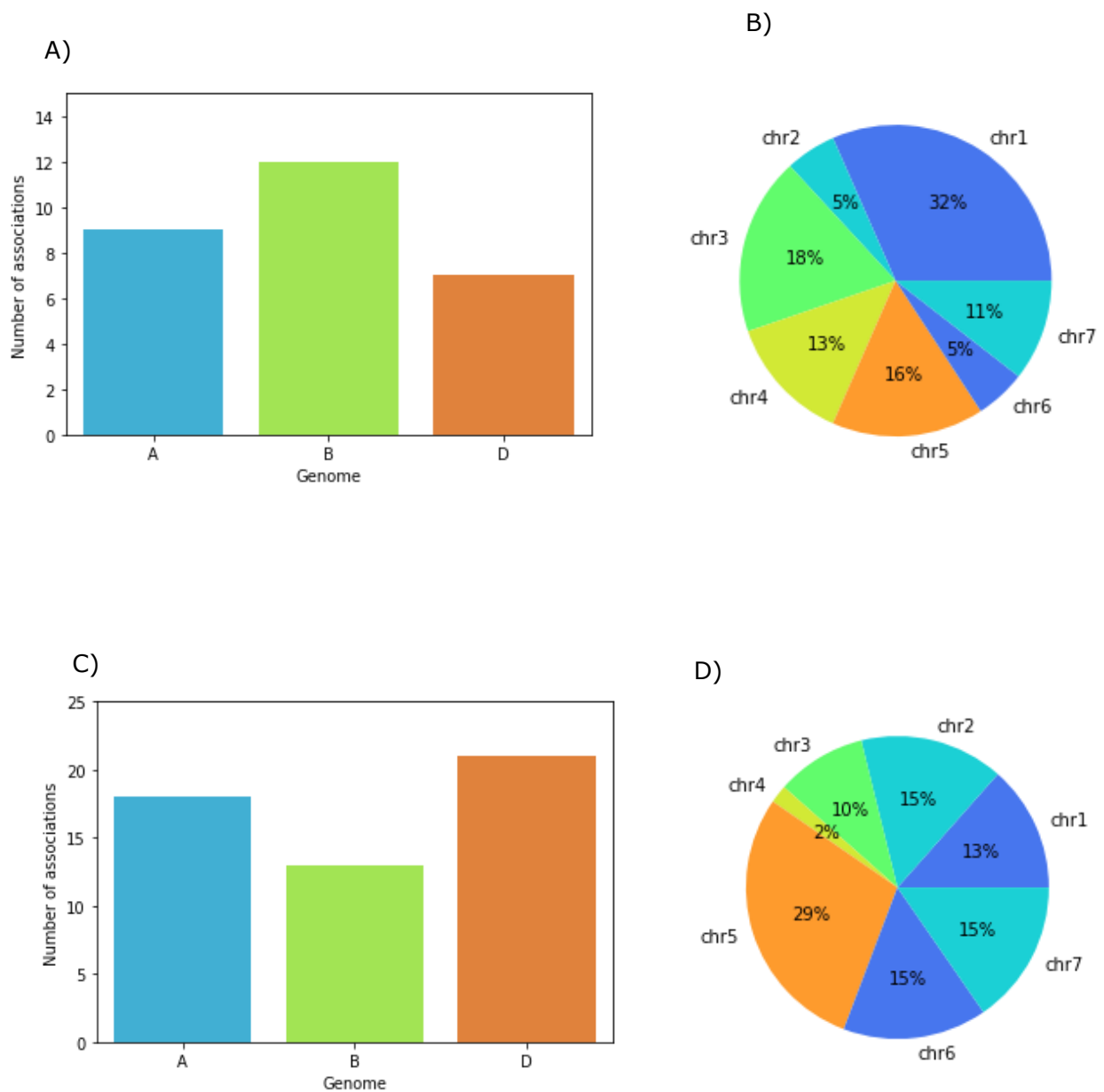


Fig 5.1. Distribution of significant marker- trait associations ($-\log_{10} < 3$) among 137 genotypes for the of the KWS winter wheat panel in 2017/18 by a A) genome and B) chromosome, and in 2018/19 field trial by c C) genome, and d D) chromosome.

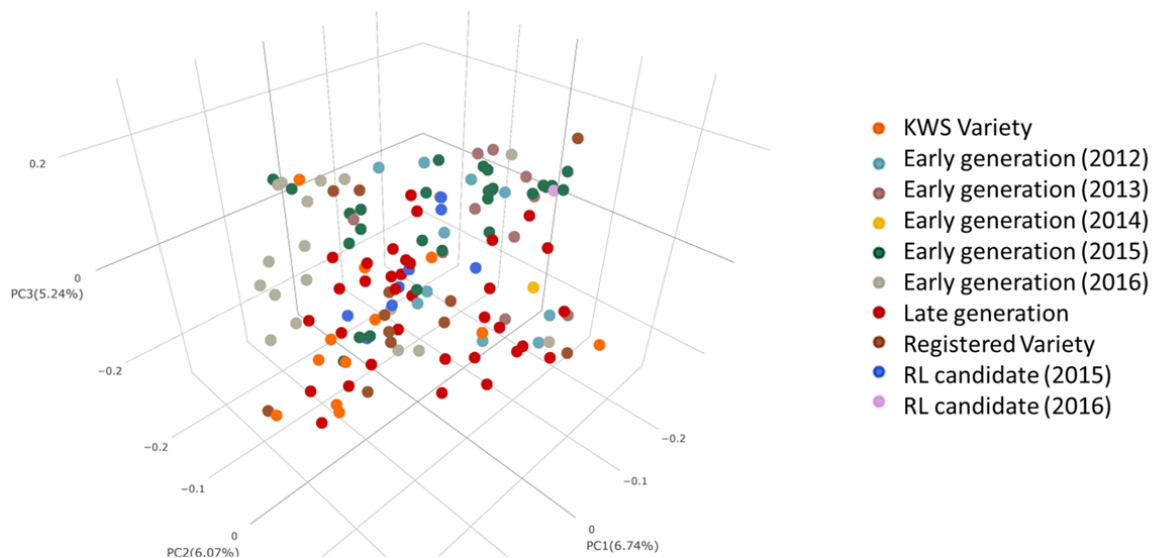


Fig. 5.2. Principal Component Analysis showing population structure of the KWS association panel.

5.3.2 Genome wide association analysis

Due to contrasting environmental conditions between years according to rainfall, as well as the complex nature of the traits being analysed, GWAS was carried out using both the BLUEs (Best linear unbiased estimates) for individual years as well as the mean across years. Association analysis was carried out on the BLUE means from the 144 total genotypes (137 genotypes in 2018 and 138 genotypes in 2019; 132 common genotypes in both seasons) used in the trial across two field seasons (2018+2019) with 7794 filtered SNP's. Results showed several MTA's with a $-\log_{10} P$ value of 3 or greater ($P < 0.001$). The number of associations detected varied significantly between models and years (Table 5.1).

Table 5.1 Summary of GWAS results obtained using a threshold of $-\log_{10} P < 3$ for two different models using both individual year means and combined means. GLM: General linear model; MLM: Mixed linear Model; PC: Principal component; K: kinship matrix; Ave: Average.

Model + Year	#	Ave marker R^2	Average ($-\log_{10} P$)
	Significant MTA's	(% phenotypic variance)	
GLM + PC5 2018	167	N/A	3.44
GLM + PC5 2019	125	N/A	3.84
GLM + PC5 combined	537	N/A	3.711
MLM PC5+K 2018	26	21.15%	4.151
MLM PC5+K 2019	52	16%	3.33
MLM PC5+K combined	50	11.90%	3.275

Both the general linear and the mixed linear models considered population structure as a covariate by utilising a PCA of the SNP data. The general linear model showed a significantly higher number of associations for each year but this was likely to include a higher number of false positive observations compared to the more stringent mixed linear model, which includes a kinship matrix. For the mixed linear model, the number of associations was lower for the 2017-8 phenotype data than the 2018-9 data, but the average marker R^2 , quantifying the percentage of phenotype variation for the trait explained by an individual marker, was much higher.

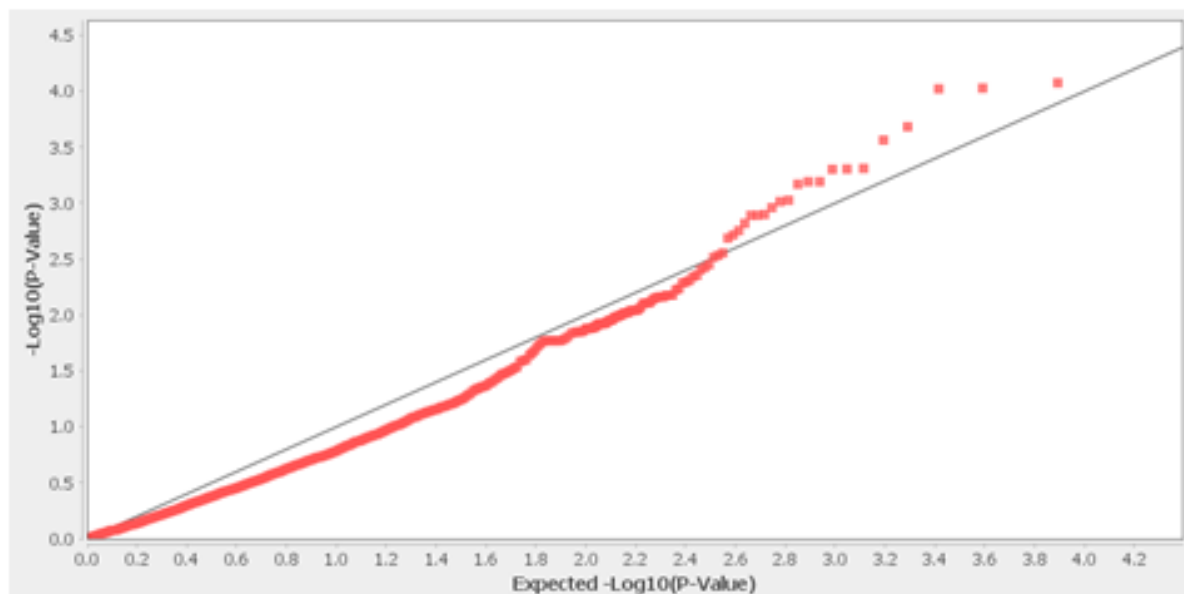
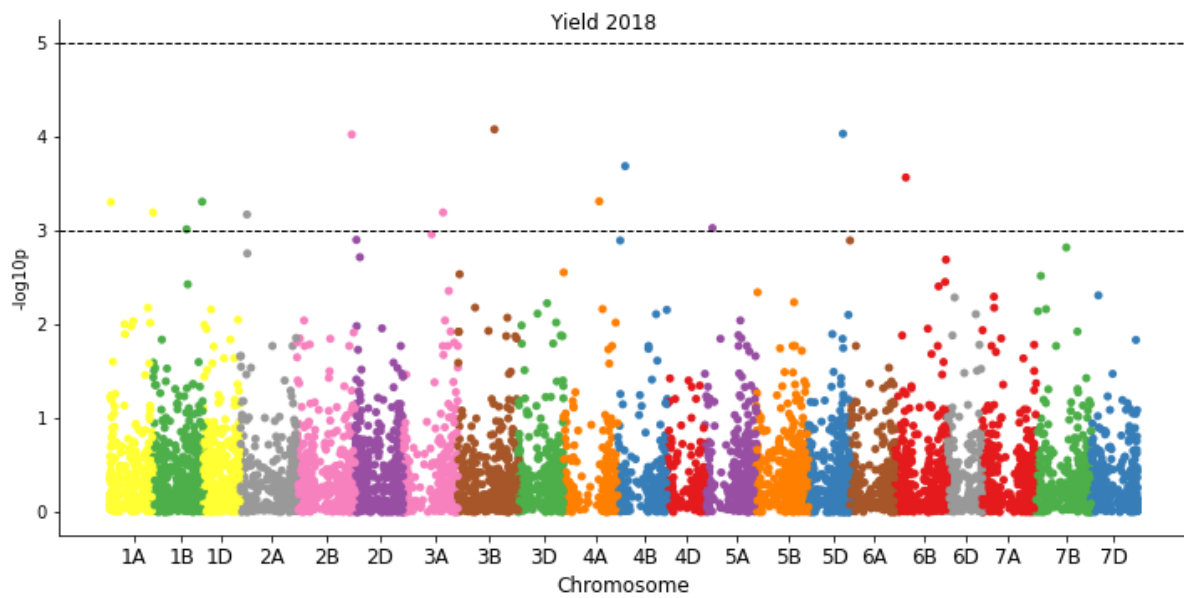


Fig 5.3 A) Manhattan plot for GWAS on the trait Grain Yield (g m^{-2}) in 2018 with $-\log_{10} p$ thresholds of 3, and 5 plotted against chromosome position and B) QQ plot with $-\log_{10}$ transformed p-values using the mixed linear model

For grain yield in 2018 using the MLM model, 11 associations were detected above the lower significance threshold (Fig 5.3A). The QQ plot values for yield in this year slightly exceeded, but were overall quite close to the expected $-\log_{10}$ p values (Fig. 5.3B). For other traits analysed using this year+ model values were slightly lower than the expected $-\log_{10}$ p values. Overall the fixed linear model showed a good fit for the data analysed.

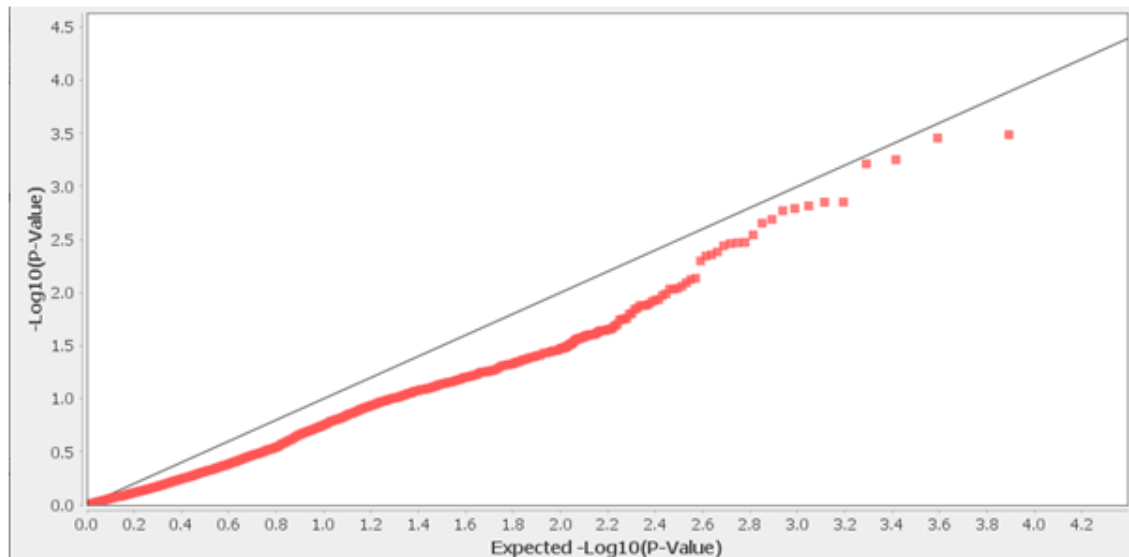
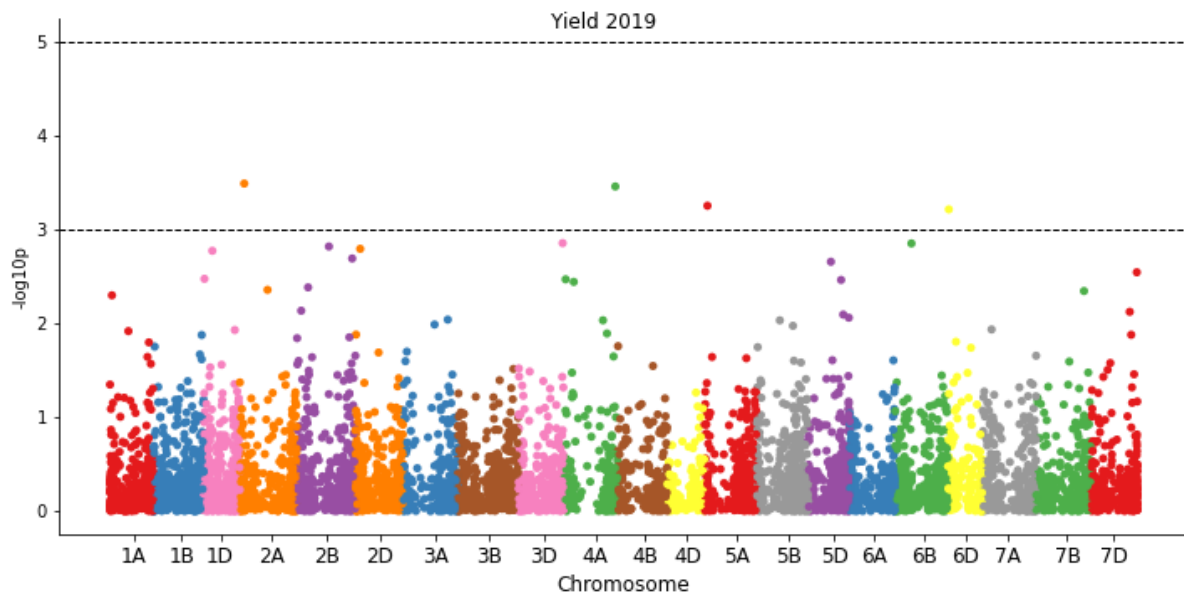


Fig 5.4. A) Manhattan plot for GWAS on the trait Grain Yield (g m^{-2}) in 2019 with $-\log_{10} p$ thresholds of 3, and 5 plotted against chromosome position and B) QQ plot with $-\log_{10}$ transformed p-values using the mixed linear model.

Contrasting with the 2018 MLM analysis, only 4 significant associations for grain yield were found for the mixed linear model using the 2019 phenotype data (Fig. 5.4A). The QQ plot showed values that were consistently lower than the expected values (Fig. 5.4B). This was consistent across other traits analysed for 2019 phenotype data using this model, with the exception of lamina partitioning index and leaf- sheath partitioning index, which matched more closely with expected values.

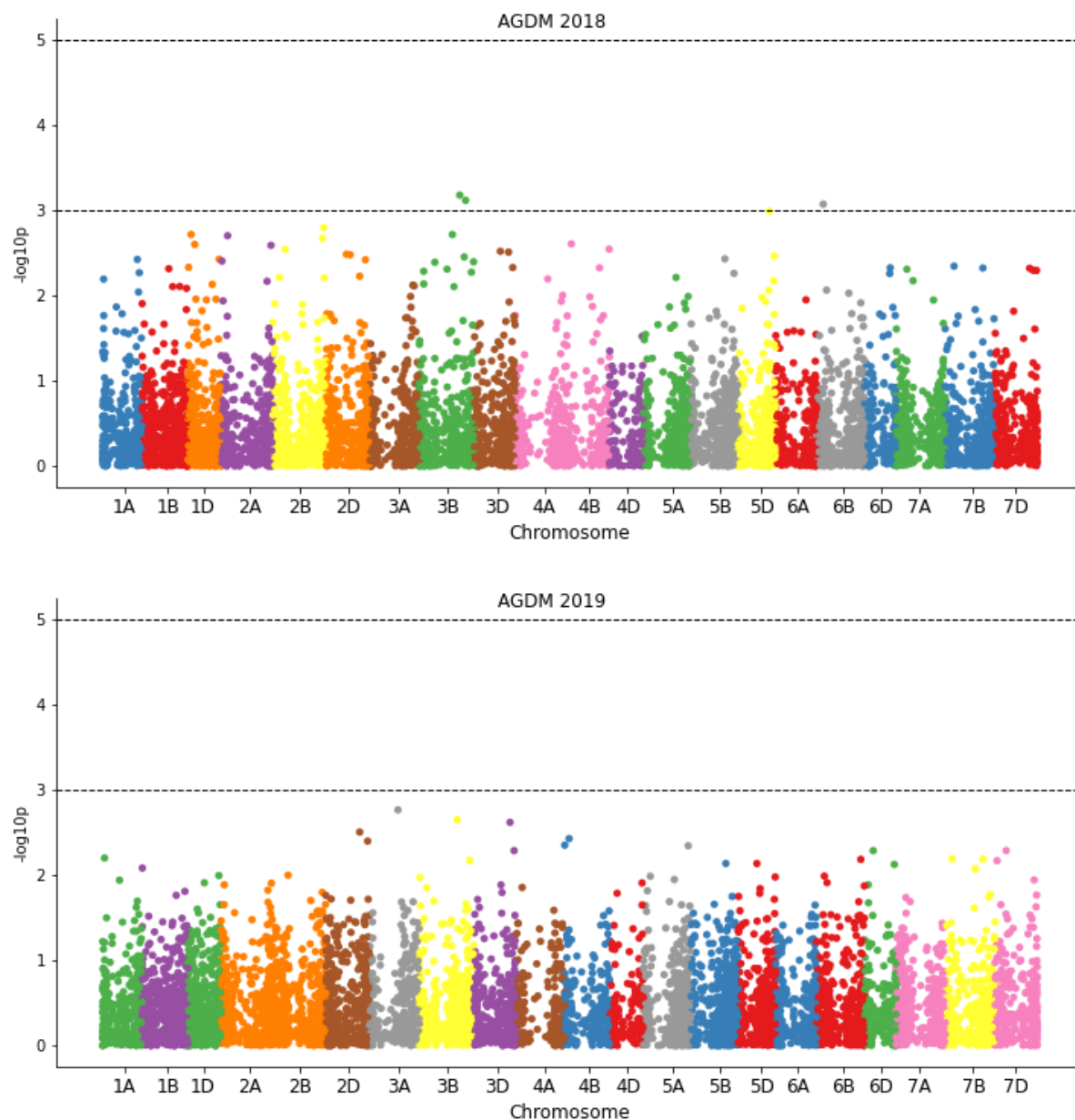


Fig. 5.5 Manhattan plot of GWAS MTAs for the above-ground DM (g m^{-2}) (AGDM) with $-\log_{10} p$ thresholds of 3, and 5 plotted against chromosome position and for 2017/18 and 2018/19.

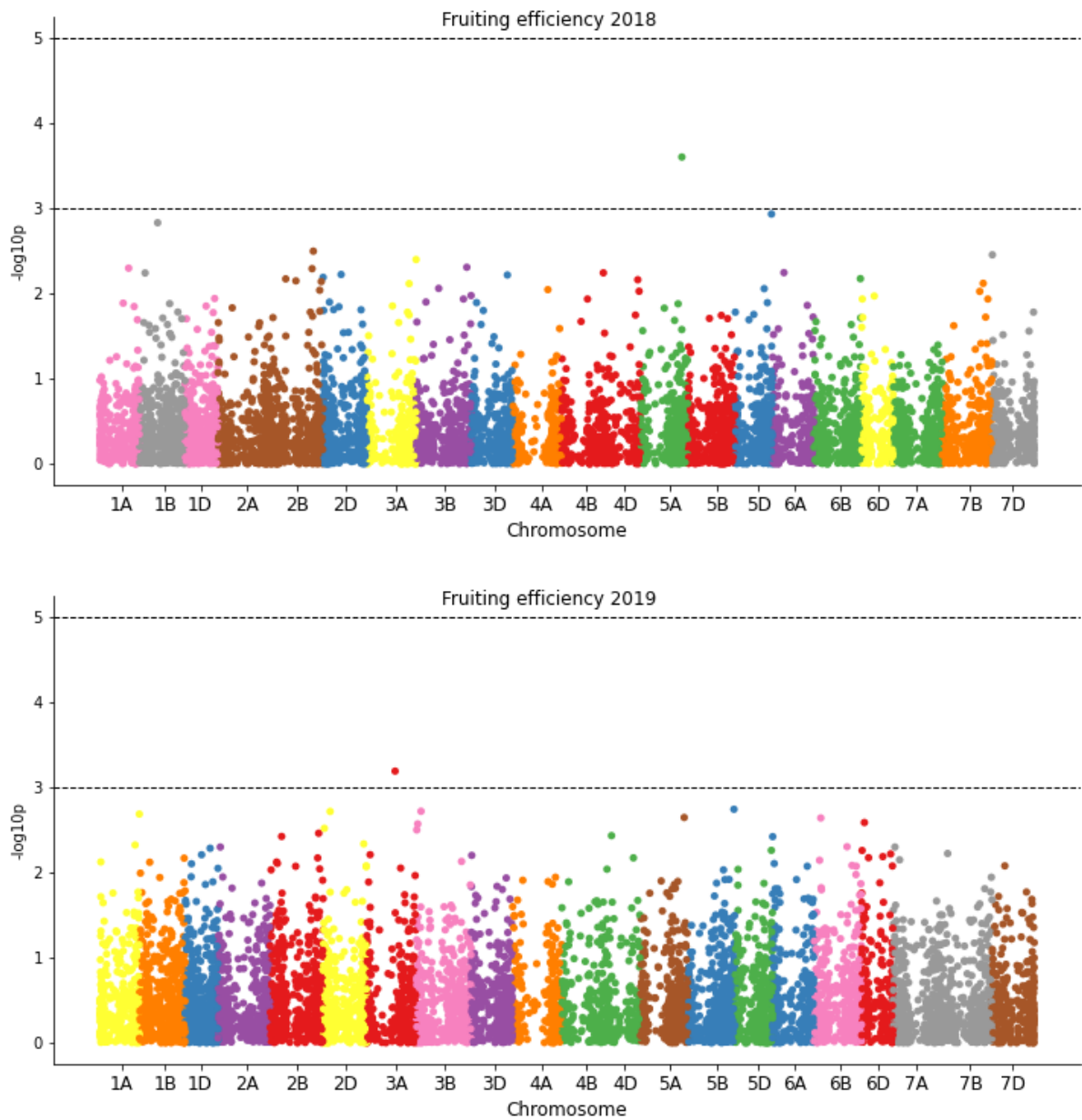


Fig. 5.6 Manhattan plot of GWAS marker trait associations for Fruiting efficiency with $-\log_{10} p$ thresholds of 3, and 5 plotted against chromosome position for 2017/18 and 2018/19.

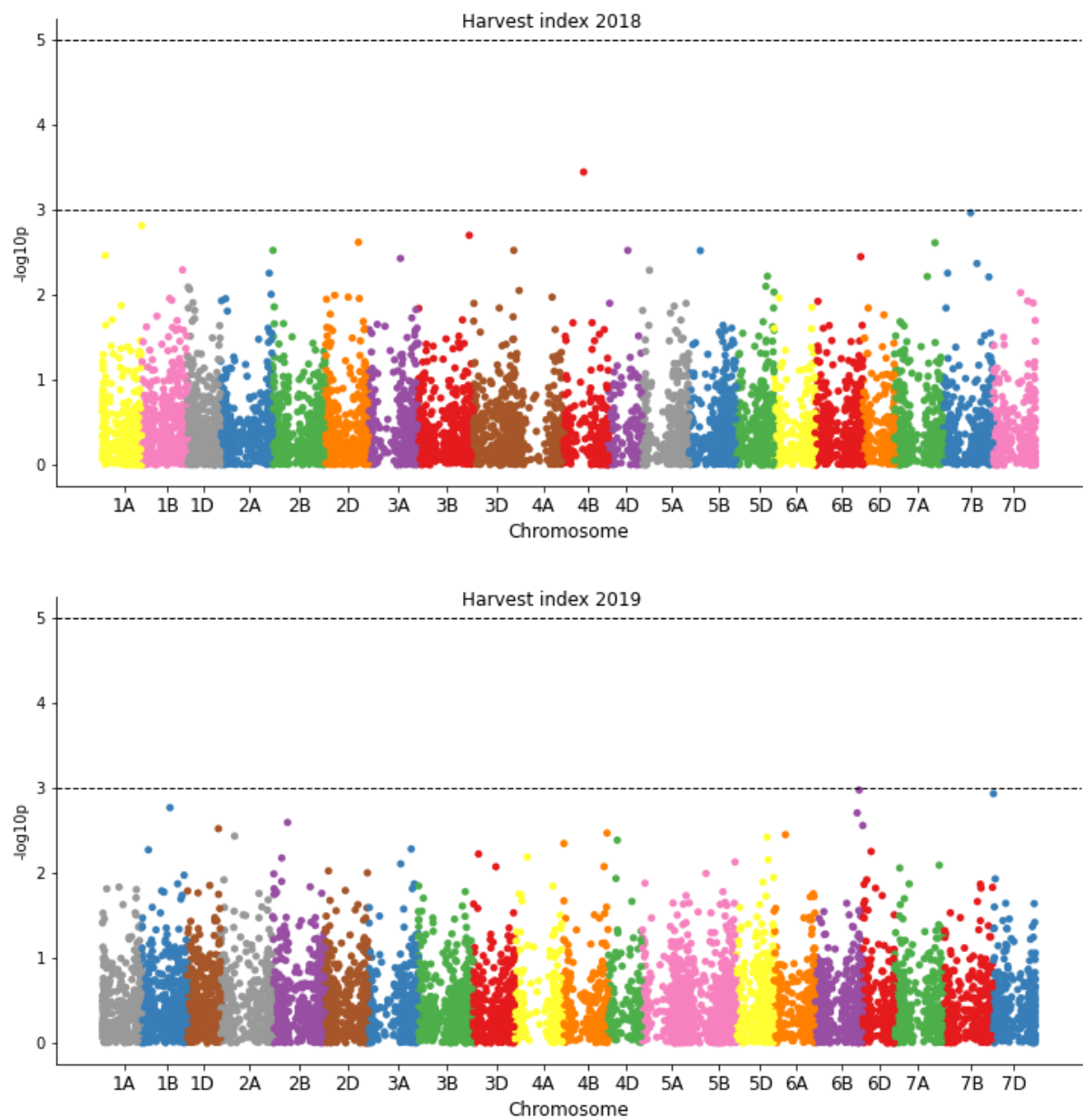


Fig. 5.7 Manhattan plot of GWAS marker trait associations for Harvest Index for 2017/18 with $-\log_{10} p$ thresholds of 3, and 5 plotted against chromosome position for 2017/18 and 2018/19.

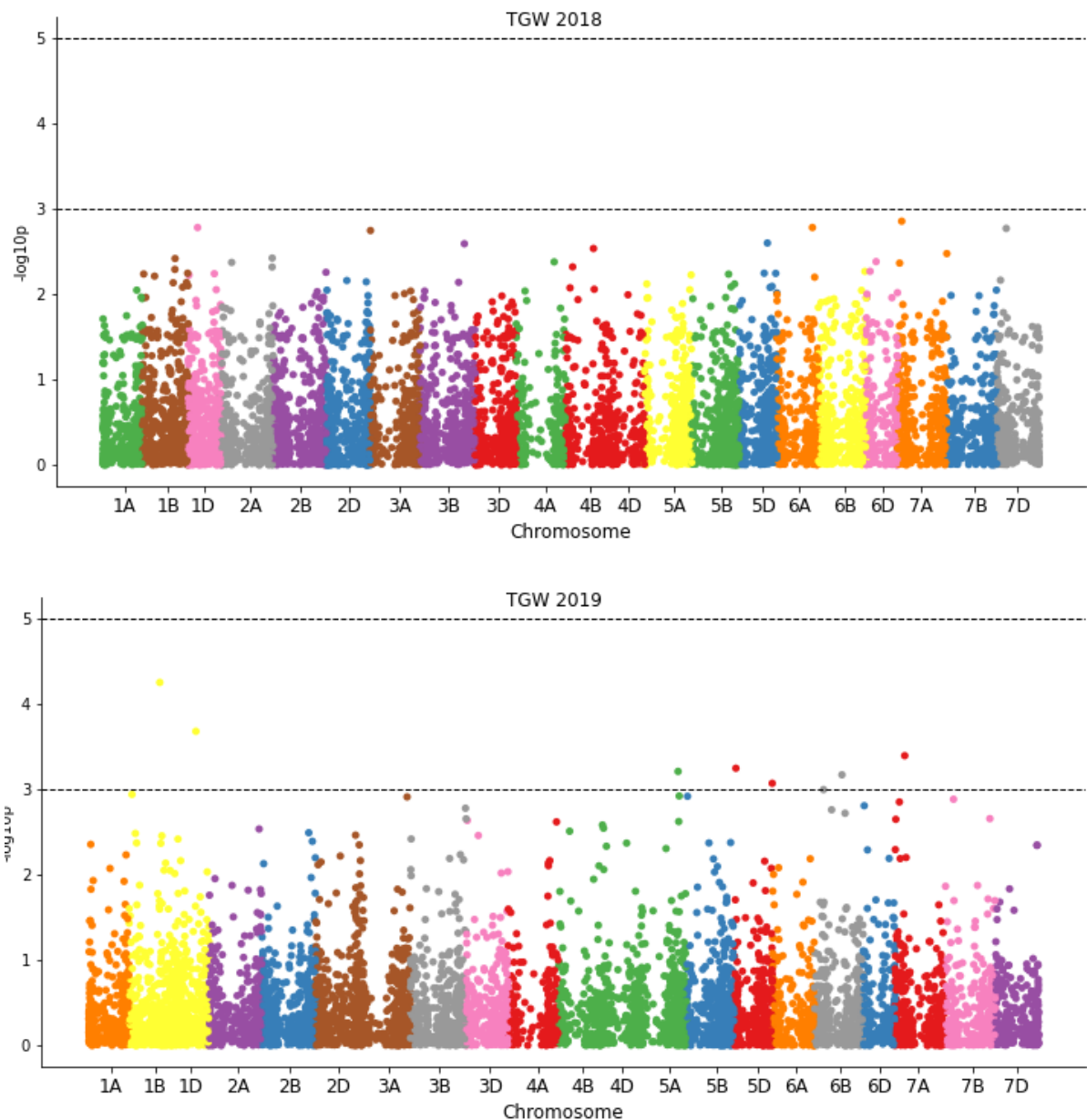


Fig. 5.8 Manhattan plot of GWAS marker trait associations for Thousand grain weight (g) with $-\log_{10} p$ thresholds of 3, and 5 plotted against chromosome position for 2018/18 and 2018/19.

For other key yield related traits, several MTA's were discovered across both years. The above -ground biomass shows a clear peak on chromosome 3B, where it has two associations above the significance threshold, of three total. However, in 2019 there were no MTA's detected for this trait (Fig 5.5). There was one marker trait association per year for fruiting efficiency, on chromosome 5A and 3A for 2018

and 2019 respectively (Fig. 5.6). For harvest index, 1 association is detected in 2018 on chromosome 4B above the significance threshold (Fig 5.7a). For harvest index in 2019 no associations are detected above the threshold, however there is one marker-trait association which is near the threshold ($-\log_{10} P = 2.97$) and is at the tip of a visible peak on chromosome 6B (Fig 5.7b) which may be worth investigation. No significant MTAs were detected for thousand grain weight in 2018 (Fig 5.8a) compared to 7 in 2019 (Fig. 5.8b).

Table 5.2. Summary of MTA's obtained from the GWAS on the KWS winter wheat association panel, by trait, year and location at chromosome and genome level. * indicates the marker co-located for multiple traits within a year. + indicates the marker was co-located for combined means and individual year means.

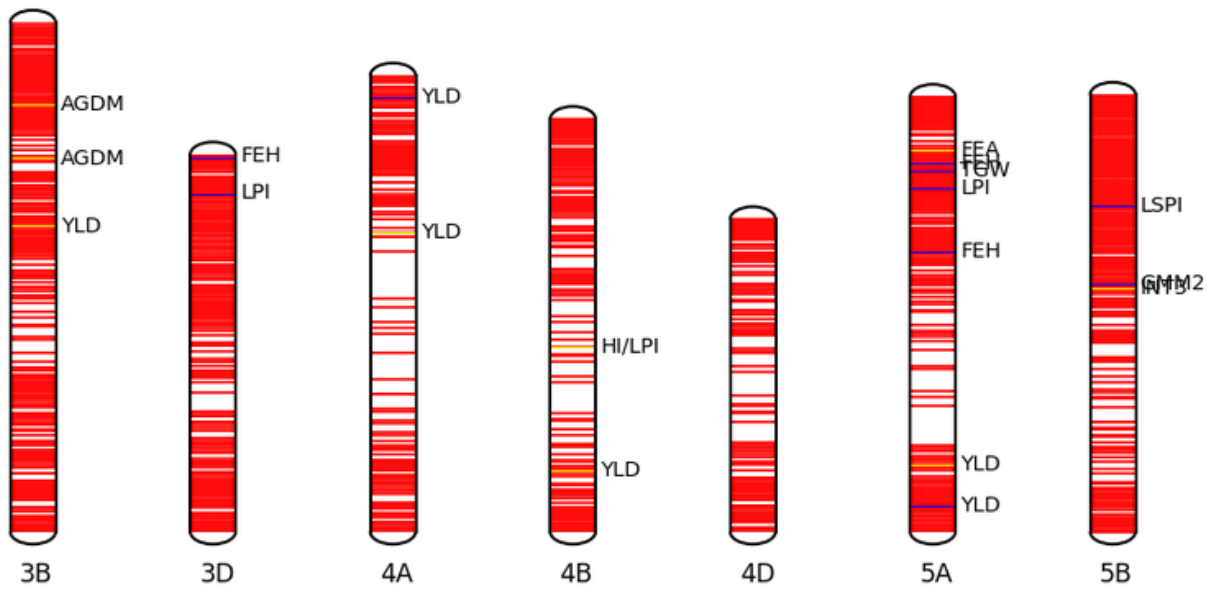
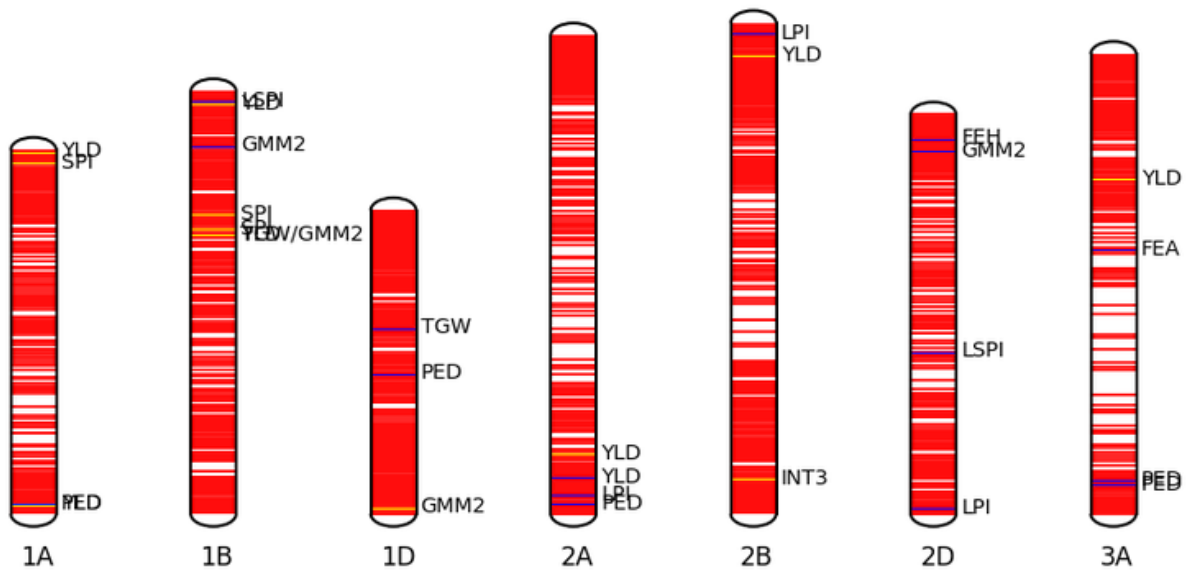
Trait	Year	Total MTA	Multitrait	Location	Average of markerR ² (Proportion phenotypic variance)
AGDM	2018	3		3B, 3B, 6B	0.205
	2019	0			
FEA	2018	1		5A	0.189
	2019	1		3A	0.101
FEH	2018	0			
	2019	11		3D, 7A, 7D, 7B,5D+ 2D, 5A, 5A, 5D, 7A	0.0998
GMM2	2018	2		6A, 1D	0.130
	2019	6	1	1B*, 1B+, 2D, 5B,5D, 6D+	0.138
HI	2018	1	1	4B*	0.160
	2019	0			
INT2	2018	0			
	2019	1		5D	0.101
INT3	2018	2		2B, 5B	0.130
	2019	0			
LPI	2018	1	1	4B*	

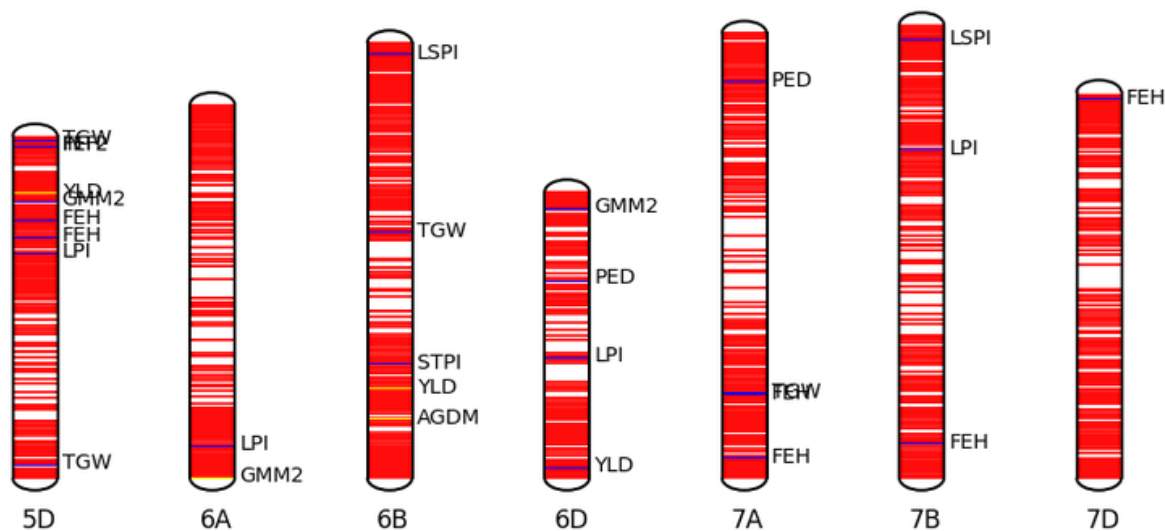
	2019	9		5A, 7B, 5D, 2B, 3D, 2A+, 2D, 6A, 6D	0.140
LSPI	2018	0			
	2019	5		2D+, 7B, 1B, 6B, 5B	0.128
PED	2018	0			
	2019	7		3A, 6D, 1A, 7A, 2A, 3A,1D	0.127
SPI	2018	3		1A+, 1B, 1B	0.150
	2019	0			
STPI	2018	0			
	2019	1		6B+	0.094
TGW	2018	0			
	2019	7	1	1B*, 1D, 7A, 5D, 5A, 6B+, 5D,	0.135
YLD	2018	13		3B, 5D, 2B, 4B, 6B, 4A, 1B, 1A, 1A, 3A, 2A, 5A, 1B	0.275
	2019	4		2A, 4A, 5A+, 6D	0.128075

AGDM above-ground dry matter ($g\ m^{-2}$); FEA fruiting efficiency (based on spike DM at GS65); FEH fruiting efficiency (based on chaff DM at maturity); GMM2 grains m^{-2} ; HI harvest index; INT2 stem-internode 2 length; INT3 stem-internode 3 length; LPI lamina partitioning index at GS65; LSPI leaf-sheath partitioning index at GS65; PEDPI peduncle partitioning index at GS65; SPI spike partitioning index at GS65; STPI stem partitioning index at GS65; TGW thousand grain weight; GLD grain yield ($g\ m^{-2}$)

Using the mixed linear model for both individual years, at least one significant marker-trait association was identified for each trait at anthesis and harvest. However, not every trait had a significant ($-\log_{10} p < 3$) association in both years. Using the Mixed linear model, a total of 26 significant associations were identified for 2018 data, of which one was co-located for multiple traits. Co-locating markers were primarily associated with grain yield, harvest index and above-ground dry matter m^{-2} . For 2019, a total of 52 significant marker-trait associations were detected, of which just one MTA was co-located, between grains m^{-2} and thousand grain weight on chromosome 1B. For the anthesis traits of partitioning indices and stem-internode lengths at anthesis and fruiting efficiency there were a total of 40 MTAs across both years. For harvest-related traits there were a total of 46 MTAs across both years. There were no markers that co-located between years. However, there were 9 marker-trait associations for individual years that were also present in association with combined phenotype BLUE means across years. Eight of these were for the 2019 analysis, and only one for 2018 (Table 5.2).

Fig. 5.9 Phenogram of MTA locations by chromosome and genome for the field trials of the KWS association panel. 2018 results are shown as blue lines, 2019 results as yellow n lines.





5.3.3. Candidate gene analysis

Potential candidate genes for key trait marker associations investigated via Knetminer are presented below. Associations for 20 marker-trait associations across individual years are presented below (Table 5.3). For spike partitioning index, two marker-trait associations were detected on chromosome 1B. However, as they were located within 20,000 base pairs of each other, candidate gene analysis was performed for both markers together.

Table 5.3 List of potential candidate genes from marker trait associations obtained from GWAS with the KWS association panel using KnetMiner, separated by year for the two individual year GWAS performed. Combined mean candidate genes can be found in the appendix.

Trait	Chromosome	Year	Gene name/accession	Potential traits involved
Yield	3B	2018	OLE9	
			PRO3	Ethylene sensitivity
			LYK3	
			VP8	Chlorophyll content, leaf size, root mass density
Yield	2B	2018	BPM1	Seed size, water use efficiency, drought tolerance, heat tolerance, germination rate, chlorophyll content
			TRAESCS2B02G55280	Plant height, chlorophyll content
			0	
Yield	5D	2018	ORC5	Days to heading

			BHLH113	Plant Height
			TRAESCS5D02G40640 0	Grain length, grain size, Harvest index
Yield	3A	2018	GSTA1	Drought tolerance, oxidative stress resistance, salt tolerance
			TRAESCS3A02G30890 0	Grain density, Drought tolerance
			TRAESCS3A02G30950 0	Grain density
Fruiting efficiency (a)	5A	2018	BZIP25	seed maturation, drought recovery, drought tolerance, water use efficiency
			BX1	
			TRAESCS5A02G44050 0	Drought tolerance
Harvest index	4B	2018	PIPK1	Seed maturation, drought tolerance, stomatal opening

			NPSN12	disease resistance
Spike partitioning index	1A	2018	NFYB4	Spikelet fertility, seed maturation, plant height, grain weight, days to heading
			TRAESCS1A02G41210	
			0	
			TRAESCS1A02G41190	
			0	
Spike partitioning index	1B	2018	DGP3	Harvest index
Internode 3 length		2018	RUB1	Plant Height
Internode 3 length			CPT1	Stem elongation
Lamina partitioning index	4B	2018	PIPK1	Seed maturation, drought tolerance, stomatal opening
			NPSN12	disease resistance

Lamina partitioning index				
Grains per m-2	1D	2018	OGR1	
Grains per m-2			PP2A1	Seed size, drought tolerance
			TRAESCS1D02G02280 0	lateral root number, drought tolerance
Thousand Grain weight	1B	2019	ARIA	Seed size, days to flowering, drought tolerance
Thousand Grain weight			CLSY3	Seed size
Lamina partitioning index	5A	2019	TRAESCS5A02G35720 0	
Lamina partitioning index			PHT4;5	Disease resistance, grain size
			TRAESCS5A02G35770 0	stem elongation

Grains per m-2	2D	2019	TRAESCS2D02G49640 0	wheat stripe rust disease resistance
Grains per m-2			ABI5	
Grains per m-2	6D	2019	SG01	
Grains per m-2			TRAESCS6D02G34790 0	plant height, drought tolerance
			TRAESCS6D02G34770 0	
Thousand Grain weight	1D	2019	SHA	Seed longevity, seed weight, chlorophyll content
Thousand Grain weight			TRAESCS1D02G21630 0	
Yield	2A	2019	PRX112	Drought tolerance, lateral root number,
Yield			BIP5	
			TRAESCS2A02G10750 0	Drought tolerance, lateral root number,

Fruiting efficiency (harvest)	3D	2019	TRAESCS3D02G53980 0	Grain weight, grain number, plant height,
Fruiting efficiency (harvest)			TRAESCS3D02G53850 0	Grain weight, grain number, grain length
			TRAESCS3D02G53760 0	Harvest index
Fruiting efficiency(a)	3A	2019	TRAESCS3A02G23090 0	
Fruiting efficiency(a)			ICME	
			TRAESCS3A02G23120 0	auxin sensitivity, stomatal opening, disease resistance
Thousand grain weight	7A	2019	GAUT9	Seed maturation
Thousand grain weight			NRP-B	leaf senescence
			GSTU10	

5.4 Discussion

5.4.1. Genetic and phenotypic variation in the KWS association panel

The KWS association panel was comprised mainly of elite cultivars and results presented in Chapter 4 confirmed that there was significant variation in grain partitioning traits, senescence traits, and flag-leaf fluorescence parameters. Grain yield in the KWS panel was strongly correlated with above-ground DM at physiological maturity which explained more of the genetic variation in grain yield than harvest index. However, no trade-off was found between above-ground DM at physiological maturity and harvest index suggesting that selecting for lines achieving both greater biomass and HI should be possible to increase grain yield (Foulkes *et al.*, 2011). Due to the association observed with fruiting efficiency another avenue to increase harvest index in high biomass backgrounds may be improving the fruiting efficiency (Slafer *et al.*, 2015).

Results in this panel showed that SPI and fruiting efficiency were associated with greater PSII activity during booting, and FE was positively associated with grain yield, harvest index and grain number per m² (see Chapter 4 for detailed discussion of the physiological determinants of SPI and FE). In summary, the association between FE and grains per m² could be related to more assimilates being available to the spike during the booting to anthesis period, enhancing floret survival and grains per spike (González, Miralles and Slafer, 2011). Harvest index was correlated with stem-internode 2 partitioning index; and spike partitioning index was negatively associated with stem-internode 3 partitioning index. It could be the case that stem internodes 2 and 3 compete more strongly with the spike for assimilate during the rapid spike growth phase from booting to anthesis than other internodes. Therefore, it is important to identify marker-trait associations for

grain partitioning traits, specifically stem-internode 2 and 3 length, and FE to enhance yield potential through increased grain number, harvest index and grain yield.

5.4.2. Marker-trait associations

Genetic studies in wheat reporting on grain partitioning traits are limited, mainly using next-generation sequencing data. In the current study the use of combined seasonal data for analysis was made difficult due to the high level of disparity in environmental conditions between years. As a result, the GWAS analysis was conducted on individual years, with MTA's being considered equally from either year. Associations for key traits were located primarily on chromosomes 3B, 4B, 1B, 6B and 5A, explaining between 9 and 21% of phenotypic variation. After examining individual years for marker-trait associations, no associations were found that were present in both years. Rainfall and temperatures between the two years were highly contrasting. In 2018, total rainfall between Anthesis and maturity was 0.3mm, compared to 90.5mm in 2019 (fig 4.1). The presence of drought in the 2018 study was reflected in the candidate gene analysis, where 9 of the potential genes have been previously associated with drought tolerance, compared to 3 for 2019. Under water limiting conditions, the analysis may be more likely to highlight drought tolerance over yield potential. In the KWS association panel field trials, thousand grain weight was significantly higher in the 2019 trial, compared to the 2018 trial which experienced drought stress during the grain filling period, and was the main trait responsible for the difference in yield between years. No markers were detected for thousand grain weight in the 2018 study, despite genetic variation being observed, possibly due to variance in grain weight being a result of multiple different stress tolerance mechanisms and yield potential. Previous GWAS work comparing grain yield traits under different

heat and drought stress conditions has shown some markers co-locating between optimal conditions and stress treatments, in contrast to the present study, using a panel of CIMMYT spring wheat lines for heat and drought nurseries in South Asia (Qaseem et al., 2019). Further work to elucidate differences in stress tolerance index and related traits such as stem WSC content, within the KWS association panel of UK winter wheat, as well as identify mechanisms of stress tolerance contributing to yield would be necessary to fully explore the difference in GWAS results between years.

In the present study with the use of the general linear model, a higher number of MTAs were obtained compared to the model in which the population structure was considered. More precise MTAs were scored using a mixed linear model (MLM) where different variables were tested to see how the interaction between the relatedness and different levels of population structure affect the detection of marker-phenotype association. Similarly, Bordes et al. (2014) for two doubled-haploid populations population reported 194 MTAs associated with grain yield and 134 for heading data, where MLM improved the power of the study. Liu et al. (2015) using 322 *Ae. tauschii* accessions reported 12,444 significant markers for phosphorus-deficiency-tolerance traits detected by the GLM and 28 by MLM from which just 18 were detected by both methods (threshold: $-\log_{10}(p) = 3.84$).

Analysis on the KWS association panel was able to detect genetic associations for key grain partitioning traits located primarily on chromosomes 3B, 4B, 1B, 6B and 5A, explaining between 9 and 21% of phenotypic variation. In the present study co-located MTAs were identified on chromosome 1B for grain number m^{-2} and thousand grain weight in 2019, and chromosome 4B for harvest index.

For harvest index a single MTA was discovered, for 2018, on chromosome 4B at the 300 MB region located near the *PIP1K1* gene. *PIP1K1* encodes a putative phosphatidylinositol 4-phosphate 5-kinase. Activity of this gene has not previously been reported for wheat. However, (H. Ma et al., 2004) reported that *OsPIP1K1* in rice was associated with negative regulation of heading. They also observed a delay in leaf emergence and development in *OsPIP1K1* deficient mutants. The observed association for the same marker with lamina partitioning index may be related to this effect on leaf emergence. The gene has also been reported in a GWAS study of perennial ryegrass (*Lolium Perenne* L) by (Shinozuka et al., 2012) where it was observed located close to several known QTL's for overall plant size and leaf extension.

For grain yield, 5 marker-trait associations were observed on chromosomes 3A, 3B, 2B, and 5D in 2018 and chromosome 2A in 2019. Yield-related marker-trait associations for chromosome 3A are well reported in the literature and it is a chromosome with a high density of yield related associations (Bordes et al., 2014; EA Edae, 2014; Hoffstetter et al., 2016; Liakat Ali et al., 2011; Neumann et al., 2011; Ogonnaya et al., 2017; Pradhan et al., 2019) lending confidence to this MTA. Related marker-trait associations have also been previously observed on chromosome 3B (Pinto et al., 2010; Sukumaran et al., 2015), 2A (Pradhan et al., 2019; S. X. Wang et al., 2017), and 5D (Pradhan et al., 2019; Qaseem et al., 2018). The study by (Pradhan et al., 2019) identified two potential genes involved with abiotic stress response on chromosome 3A. Similarly, the association detected in this study for chromosome 3A was located near *GSTA1* and *TRAESCS3A02G308900*, both of which were also associated with abiotic stress response. As this marker did not show up in the 2019 study, it could be related to the effect of stress response on yield in the drought-affected 2018 experiment. Of

genes nearby the MTA on chromosome 5D identified in this study, only one has been reported in the literature for wheat, *BHLH113*, which encodes a transcription factor affecting abiotic stress response (Shen et al., 2020). However, it is also located near a previously unreported gene with associations with grain length, size, and harvest index, *TRAESCS5D02G406400*, making it a prime candidate for further exploration. Yield-related MTA's have also been previously reported on chromosome 2A (Pradhan et al., 2019; S. X. Wang et al., 2017). The MTA for chromosome 2A is located close to two genes both associated with lateral root number and drought tolerance, *PRX112* and *BIP5*. Grain yield associations for the MTA on chromosome 2B have not previously been reported. Potential genes include *BPM1* due to its association with seed size, or *TRAESCS2B02G552800* due to its association with plant height.

For fruiting efficiency as measured by grain number per unit of spike dry matter at anthesis, marker-trait associations were detected on chromosome 5A in 2018, and 3A in 2019. For fruiting efficiency calculated using spike chaff weight, an MTA was detected on chromosome 3D in 2019 only. Literature exploring the genetic basis of fruiting efficiency is relatively sparse. However, associations have been reported on chromosome 5A (Basile, 2019; Gerard et al., 2020; Pretini et al., 2021) and chromosome 3 (Pretini et al., 2021). The well-known *GNI-A1* gene located on chromosome 2A is a HD-Zip1 transcription factor responsible for increased floret development (Sakuma et al., 2019) that has been previously linked to increased spikelet number and fruiting efficiency (J. Ma et al., 2019). It was not detected in this study for either individual year of physiological data. However, a significant marker-trait association for fruiting efficiency (chaff) was detected on chromosome 2A for analysis performed on combined means. *GNI1* is a reduced function variant that increases floret and grain number, compared to

the WT allele which serves to depress it. If the mutant allele of the gene is present in UK populations, it should be explored further as a potential candidate gene. No marker-trait associations have previously been reported for the MTA on chromosome 3D, which was located nearby two unreported genes associated with grain number *TRAESCS3D02G539800* and *TRAESCS3D02G538500*. Both of these warrant investigation as potential candidate genes for fruiting efficiency.

For thousand grain weight, 7 marker-trait associations were detected in this study, all in 2019, on chromosomes 1B, 1D, 5A, 6B, 7A and two on 5B. MTA's have been previously reported for TGW on chromosome 1B (Ma et al., 2018; Sukumaran, Lopes, et al., 2018), 5A S (F. Ma et al., 2018; Qaseem et al., 2018; Sukumaran et al., 2015), (Sukumaran et al., 2015, 2018; Sun et al., 2017) and 7A (F. Ma et al., 2018; Qaseem et al., 2018; Sun et al., 2017; Wang et al., 2017).

For spike partitioning index three marker-trait associations were identified in the 2018, one on chromosome 1A and two on chromosome 1B. The MTA on chromosome 1A was located near the *NFYB4* gene, associated with increased spikelet fertility. This gene has not previously been studied in wheat populations; an analogue, however, has been reported as highly expressed in maize ears (Liu et al., 2021) encoding a Squamosa-promoter binding protein transcription factor. This family of proteins has been linked to a number of plant developmental processes in other crop species and model plants, including ear development (Preston & Hileman, 2013). The two associations located on chromosome 1B were situated very close together, and the same gene is likely responsible for both markers. The most likely candidate gene is *NPF5.10*, belonging to a family of nitrate transporters and associated with increased seed size as well as nitrate

uptake. The NPF family of genes is responsible for nitrate uptake, remobilisation, and transport. Improvements to overall crop NUE have been linked to increased grain yield in wheat (Slafer et al., 1990), and overexpression studies of NPF family orthologue genes have been shown to improve crop yield and NUE in rice (Fan et al., 2016; Hu et al., 2015; Y. Y. Wang et al., 2018). Additional nitrate availability to the spike may improve spike development, leading to greater sink strength and gains in yield.

In the present study co-located MTAs were identified on chromosome 1B for grain number m^{-2} and thousand grain weight in 2019, and chromosome 4B for harvest index. For Harvest index a single MTA was discovered, in 2018, on chromosome 4B at the 300 MB region, located near the *PIP1* gene. *PIP1* encodes a putative phosphatidylinositol 4-phosphate 5-kinase. Activity of this gene has not previously been reported for wheat. However, Ma et al. (2004) reported that *OsPIP1* in rice was associated with negative regulation of heading. They also observed a delay in leaf emergence and development in *OsPIP1* deficient mutants, possibly explaining the effect on HI.

In summary, novel MTA's were discovered for spike partitioning index, fruiting efficiency and grain yield. The identification of these new MTAs hopefully will be corroborated in further studies. The incorporation of these partitioning-based traits, such as fruiting efficiency, spike partitioning index and reduced stem-internode 3 length, into breeding programmes has significant scope to accelerate gains in harvest index and yield potential.

5.5 Supplementary material

5.5.1 Combined mean GWAS marker-trait associations

Trait	Marker	Chr	MarkerR2
FEH	AX-94481367	1A	0.11201
HI	AX-95255804	1A	0.12376
LPI	AX-95188181	1A	0.1151
FEH	AX-94479851	1B	0.11306
GMM2	AX-94733911	1B	0.11467
HI	AX-94598588	1B	0.14985
HI	AX-94495814	1B	0.11739
HI	AX-94941077	1B	0.12176
FEH	AX-94654446	2A	0.10806
HI	AX-94511927	2A	0.11202
LPI	AX-94381641	2A	0.12865
FEA	AX-94510910	2B	0.09353
INT2	AX-94476746	2B	0.11551
SPI	AX-95255851	2B	0.12074
AGDM	AX-94589256	2D	0.11
HI	AX-94399237	2D	0.13974
LPI	AX-94409188	2D	0.10172
LSPI	AX-94399340	2D	0.11366
SPI	AX-94960858	2D	0.1226
HI	AX-94528644	3B	0.11757
HI	AX-94591477	3B	0.11252
LSPI	AX-94646097	3B	0.11274
HI	AX-94583481	3D	0.1476
STPI	AX-94874313	3D	0.12097
FEH	AX-95098004	4B	0.11143
FEH	AX-95222901	4D	0.11518
AGDM	TRAESCS5A02G095900	5A	0.11607
HI	AX-94510137	5A	0.11797
YLD	AX-94984528	5A	0.11911

HI	AX-94402018	5B	0.12128
HI	AX-94807708	5B	0.12245
INT2	AX-94825562	5B	0.11828
FEH	AX-94929524	5D	0.08736
HI	AX-94924969	5D	0.15151
HI	AX-94923627	5D	0.13201
FEA	AX-95114964	6A	0.1149
HI	AX-94416604	6A	0.10508
HI	AX-94449689	6A	0.13133
TGW	AX-94556575	6A	0.11362
GMM2	AX-94832771	6B	0.14731
HI	AX-94492766	6B	0.13429
HI	AX-95162393	6B	0.12033
STPI	AX-95255344	6B	0.09487
AGDM	AX-94881375	6D	0.10748
LSPI	AX-94392519	6D	0.11899
HI	AX-94517269	7B	0.11536
AGDM	AX-94533907	7D	0.1135
HI	AX-94533907	7D	0.14648
LPI	AX-94638691	7D	0.11643
STPI	AX-94638691	7D	0.11825

Chapter 6. Source/Sink traits and association with HI and grain yield in a subset of a UK KWS winter wheat association panel in glasshouse experiments

6.1 Introduction

Grain yield increased during the green revolution through introgression of Rht semi-dwarfing genes that resulted in height reduction favouring assimilate partitioning to the spike during stem elongation and increasing spike growth and grain number (Hedden, 2003). Despite this major advancement in the 1960s and 1970s, we presently need to double wheat production by 2050 in novel ways for food security (Reynolds et al, 2021). Grain yield of modern cultivars is still limited by grain sink strength and grain number under favourable conditions (Rivera-Amado et al, 2020).

Recent studies in wheat show that genetic variation in fruiting efficiency (ratio of grain number to spike dry matter at anthesis, FE) is associated with grains m^{-2} (Garcia et al, 2014; Gonzalez et al, 2011). However, FE has not been actively selected for in breeding, and there are limited investigations which have quantified the genetic basis of FE. In order to deploy FE in breeding an understanding of its genetic basis is required to help breeders develop molecular markers for marker-assisted selection. Strategies to increase FE include increasing assimilate partitioning to the developing florets in the spike rather than the structural components (glumes, palea, lemma etc) (Ferrante et al, 2013). Some work has shown a trade-off between FE and SPI (Dreccer et al, 2009; Sierra-Gonzalez, 2020; Terrile et al, 2017), possibly because the plants are unable to allocate

enough resources from the rest of the spike to the florets, or that restricted vascular connections limiting assimilate supply (Bancal & Soltani, 2002). The interaction between FE and SPI is yet to be fully understood. There is also evidence that genetic variation in FE is influenced by levels of spike hormones, in particular, cytokinins (Love 2022, Jameson et al, 1982, Zheng 2016). Cytokinins (CKs) play a key role in the stimulation of cell division and nucleic acid metabolism. (Wang et al., 2001). One gene currently identified for CK degradation is CK oxidase/dehydrogenase (OsCKX2), found in QTL Gn1a in rice. When the expression of OsCKX2 is reduced, CK accumulates in the inflorescence meristems of rice (Ashikari et al, 2005). Increases to FE as a result of additional high spike cytokinin levels appear to be linked to increases in grain number, due to an increased number of fertile florets at anthesis. The study by (Zheng (2016), applied 6-benzylaminopurine (6-BA), a synthetic cytokinin as a foliar spray in winter wheat in China and reported a 77% decrease in abortion rate of basal, central, and apical spike florets compared to the control. Similarly, RNAi experiments suppressing cytokinin-oxidase dehydrogenases which degrade cytokinins in wheat reported increases in spike cytokinin levels and moderate increases in grain number per spike (Li et al., 2018, Jablonski et al., 2020).

Changes in spike morphology as a result of targeting increased FE may also affect source/sink dynamics of wheat. Although at present it appears that UK winter wheat is either sink limited or co-limited, previous work has shown that up to 30% of incident radiation is intercepted by the spike in wheat (Sanchez-Bragado et al., 2014), making spike photosynthesis a significant factor in future increases to yield potential. Spike photosynthesis has been shown to correlate with yield, thousand grain weight, and spike length in CIMMYT spring wheat varieties, as well as

showing high genetic variation within the panel (Molero and Reynolds 2020). By selecting for larger spikes, not only could pre-anthesis sink strength be improved, but there may also be gains to post-anthesis source.

If these novel targets determining FE are identified, then molecular markers can be found and used in marker-assisted selection to accelerate yield gains. Therefore, glasshouse experiments were carried out over two years to quantify genetic variation in fruiting efficiency and investigate whether leaf photosynthesis rate correlates with ear biomass and fruiting efficiency.

6.2 Materials and methods

6.2.1 Experimental design and growth conditions

Both the experiments in 2019 and 2021 consisted of 8 lines selected from the 30-line subset (Subset 1) of the KWS association panel. Selection of the initial subset of 25 was based upon variation in spike/stem partitioning index and spikelet number/ rachis length. The 8 lines selected for the glasshouse experiments were selected based on contrasting high and low values for fruiting efficiency in the field experiment in 2017/18. The plants in the experiment in 2021 were divided into 2 sampling groups, one for physiological maturity (GS91) one for anthesis (GS65). The plants in both experiments were grown in 2 L pots (1 plant per pot) using John Innes no 2 compost as soil medium. A single plant was transplanted per 2 L pot. Pots were arranged in a 10 x 8 configuration with border plants placed around the whole experiment. Pots were placed in contact with each other with no space between pots. Plants were drip irrigated automatically with complete nutrient solution to ensure optimal nutrition. Fungicide and pesticides were added

as necessary to minimise effects of pests and disease. The 2019 experiment was sown on "" and harvested on "". The experiment was sown on the 6th of Jan 2021 and harvested on 20th July 2021. After removal from vernalisation, plants were put on a 16-hour photoperiod at 21c. A randomised complete block design was used and there were three biological replicates for each sampling per genotype.

6.2.2 Crop measurements

Samples were collected at anthesis (GS65) and physiological maturity (GS91) in 2021. Growth stage was taken on the main shoot (MS) of each plant by assessment twice a week according to the Zadoks growth stages (Zadoks et al, 1974).

Growth analysis at anthesis

Plants were separated into MS, other fertile shoots, and infertile shoots. Each fertile shoot was then separated into spike, leaf lamina and stem (true stem and leaf sheath attached, MS separately). The lengths of the peduncle, internode 2 and internode 3 were recorded for the MS, as well as the plant height (measured from soil surface to tip of the spike, excluding awns). Each plant component was then dried for 48 hours at 70 °C. Dry weight of each component was then recorded, and partitioning index (PI) was calculated for the component as the proportion of above-ground biomass.

Growth analysis at physiological maturity

At physiological maturity, for all fertile shoots the spike was separated from the straw (stem and leaves), and DM of the straw and spike was recorded separately

after drying for 48 hours at 70 °C. The number of spikes were counted and then threshed by hand to obtain the DM weight of grains and chaff, and grain number. These data were then used to calculate harvest index (HI, proportion of above-ground DM in the grain), above-ground DM (AGDM_{PM}) and fruiting efficiency (FE, ratio of grain number to spike DM at anthesis or ratio of grain number to chaff DM at maturity).

Flag-leaf photosynthesis rate measurements

Flag-leaf photosynthesis rate measurements were taken at two assessment dates (26 April and 15 May) in the experiment in 2019. Photosynthesis rate was measured for each plant on the flag leaf of the main shoot using a LI-COR 6400 XT Portable Photosynthesis System (Li-Cor Biosciences, NE, USA) pre-anthesis and post-anthesis. Light-saturated photosynthetic rate (A_{max}) and stomatal conductance (g_s) were measured on the flag-leaf. One measurement per flag leaf in each of three replicates was taken between 10.00 and 14.00. The settings for the cuvette used a flow rate of 400 $\mu\text{mol s}^{-1}$, block temperature of 25°C, and light intensity of 1800 $\mu\text{mol m}^{-2} \text{s}^{-1}$ photosynthetically active radiation (PAR). Relative humidity (RH %) was set between 50 and 70% (aiming for 55%).

6.3 Results

6.3.1. Genetic variation in experiments

For the eight genotypes in the 2021 experiment, the genetic variation was not significant for spike biomass per MS, biomass per MS or MS per plant (Table 6.1).

There was genetic variation in stem-internode length 2 in the range 11.0 – 13.2 cm ($P < 0.05$) and a trend for variation in peduncle length in the range 17.2 – 32.0 cm ($P = 0.11$). For the yield and yield-related traits at physiological maturity, the genetic variation was not significant for the eight genotypes, although there was an apparent trend for differences for some of the harvest traits, e.g., grains per ear, HI, and grain weight per plant ($P < 0.15$; Table 6.2).

With regard to the flag-leaf gas exchange traits in the experiment in 2019, the flag-traits pre-anthesis did not show significant genetic variation. Post-anthesis, the eight genotypes ranged from 233.9 – 272.6 ppm for internal concentration of CO₂ ($P < 0.05$) and in transpiration efficiency from 1.69 – 4.10 mmol m⁻² s⁻¹.

Table 6.1. Biomass, dry matter partitioning and stem-internode lengths at anthesis for eight winter wheat genotypes in glasshouse experiment in 2021

	Average	Min	Max	F. Pr	S.E
	e				
Spike partitioning index	0.23	0.18	0.28	0.18	0.01
Peduncle length (cm)	27.09	17.20	32.00	0.11	0.83
Internode 2 length (cm)	13.20	11.00	18.10	0.04	0.43
Internode 3 length(cm)	9.63	4.90	13.10	0.16	0.47
Main shoot biomass g shoot ⁻¹	3.80	2.08	5.42	0.23	0.20
Fertile shoots plant ⁻¹	5.25	4.00	8.00	0.15	0.23
Aboveground biomass at anthesis g plant ⁻¹	15.21	8.97	22.21	0.22	0.72

Table 6.2. Grain yield per plant, biomass per plant, HI, and yield components for eight winter wheat genotypes in glasshouse experiment in 2021

	Average	Min	Max	F. Pr	S.E
	e				
Harvest index	0.36	0.28	0.46	0.14	0.01
Grain weight (g plant ⁻¹)	13.40	7.52	19.86	0.15	0.85
Thousand grain weight g	28.99	18.00	40.39	0.31	1.23
Grains plant ⁻¹	464.90	307.00	654.00	0.74	25.57
Fruiting efficiency grains g ⁻¹	96.81	65.50	143.00	0.85	4.30
Ears plant ⁻¹	8.25	4.00	11.00	0.60	0.29
Grains ear ⁻¹	56.29	40.20	73.62	0.13	2.31
Aboveground biomass g plant ⁻¹	36.33	23.90	51.90	0.35	1.64

Table 6.3. 2019 Glasshouse experiment in 2019. Flag-leaf photosynthesis rate (a_{max}), stomatal conductance, CO₂ internal conc (ppm) and transpiration rate for eight winter wheat genotypes

Date	Genotype	a_{max} (mmol m ⁻² s ⁻¹)	Stomatal conductance (mol m ⁻² s ⁻¹)	CO ₂ internal concentration (ppm)	Transpiration rate (mmol m ⁻² s ⁻¹)

April 26	ST13_24200	37.76	0.45	235.94	5.96
Pre-anthesis	Santiago	45.63	0.53	235.11	6.82
	St13_24090	28.89	0.45	272.59	5.70
	TC16_128	38.35	0.45	243.67	5.92
	TC16_417	50.63	0.55	223.88	7.26
	TC16_97	43.01	0.46	223.76	6.23
	W309	41.22	0.45	231.31	6.37
	Zyatt	44.07	0.50	229.42	6.38
May 16	ST13_24200	12.45	0.13	208.10	4.03
Post-anthesis	Santiago	20.39	0.24	239.24	2.86
	St13_24090	15.40	0.14	179.00	4.10
	TC16_128	17.38	0.20	239.21	2.15
	TC16_417	18.49	0.21	231.58	1.69
	TC16_97	21.25	0.25	244.22	2.11
	W309	17.18	0.18	204.03	2.19
	Zyatt	20.15	0.23	218.29	3.40

Table 6.4. Genetic range, average and significance for flag-leaf gas exchange traits data for the 2019 glasshouse experiment

	Min	Max	Mean	F.Pr	S.E
a_{\max} (mmol m ⁻² s ⁻¹)	28.89	44.07	41.6	0.63	2.2
			9		2

Pre- Anthesis	Stomatal cond. (mol m ⁻² s ⁻¹)	0.45	0.55	0.48	0.47	0.0
	CO ₂ internal conc. (ppm)	223.8	272.8	237.	0.67	5.7
	Transpiration rate (mmol m ⁻² s ⁻¹)	5.92	7.26	6.38	0.64	0.1
	a _{max} (mmol m ⁻² s ⁻¹)	12.45	21.25	17.8	0.65	1.0
Post- Anthesis	Stomatal cond. (mol m ⁻² s ⁻¹)	0.13	0.25	0.19	0.58	0.0
	CO ₂ internal conc. (ppm)	179.0	239.2	220.	0.02	5.7
	Transpiration rate (mmol m ⁻² s ⁻¹)	1.69	4.10	2.82	0.04	0.2

6.3.2 Correlation between genetic variation in traits in glasshouse experiments and traits in field experiments.

Six genotypes were common in the field and glasshouse experiments. The correlation amongst genotypes between the pre-anthesis flag-leaf gas-exchange traits in the glasshouse and the field physiology traits is shown in Fig. 6.1. The corresponding correlations for the post-anthesis gas-exchange traits with field

physiology traits are showing in Fig. 6.2. In summary, significant correlation between pre-anthesis gas-exchange traits and grain yield and yield components in the field experiments were not observed. However, for post-anthesis flag-leaf traits there was a trend for a positive association between flag-leaf transpiration rate and 1,000 grain weight ($r = 0.31$) and trend for negative association with grains m^{-2} ($r = -0.37$) and fruiting efficiency ($r = -0.36$).

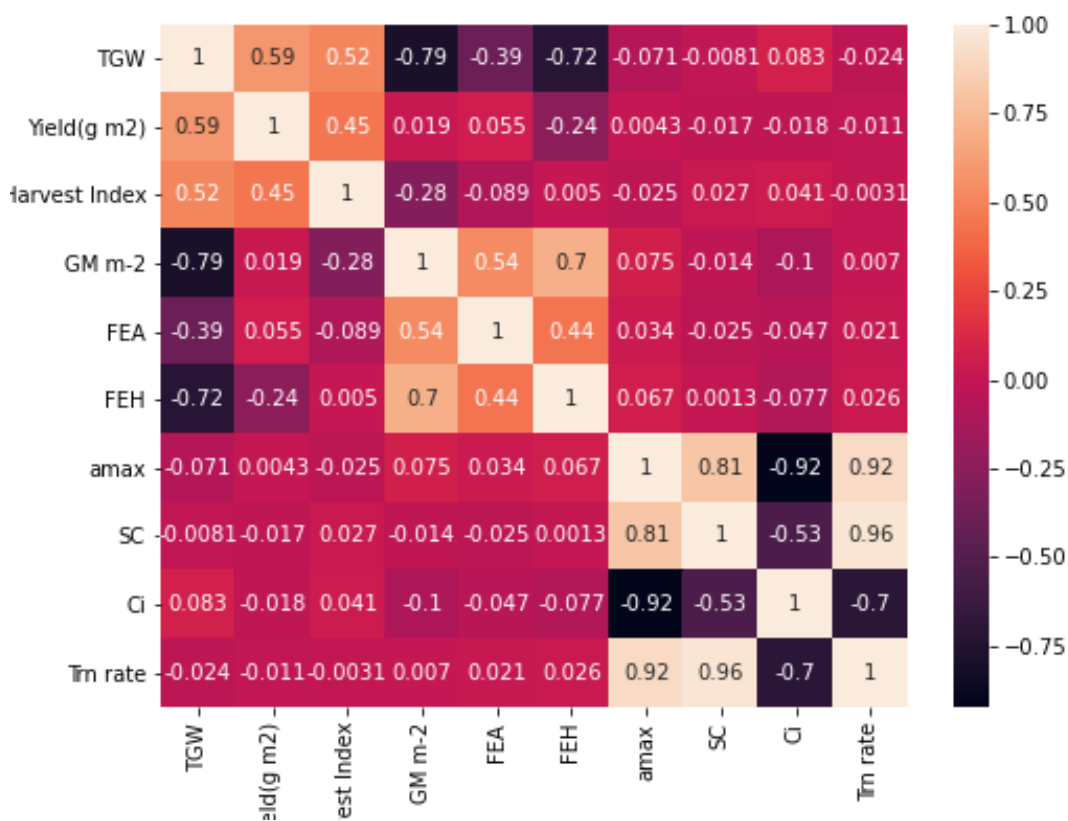


Fig 6.1. Correlation of field physiology traits (Thousand grain weight, yield $g\ m^{-2}$, Harvest index, grains m^{-2} , Fruiting efficiency (anthesis) and Fruiting efficiency (harvest), with photosynthetic traits from the 2019 glasshouse experiment pre-anthesis LICOR measurements (a_{max} = Leaf A_{max}, SC = Stomatal conductance, C_i = Internal concentration CO₂, Trn rate = Transpiration rate).

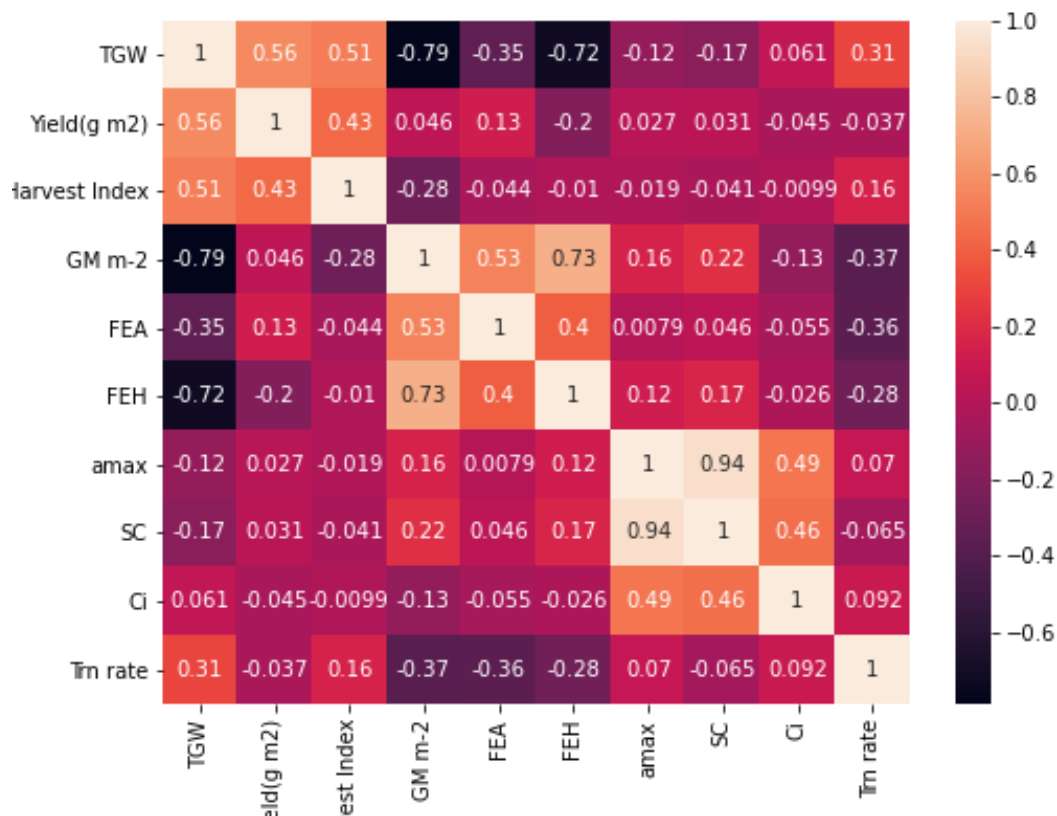


Fig 6.2. Correlation of field physiology traits (Thousand grain weight, yield g m⁻², Harvest index, grains m⁻², Fruiting efficiency (anthesis) and Fruiting efficiency (harvest), with photosynthetic traits from the 2019 glasshouse experiment post-anthesis LICOR measurements (amax = Light saturated leaf photosynthesis rate, SC = Stomatal conductance, Ci = Internal concentration CO₂, Trn rate = Transpiration rate).

6.4 Discussion

6.4.1. Pre-anthesis partitioning and spike growth

In previous field experiments in spring wheat (Sierra-Gonzalez et al., 2020; Rivera-Amado et al., 2019) and in field experiments in the present study, the true-

stem internode 2 and 3 PIs were negatively associated with spike PI. However, in the subset in the glasshouse experiments, internode TS 2 and 3 lengths were not associated with spike PI (linear regressions of (SPI versus stem internode Int 2 length, $R^2 = 0.01$, $p = 0.659$. and SPI versus stem internode 3 length, $R^2 = 0.09$, $p = 0.695$). These correlations differ with those in the field experiments, perhaps because of the different environmental conditions in the glasshouse experiments compared to the field experiments affecting tillering. There may have been effects on inter-shoot competition for assimilates according to the differences between single plants grown in the glasshouse and populations of plants in the field experiments. In the glasshouse, light interception per shoot is likely much greater than in the field, so competition between spike and stem for assimilates due to mutual shading may occur at a relatively later stage during stem extension, i.e. during peduncle extension rather than stem internode 2 and 3 extension. There were also differences in the phenology between the glasshouse and field experiments.

6.4.2 Source/sink traits and grain growth

The flag-leaf photosynthetic rate and other gas-exchange traits pre-anthesis were not correlated with grain yield or yield components in the field experiments. However post-anthesis transpiration efficiency was correlated positively with both FE and grains per m^2 . Grain number is determined partly by spike growth from booting to anthesis (Gonzalez et al., 2011), while grain weight is determined by post-anthesis growth, so it would be expected that the post-anthesis transpiration efficiency is correlating positively with grain weight. A positive association between genetic variation in post-anthesis photosynthesis and yield has been reported

previously in wheat (Reynolds et al., 2005; Gaju et al., 2016). However, other studies found no correlation between post-anthesis gas exchange and grain yield (Xue et al., 2002). Pre-anthesis photosynthesis rate would be expected to be associated with grains m^{-2} , but this was not observed in the present experiments. As environmental effects on gas exchange can be large (Reynolds et al., 2000), it is possible that more time points of leaf photosynthesis rate measurements may have increase the associations in the present experiments.

Chapter 7. General Discussion

7.1 Summary of Hypotheses

The specific hypotheses of the thesis were:

1. Genetic variation in grain yield in the KWS panel is correlated with both harvest index and above-ground dry matter at maturity.

This hypothesis is fully supported by the field experiment results from chapter 4, which showed significant positive associations between grain yield and above-ground biomass, and grain yield and harvest index. Biomass was the main determinant of genetic variation in grain yield in both experiments.

2. Grain number is positively associated with spike partitioning index and fruiting efficiency among genotypes in the KWS panel.

This hypothesis was partially supported by the field experiment results from chapter 4, which showed a strong association between grain number per m² and fruiting efficiency. The association between grain number per m² and spike partitioning index was very weak, but negative and significant. This might indicate that high spike dry matter genotypes do not optimally partition dry matter to the florets within the spike.

3. A trade-off is observed between spike partitioning index and fruiting efficiency among the KWS panel genotypes.

This hypothesis was fully supported by field experiment results from chapter 4, which showed a strong negative relationship between fruiting efficiency and

spike partitioning index, as well as a strong negative relationship between fruiting efficiency and spike dry matter m^{-2} .

4. Competition observed between spike growth and stem internodes 2 and 3 is stronger than between spike growth and the peduncle , so that the association with each of Spike PI and grains m^{-2} is stronger for true-stem internodes 2 and 3 partitioning indices than the true-stem peduncle partitioning indices

This hypothesis was partially supported by the field experiment results in chapter 4. For subset 1, spike partitioning index 3 was observed to have a significant negative association with true-stem internode 2 PI, but not TS peduncle or TS stem-internode 3 PI. For the 137 genotypes, stem-internode 2 and 3 lengths were negatively associated with SPI but there was no association with peduncle length. However, the TS stem-internode 2 and 3 PIs and stem-internode 2 and 3 lengths were not associated with grains m^{-2} .

5. In the glasshouse, a positive association is observed in flag leaf photosynthesis rate pre-anthesis and spike biomass and grain number per spike in the KWS panel subset

This hypothesis was not supported by the glasshouse experiment results in chapter 6. No significant associations between flag-leaf photosynthetic traits and spike biomass or grains per spike were observed pre-anthesis.

6. Field and glasshouse expression of grain number traits are positively correlated among the KWS panel genotypes

This hypothesis was generally not supported by the glasshouse experiment results in chapter 6.

7. Marker-trait associations can be identified for the key grain partitioning traits, fruiting efficiency and grain number per m²

This hypothesis was fully supported by the GWAS results in chapter 5. At least one marker-trait association was detected for all key grain partitioning traits and fruiting efficiency.

8. Co-locating markers will be identified for fruiting efficiency and grains m⁻².

This hypothesis was not supported by the GWAS results in chapter 5. Only two markers were co-locating for different traits, a marker-trait association for harvest index/LPI, and one for grains m⁻² and thousand grain weight. No MTA for fruiting efficiency co-located with other traits, or across years.

9. Candidate genes for the key SNPs associating with grain partitioning and grain number traits will be identified and confirmed with reference to previous literature.

This hypothesis was supported by the GWAS results in chapter 5. Several potential candidate genes were identified for key grain partitioning traits and fruiting efficiency, including *GNI-1*, as previously reported by (Sakuma et al., 2019). Additional work is required to confirm and validate potential candidate genes identified.

7.2 Implications for breeders

One primary conclusion drawn from this thesis is that associations between increased spike partitioning index and decreased stem-internode 2 and 3 length/PI reported in spring wheat varieties are also expressed in this UK winter wheat breeding panel.. However, there was a trade-off between SPI and FE, so that the stem-internode traits were not associated with grains m⁻². Breeding for additional spike biomass resulted in diminishing rates of gain due to the corresponding decrease in FE, possibly due to suboptimal partitioning of additional dry matter. Gains in grain yield could alternatively be achieved by targeting FE increases to increase harvest index and grain yield in already high biomass varieties. For FE measured in the KWS panel field experiments field sampling and growth analysis at anthesis was required which is relatively time-consuming, but this is only feasible on a panel containing ca.100-150 genotypes. The internode-length traits are not a destructive measurement and there may be scope for developing high-throughput imaging techniques to process samples for these traits, but presently, internode length could be measured on shoots in situ on hundreds but not thousands of field plots. Measuring FE using the chaff DM instead of the anthesis spike DM removed the requirement for a destructive sampling at anthesis but necessitated increased processing at physiological maturity. For traits where high-throughput phenotyping cannot be developed, such as FE, molecular markers need to be developed. Identification and incorporation of the genetic basis of these traits will allow markers for them to be included in future breeding programs.

7.3 Future work

7.3.1 Optimising spike partitioning and validation of physiological relationships

Future work on this material would include more detailed spike morphological component (glumes, palea, lemma, rachis awn) partitioning to identify the physiological basis of the observed trade-off between fruiting efficiency and spike partitioning index. Although prior work (Sierra-Gonzalez et al., 2021) has identified reduced awn partitioning index as associated with increased fruiting efficiency, this is unlikely to be the cause of the trade-off observed in this panel as all but two genotypes did not possess awns. It has been suggested by (The most likely competitor in this panel for spike dry matter would be the Rachis. Previous work by (Rivera-amado et al, 2019) identified an association between decreased Rachis specific weight /rachis partitioning index and fruiting efficiency. Uncovering the chief competitor of grain for spike dry matter would help in optimising spike morphological partitioning to reduce the observed trade off with FE. Furthermore, phenotyping of more European winter wheat breeding material in different growing environments to validate further the physiological relationships and results observed here would be useful in developing novel breeding targets and traits for the improvement of grain yield in future varieties. Also, further wider germplasm could be investigated for novel trait expression, for example, Relevant wider germplasm for screening could be the A.E. Watkins landrace collection curated at John Innes Centre, UK, with 700 landraces that cover origins from many Asian and European countries, and the CIMMYT primary synthetics diversity panel (160 genotypes) and the CIMMYT bread wheat diversity panel (370 genotypes).

7.3.2 Further exploration of flag-leaf fluorescence parameters

Detailed exploration of flag-leaf fluorescence photosynthetic parameters such as PSII quantum yield and NPQ was restricted by experimental conditions and the large number of genotypes to be assessed. The preliminary work here shows some promising relationships between grain partitioning traits and increased flag-leaf quantum yield that could be further explored in additional experiments with a smaller number of contrasting genotypes and more rigorous testing protocols. The use of high-throughput measuring techniques for radiation-use efficiency, e.g., hyperspectral reflectance techniques could allow for measurements in breeders' plots in larger numbers of genotypes to better observe how these traits affect partitioning traits during different developmental stages and generate more robust data sets. In addition, these flag-leaf fluorescence traits should be studied in other cereals which have yet to be quantified in the future.

7.3.3 Validation of potential candidate genes

Field experiments on several doubled-haploid mapping populations derived from biparental crosses would allow the confirmation of phenotype effects and marker-trait associations across a range of genetic backgrounds in plant breeders' programs. The validation of potential candidate genes identified here via Knetminer, and marker-trait associations would be required for the development of more precise markers for marker-assisted breeding programs. Candidate gene validation could be conducted by the generation and characterisation of mutant genotypes via TILLING mutants. This would allow the validation of different alleles of candidate genes, such as in *GNI-A1* and generation of KASP markers. Finally, expression profiles of candidate genes could be explored via RNAseq, as originally intended in this study.

7.3.4 Exploration of stem WSC content and drought tolerance in high spike biomass varieties.

Optimisation of dry matter allocation to favour high spike biomass varieties may introduce trade – offs with drought tolerance due to reduced reserves of water-soluble carbohydrates in the stem, which act as a buffer in times of low water availability. The 2018 field trial experienced drought at a severity highly unusual for the UK, and grain yield and grain weight were significantly lower in that trial compared to the 2019 trial. Further work could be undertaken to compare stem WSC content in UK winter wheat populations and explore the relationship between spike partitioning index, stem WSC content and yields in varying environmental conditions.

8. References

1. Abbate, P. E., Andrade, F. H., Lazaro, L., Bariffi, J. H., Berardocco, H. G., Inza, V. H. & Marturano, F. (1998) Grain yield increase in recent argentine wheat cultivars. *Crop Science*, 38(5), 1203-1209.
2. Acevedo, E., Silva, P., and Silva, H. (2002). *Wheat Growth and Physiology*. FAO Corporate Document Repository. Rome: FAO, 1–31.
3. Acreche, M. M., Briceno-Felix, G., Sanchez, J. A. M. & Slafer, G. A. (2008) Physiological bases of genetic gains in Mediterranean bread wheat yield in Spain. *European Journal of Agronomy*, 28(3), 162-170.

4. Ahmadi, A., M. Joudi and M. Janmohammadi, 2009. Late defoliation and wheat yield: Little evidence of post-anthesis source limitation. *Field Crops Res.*, 113: 90-93.
5. Aisawi, K. A. B., Reynolds, M. P., Singh, R. P. & Foulkes, M. J. (2015) The Physiological Basis of the Genetic Progress in Yield Potential of CIMMYT Spring Wheat Cultivars from 1966 to 2009. *Crop Science*, 55(4), 1749-1764.
6. Alqudah, A. M., Haile, J. K., Alomari, D. Z., Pozniak, C. J., Kobiljski, B. & Borner, A. (2020) Genome-wide and SNP network analyses reveal genetic control of spikelet sterility and yield-related traits in wheat. *Scientific Reports*, 10(1).
7. Alonso-Blanco, C., Aarts, M. G. M., Bentsink, L., Keurentjes, J. J. B., Reymond, M., Vreugdenhil, D. & Koornneef, M. (2009) What Has Natural Variation Taught Us about Plant Development, Physiology, and Adaptation? *Plant Cell*, 21(7), 1877-1896.
8. Alvarado, G. et al. (2020) "META-R: A software to analyze data from multi-environment plant breeding trials," *The Crop Journal*, 8(5), pp. 745–756. doi: 10.1016/J.CJ.2020.03.010.
9. Amalova, A., Abugalieva, S., Babkenov, A., Babkenova, S. & Turuspekov, Y. (2021) Genome-wide association study of yield components in spring wheat collection harvested under two water regimes in Northern Kazakhstan. *Peerj*, 9.
10. Bindraban, P.S.; Sayre, K.D.; Solis-Moya, E. 1998. Identifying factors that determine kernel number in wheat. *Field Crops Research* 58, 223 - 234. [https://doi.org/10.1016/S0378-4290\(98\)00097-5](https://doi.org/10.1016/S0378-4290(98)00097-5)

11. Breakout session P1.1 National Food Security-The Wheat Initiative-an International Research Initiative for Wheat Improvement (no date). Available at: www.wheatinitiative.org (Accessed: August 3, 2020).
12. Calderini, D.F., Abeledo, L.G., Slafer, G.A., 2000. Physiological maturity in wheat based on kernel water and dry matter. *Agron. J.* 92, 895–901
13. Cartelle J, Pedró A, Savin R, Slafer GA. 2006. Grain weight responses to post-anthesis spikelet-trimming in an old and a modern wheat under Mediterranean conditions. *Europ J Agron* 25, 365–371
14. Cortes, L. T., Zhang, Z. W. & Yu, J. M. (2021) Status and prospects of genome-wide association studies in plants. *Plant Genome*, 14(1).
15. M.F. Dreccer, K.B. Wockner, J.A. Palta, C.L. McIntyre, M.G. Borgognone, M. Bourgault, M.P. Reynolds, D.J. Miralles More fertile florets and grains per spike can be achieved at higher temperature in wheat lines with high spike biomass and sugar content at booting *Funct. Plant Biol.*, 41 (2014), pp. 482-495, 10.1071/FP13232
16. FAO (2009) How to Feed the World in 2050, Insights from an expert meeting at FAO. doi: 10.1111/j.1728-4457.2009.00312.x.
17. FAO (2017) FAO Cereal Supply and Demand Brief | World Food Situation | Food and Agriculture Organization of the United Nations. Available at: <http://www.fao.org/worldfoodsituation/csdb/en/> (Accessed: November 3, 2017).
18. Fischer, R. A. & Stockman, Y. M. (1980) Kernel number per spike in wheat (*Triticum-aestivum* L) - responses to preanthesis shading. *Australian Journal of Plant Physiology*, 7(2), 169-180.
19. Fischer, RA 1983 Growth and yield of wheat Smith W.H., Banta S.J. (Eds.), *Potential Productivity of Field Crops under Different Environments*, IRRI, Los Ban~os (1983), pp. 129-154 IRRI, Los Ban~os

20. Fischer, R.A.. (2008). The importance of grain or kernel number in wheat: A reply to Sinclair and Jamieson. *Field Crops Research*. 105. 15-21. 10.1016/j.fcr.2007.04.002.
21. Fischer, RA 1985. Number of kernels in wheat crops and the influence of solar radiation and temperature. *J. Agric. Sci.*, 105 (1985), pp. 447-461, 10.1017/S0021859600056495
22. Foulkes, Michael & Sylvester-Bradley, Roger & Weightman, R. & Snape, John. (2007). Identifying physiological traits associated with improved drought resistance in winter wheat. *Field Crops Research*. 103. 11-24. 10.1016/j.fcr.2007.04.007.
23. Ferrante, A., Cartelle, J., Savin, R. & Slafer, G. A. (2017) Yield determination, interplay between major components and yield stability in a traditional and a contemporary wheat across a wide range of environments. *Field Crops Research*, 203, 114-127.
24. Gaju, O., Reynolds, M. P., Sparkes, D. L. & Foulkes, M. J. (2009) Relationships between Large-Spike Phenotype, Grain Number, and Yield Potential in Spring Wheat. *Crop Science*, 49(3), 961-973.
25. Gaju, O., Reynolds, M. P., Sparkes, D. L., Mayes, S., Ribas-Vargas, G., Crossa, J. & Foulkes, M. J. (2014) Relationships between physiological traits, grain number and yield potential in a wheat DH population of large spike phenotype. *Field Crops Research*, 164, 126-135.
26. Garcia, G. A., Serrago, R. A., Gonzalez, F. G., Slafer, G. A., Reynolds, M. P. & Miralles, D. J. (2014) Wheat grain number: Identification of favourable physiological traits in an elite doubled-haploid population. *Field Crops Research*, 168, 126-134.
27. Gerard, G. S., Alqudah, A., Lohwasser, U., Borner, A. & Simon, M. R. (2019) Uncovering the Genetic Architecture of Fruiting Efficiency in Bread Wheat: A Viable Alternative to Increase Yield Potential. *Crop Science*, 59(5), 1853-1869.

28. Gonzalez, F. G., Miralles, D. J. & Slafer, G. A. (2011) Wheat floret survival as related to pre-anthesis spike growth. *Journal of Experimental Botany*, 62(14), 4889-4901.
29. Lazaro, L. & Abbate, P. E. (2012) Cultivar effects on relationship between grain number and photothermal quotient or spike dry weight in wheat. *Journal of Agricultural Science*, 150, 442-459.
30. García, G. A. et al. (2014) "Wheat grain number: Identification of favourable physiological traits in an elite doubled-haploid population," *Field Crops Research*, 168, pp. 126–134. doi: 10.1016/j.fcr.2014.07.018.
31. Gonzalez-Navarro, O. E. et al. (2016) "Variation in developmental patterns among elite wheat lines and relationships with yield, yield components and spike fertility," *Field Crops Research*, 196, pp. 294–304. doi: 10.1016/j.fcr.2016.07.019.
32. T. Gebbing and S. Schnyder, "Pre-anthesis Reserve Utilization for Protein and Carbohydrate Synthesis in Grains of Wheat," *Plant Physiology*, Vol. 121, No. 3, 1999, pp. 871-878. doi:10.1104/pp.121.3.871
33. Gonzalez, F.G., Slafer, G.A. and Miralles, D.J. (2003) Floret Development and Spike Growth as Affected by Photoperiod during Stem Elongation in Wheat. *Field Crop Research*, 81, 29-38. [http://dx.doi.org/10.1016/S0378-4290\(02\)00196-X](http://dx.doi.org/10.1016/S0378-4290(02)00196-X)
34. Guo, Z. F., Chen, D. J., Alqudah, A. M., Roder, M. S., Ganai, M. W. & Schnurbusch, T. (2017) Genome-wide association analyses of 54 traits identified multiple loci for the determination of floret fertility in wheat. *New Phytologist*, 214(1), 257-270.
35. Guo Z, Slafer GA, Schnurbusch T. 2016. Genotypic variation in spike fertility traits and ovary size as determinants of floret and grain survival rate in wheat. *Journal of Experimental Botany* 67, 4221-4230.

36. Haas, M., Schreiber, M. & Mascher, M. (2019) Domestication and crop evolution of wheat and barley: Genes, genomics, and future directions. *Journal of Integrative Plant Biology*, 61(3), 204-225.
37. Harris, C. R. et al. (2020) "Array programming with NumPy," *Nature* 2020 585:7825, 585(7825), pp. 357–362. doi: 10.1038/s41586-020-2649-2.
38. Kirby, E.J.M. 2002, 'Botany of the wheat plant'. In: Curtis BC, Rajaram, S and Gomez. Macpherson, H (eds) 2002, Bread wheat improvement and production.
39. Kirby, E.J.M., Appleyard, M. & Simpson, N.A. 1994. Co-ordination of stem elongation and Zadoks growth stages with leaf emergence in wheat and barley. *J. Agric. Sci.*, 122: 21-29.
40. Kumar, J., Pratap, A., Solanki, R. K., Gupta, D. S., Goyal, A., Chaturvedi, S. K., Nadarajan, N. & Kumar, S. (2012) Genomic resources for improving food legume crops. *Journal of Agricultural Science*, 150, 289-318.
41. Kuhlert, S. et al. (2016) "MultispeQ Beta: a tool for large-scale plant phenotyping connected to the open PhotosynQ network," *Royal Society Open Science*, 3(10). doi: 10.1098/RSOS.160592.
42. Large, E. C. (1954) Growth stages in cereals-illustration of the Feekes scale. *Plant Pathology*, 3, 128-129.
43. Liu, J., Feng, B., Xu, Z. B., Fan, X. L., Jiang, F., Jin, X. F., Cao, J., Wang, F., Liu, Q., Yang, L. & Wang, T. (2018) A genome-wide association study of wheat yield and quality-related traits in southwest China. *Molecular Breeding*, 38(1).
44. Loomis R.S., Williams W.A. (1963). Maximum crop productivity: An estimate. *Crop Sci.* 3: 67–72.
45. Lozada, D. N., Mason, R. E., Babar, M. A., Carver, B. F., Guedira, G. B., Merrill, K., Arguello, M. N., Acuna, A., Vieira, L., Holder, A., Addison, C., Moon, D. E., Miller, R. G. & Dreisigacker, S. (2017) Association mapping reveals loci associated with multiple traits that affect grain yield and adaptation in soft winter wheat. *Euphytica*, 213(9).

46. Lucas, H. (2012) "Breakout session P1.1 National Food Security – The Wheat Initiative – an International Research Initiative for Wheat Improvement Context – the problems being addressed," GCARD - Second Global Conference on Agricultural Research for Development, (September), pp. 1–3. Available at: [http://www.fao.org/docs/eims/upload/306175/Briefing Paper \(3\)-Wheat Initiative - Hélène Lucas.pdf](http://www.fao.org/docs/eims/upload/306175/Briefing_Paper_(3)-Wheat_Initiative_-_Hélène_Lucas.pdf) (Accessed: November 3, 2017).
47. Melrose, J., Perroy, R. and Careas, S. (2015) "World population prospects," United Nations, 1(6042), pp. 587–92. doi: 10.1017/CBO9781107415324.004.
48. Neumann, K., Kobiljski, B., Dencic, S., Varshney, R. K. & Borner, A. (2011) Genome-wide association mapping: a case study in bread wheat (*Triticum aestivum* L.). *Molecular Breeding*, 27(1), 37-58.
49. Pedregosa, F. et al. (2011) "Scikit-learn: Machine Learning in Python," *Journal of Machine Learning Research*, 12(85), pp. 2825–2830.
50. Pask, A., Pietragalla, J., Mullan, D. & Reynolds, M. (2012) *Physiological breeding II: A field guide to wheat phenotyping*. CIMMYT, Mexico.
51. Pinera-Chavez, F. J., Berry, P. M., Foulkes, M. J., Jesson, M. A. & Reynolds, M. P. (2016) Avoiding lodging in irrigated spring wheat. I. Stem and root structural requirements. *Field Crops Research*, 196, 325-336.
52. Reynolds, M. et al. (2012) "Achieving yield gains in wheat," *Plant, Cell and Environment*, 35(10), pp. 1799–1823. doi: 10.1111/j.1365-3040.2012.02588.x.
53. Rivera-Amado, Alma & Trujillo-Negrellos, Eliseo & Molero, Gemma & Reynolds, Matthew & Sylvester-Bradley, Roger & Foulkes, Michael. (2019). Optimizing dry-matter partitioning for increased spike growth, grain number and harvest index in spring wheat. *Field Crops Research*. 240. 10.1016/j.fcr.2019.04.016.
54. Osmar Rodrigues, Mauro César Celaro Teixeira, Edson Roberto Costenaro, Leandro Vargas, Rafael Damo 2014. Influence of Vernalization and Photoperiod on the Duration of Stem Elongation and Spikelet Fertility in

55. Sehgal, D., Mondal, S., Crespo-Herrera, L., Velu, G., Juliana, P., Huerta-Espino, J., Shrestha, S., Poland, J., Singh, R. & Dreisigacker, S. (2020) Haplotype-Based, Genome-Wide Association Study Reveals Stable Genomic Regions for Grain Yield in CIMMYT Spring Bread Wheat. *Frontiers in Genetics*, 11.
56. Soto-Cerda, B. J. & Cloutier, S. (2012) Association Mapping in Plant Genomes. *Genetic Diversity in Plants*, 29-54.
57. Slafer, G. A., Elia, M., Savin, R., Garcia, G. A., Terrile, II, Ferrante, A., Miralles, D. J. & Gonzalez, F. G. (2015) Fruiting efficiency: an alternative trait to further rise wheat yield. *Food and Energy Security*, 4(2), 92-109.
58. Sreenivasulu, N. & Schnurbusch, T. (2012) A genetic playground for enhancing grain number in cereals. *Trends in Plant Science*, 17(2), 91-101.
59. Terrile, II, Miralles, D. J. & Gonzalez, F. G. (2017) Fruiting efficiency in wheat (*Triticum aestivum* L): Trait response to different growing conditions and its relation to spike dry weight at anthesis and grain weight at harvest. *Field Crops Research*, 201, 86-96.
60. Sayre, K.D., S. Rajaram and R.A. Fischer. 1997. Yield potential progress in short bread wheats in Northwest Mexico. *Crop Sci.* 37: 36-42.
61. Shearman, V., Sylvester-Bradley, R., Scott, R. & Foulkes, M. (2005) Physiological processes associated with wheat yield progress in the UK. *Crop Science*, 45(1), 175-185.
62. Shewry, W. P. R. (2009) "DARWIN REVIEW," *Journal of Experimental Botany*, 60(6), pp. 1537-1553. doi: 10.1093/jxb/erp058.
63. Sinclair, T.R. & Jamieson, P.D.. (2006). Grain number, wheat yield, and bottling beer: An analysis. *Field Crops Research*. 98. 60-67. 10.1016/j.fcr.2005.12.006.

64. Slafer, G. A., Andrade, F. H. & Satorre, E. H. (1990) Genetic-improvement effects on pre-anthesis physiological attributes related to wheat grain-yield. *Field Crops Research*, 23(3), 255-263.
65. Slafer, G. A. & Andrade, F. H. (1993) Physiological attributes related to the generation of grain-yield in bread wheat cultivars released at different eras. *Field Crops Research*, 31(3-4), 351-367.
66. Slafer, G. A. & Rawson, H. M. (1994) Sensitivity of wheat phasic development to major environmental factors - A re-examination of some assumptions made by physiologists and modelers *Australian Journal of Plant Physiology*, 21(4), 393-426.
67. Stockman and Ralph A. Fischer and E. G. Brittain 1983. Assimilate Supply and Floret Development Within the Spike of Wheat (*Triticum aestivum* L. *Australian Journal of Plant Physiology*, 10, 585-594}
68. Whitechurch, Slafer & Miralles (2007) *J Agron Crop Sci* 193, 138-145. Variation in stem elongation phase (independent of cycle length).
69. Yan L, Loukoianov A, Tranquilli G, Helguera M, Fahima T, Dubcovsky J (2003) Positional cloning of the wheat vernalization gene VRN1. *Proc Natl Acad Sci USA* 100: 6263–6268
70. Yan L, Loukoianov A, Blechl A, Tranquilli G, Ramakrishna W, SanMiguel P, Bennetzen JL, Echenique V, Dubcovsky J (2004 a) The wheat VRN2 gene is a flowering repressor down-regulated by vernalization. *Science* 303: 1640–1644
71. Youssef, H. M., Eggert, K., Kopplu, R., Alqudah, A. M., Poursarebani, N., Fazeli, A., Sakuma, S., Tagiri, A., Rutten, T., Govind, G., Lundqvist, U., Graner, A., Komatsuda, T., Sreenivasulu, N. & Schnurbusch, T. (2017) VRS2 regulates hormone-mediated inflorescence patterning in barley. *Nature Genetics*, 49(1), 157-161.

72.Zadoks, J. C., Chang, T. T. and Konzak, C. F. (1974) "A decimal code for the growth stages of cereals," *Weed Research*, 14(6), pp. 415–421. doi: 10.1111/j.1365-3180.1974.tb01084.x.

Abbate, P. E., Andrade, F. H., & Culot, J. P. (1995). The effects of radiation and nitrogen on number of grains in wheat. *The Journal of Agricultural Science*, 124(03), 351. <https://doi.org/10.1017/S0021859600073317>

Abbate, P. E., Andrade, F. H., Culot, J. P., & Bindraban, P. S. (1997). Grain yield in wheat: Effects of radiation during spike growth period. *Field Crops Research*, 54(2–3), 245–257. [https://doi.org/10.1016/S0378-4290\(97\)00059-2](https://doi.org/10.1016/S0378-4290(97)00059-2)

Abbate, P. E., Andrade, F. H., Lázaro, L., Bariffi, J. H., Berardocco, H. G., Inza, V. H., & Marturano, F. (1998). Grain yield increase in recent Argentine wheat cultivars. *Crop Science*, 38(5), 1203–1209. <https://doi.org/10.2135/cropsci1998.0011183X003800050015x>

Acevedo, E., Silva, P., Silva, H. (2002). Bread wheat. Improvement and Production. FOOD AND AGRICULTURE ORGANIZATION OF THE UNITED NATIONS, Rome. <http://www.fao.org/docrep/006/y4011e/y4011e06.htm#bm06>

Acevedo, E., Silva, P., Silva, H. (2015). Wheat Growth and Physiology. FAO. <http://www.fao.org/docrep/006/y4011e/y4011e06.htm>

Acreche, M. M., Briceño-Félix, G., Sánchez, J. A. M., & Slafer, G. A. (2008). Physiological bases of genetic gains in Mediterranean bread wheat yield in Spain. *European Journal of Agronomy*, 28(3), 162–170. <https://doi.org/10.1016/J.EJA.2007.07.001>

Ahmadi, A., Joudi, M., & Janmohammadi, M. (2009). Late defoliation and wheat yield: Little evidence of post-anthesis source limitation. *Field Crops Research*, 113(1), 90–93. <https://doi.org/10.1016/J.FCR.2009.04.010>

Aisawi, K. A. B., Reynolds, M. P., Singh, R. P., & Foulkes, M. J. (2015). The physiological basis of the genetic progress in yield potential of CIMMYT spring

wheat cultivars from 1966 to 2009. *Crop Science*, 55(4), 1749–1764.
<https://doi.org/10.2135/CROPSCI2014.09.0601>

Alonso-Blanco, C., Aarts, M. G. M., Bentsink, L., Keurentjes, J. J. B., Reymond, M., Vreugdenhil, D., & Koornneef, M. (2009). What Has Natural Variation Taught Us about Plant Development, Physiology, and Adaptation? *The Plant Cell*, 21(7), 1877–1896. <https://doi.org/10.1105/TPC.109.068114>

Alqudah, A. M., Sallam, A., Stephen Baenziger, P., & Börner, A. (2020). GWAS: Fast-forwarding gene identification and characterization in temperate Cereals: lessons from Barley – A review. *Journal of Advanced Research*, 22, 119–135. <https://doi.org/10.1016/J.JARE.2019.10.013>

Araus, J. L., & Cairns, J. E. (2014). Field high-throughput phenotyping: The new crop breeding frontier. *Trends in Plant Science*, 19(1), 52–61.
<https://doi.org/10.1016/j.tplants.2013.09.008>

Austin, R. B. (1982). Crop Characteristics and the Potential Yield of Wheat. *The Journal of Agricultural Science*, 98(02), 447–453.
<https://doi.org/10.1017/S002185960004199X>

Barraclough, P. B., Lopez-Bellido, R., & Hawkesford, M. J. (2014). Genotypic variation in the uptake, partitioning and remobilisation of nitrogen during grain-filling in wheat. *Field Crops Research*, 156, 242–248.
<https://doi.org/10.1016/j.fcr.2013.10.004>

Basile, S. L. (2019). Haplotype block analysis of an Argentinean hexaploid wheat collection and GWAS for yield components and adaptation. *BMC Plant Biol.*, 19.

Battenfield SD, Sheridan JL, Silva LDCE, Miclaus KJ, Dreisigacker S, et al. (2018) Breeding-assisted genomics: Applying meta-GWAS for milling and baking quality in CIMMYT wheat breeding program. *PLOS ONE* 13(11): e0204757. <https://doi.org/10.1371/journal.pone.0204757>

Beche, E., Benin, G., da Silva, C. L., Munaro, L. B., & Marchese, J. A. (2014). Genetic gain in yield and changes associated with physiological traits in Brazilian wheat during the 20th century. *European Journal of Agronomy*, 61(61), 49–59. <https://doi.org/10.1016/j.eja.2014.08.005>

- Berry, P. M., Rounsevell, M. D. A., Harrison, P. A., & Audsley, E. (2006). Assessing the vulnerability of agricultural land use and species to climate change and the role of policy in facilitating adaptation. *Environmental Science & Policy*, 9(2), 189–204. <https://doi.org/10.1016/j.envsci.2005.11.004>
- Berry, P. M., Spink, J. H., Foulkes, M. J., & Wade, A. (2003). Quantifying the contributions and losses of dry matter from non-surviving shoots in four cultivars of winter wheat. *Field Crops Research*, 80(2), 111–121. [https://doi.org/10.1016/S0378-4290\(02\)00174-0](https://doi.org/10.1016/S0378-4290(02)00174-0)
- Bindraban, P. S., Sayre, K. D., & Solis-Moya, E. (1998). Identifying factors that determine kernel number in wheat. *Field Crops Research*, 58(3), 223–234. [https://doi.org/10.1016/S0378-4290\(98\)00097-5](https://doi.org/10.1016/S0378-4290(98)00097-5)
- Boken, V. K., & Shaykewich, C. F. (2010). Improving an operational wheat yield model using phenological phase-based Normalized Difference Vegetation Index. <https://doi.org/10.1080/014311602320567955>, 23(20), 4155–4168. <https://doi.org/10.1080/014311602320567955>
- Bordes, J., Goudemand, E., Duchalais, L., Chevarin, L., Oury, F. X., Heumez, E., Lapierre, A., Perretant, M. R., Rolland, B., Beghin, D., Laurent, V., le Gouis, J., Storlie, E., Robert, O., & Charmet, G. (2014). Genome-wide association mapping of three important traits using bread wheat elite breeding populations. *Molecular Breeding*, 33(4), 755–768. <https://doi.org/10.1007/S11032-013-0004-0/FIGURES/4>
- Borrás, L., Slafer, G. A., & Otegui, M. E. (2004). Seed dry weight response to source-sink manipulations in wheat, maize and soybean: A quantitative reappraisal. *Field Crops Research*, 86(2–3), 131–146. <https://doi.org/10.1016/j.fcr.2003.08.002>
- Brancourt-Hulmel, M., Doussinault, G., Lecomte, C., Bérard, P., le Buanec, B., & Trottet, M. (2003). Genetic Improvement of Agronomic Traits of Winter Wheat Cultivars Released in France from 1946 to 1992. *Crop Science*, 43(1), 37. <https://doi.org/10.2135/cropsci2003.3700>
- Calderini, D. F., Abeledo, L. G., & Slafer, G. A. (2000). Physiological Maturity in Wheat Based on Kernel Water and Dry Matter. *Agronomy Journal*, 92(5), 895. <https://doi.org/10.2134/agronj2000.925895x>

Calderini, D. F., Dreccer, M. F., & Slafer, G. A. (1995). Genetic improvement in wheat yield and associated traits. A re-examination of previous results and the latest trends. *Plant Breeding*, 114(2), 108–112.

<https://doi.org/10.1111/j.1439-0523.1995.tb00772.x>

Calderini, D. F., & Slafer, G. A. (1998). Changes in yield and yield stability in wheat during the 20th century. *Field Crops Research*, 57(3), 335–347.

[https://doi.org/10.1016/S0378-4290\(98\)00080-X](https://doi.org/10.1016/S0378-4290(98)00080-X)

Cartelle, J., Pedró, A., Savin, R., & Slafer, G. A. (2006). Grain weight responses to post-anthesis spikelet-trimming in an old and a modern wheat under Mediterranean conditions. *European Journal of Agronomy*, 25(4), 365–371. <https://doi.org/10.1016/J.EJA.2006.07.004>

CASAL, J. J. (1988). Light quality effects on the appearance of tillers of different order in wheat (*Triticum aestivum*). *Annals of Applied Biology*, 112(1), 167–173. <https://doi.org/10.1111/j.1744-7348.1988.tb02052.x>

CHAI, J. fang, ZHANG, C. mian, MA, X. ying, & WANG, H. bo. (2016). Molecular identification of ω -secalin gene expression activity in a wheat 1B/1R translocation cultivar. *Journal of Integrative Agriculture*, 15(12), 111111. [https://doi.org/10.1016/S2095-3119\(15\)61290-4](https://doi.org/10.1016/S2095-3119(15)61290-4)

Collard, B. C. Y., Jahufer, M. Z. Z., Brouwer, J. B., & Pang, E. C. K. (2005). An introduction to markers, quantitative trait loci (QTL) mapping and marker-assisted selection for crop improvement: The basic concepts. *Euphytica*, 142, 169–196. <https://doi.org/10.1007/s10681-005-1681-5>

Crain, J., Mondal, S., Rutkoski, J., Singh, R. P., & Poland, J. (2018). Combining High-Throughput Phenotyping and Genomic Information to Increase Prediction and Selection Accuracy in Wheat Breeding. *The Plant Genome*, 11(1), 170043.

<https://doi.org/10.3835/PLANTGENOME2017.05.0043/FORMAT/PDF>

Curtis, B. C. (2002). *Wheat in the world* - B.C. Curtis. FAO.

<http://www.fao.org/docrep/006/y4011e/y4011e04.htm>

Delgado, C. (2003). Rising Consumption of Meat and Milk in Developing Countries Has Created a New Food Revolution. *The Journal of Nutrition*,

133(5), 3875S-4061S.

<https://doi.org/http://jn.nutrition.org/content/133/11/3907S.abstract>

Demmig-Adams, B., Cohu, C. M., Muller, O., & Adams, W. W. (2012). Modulation of photosynthetic energy conversion efficiency in nature: from seconds to seasons. *Photosynthesis Research* 2012 113:1, 113(1), 75–88. <https://doi.org/10.1007/S11120-012-9761-6>

Dore, M. H. I. (2005). Climate change and changes in global precipitation patterns: What do we know? In *Environment International* (Vol. 31, Issue 8, pp. 1167–1181). Pergamon. <https://doi.org/10.1016/j.envint.2005.03.004>

Dreccer, M. F., Wockner, K. B., Palta, J. A., McIntyre, C. L., Borgognone, M. G., Bourgault, M., Reynolds, M., & Miralles, D. J. (2014). More fertile florets and grains per spike can be achieved at higher temperature in wheat lines with high spike biomass and sugar content at booting. *Functional Plant Biology : FPB*, 41(5), 482–495. <https://doi.org/10.1071/FP13232>

Dreisigacker, S., Kishii, M., Lage, J., & Warburton, M. (2008). Use of synthetic hexaploid wheat to increase diversity for CIMMYT bread wheat improvement. *Australian Journal of Agricultural Research*, 59(5), 413. <https://doi.org/10.1071/AR07225>

EA Edae, P. B. S. H. (2014). Genome-wide association mapping of yield and yield components of spring wheat under contrasting moisture regimes. *Theor Appl Genet*.

Ehdaie, B., & Waines, J. G. (1996). Dwarfing genes, water-use efficiency and agronomic performance of spring wheat. *Canadian Journal of Plant Science*, 76(4), 707–714. <http://www.nrcresearchpress.com/doi/pdf/10.4141/cjps96-122>

Elía, M., Savin, R., & Slafer, G. A. (2016). Fruiting efficiency in wheat: Physiological aspects and genetic variation among modern cultivars. *Field Crops Research*, 191, 83–90. <https://doi.org/10.1016/j.fcr.2016.02.019>

Evans, L. T. (1997). *Crop Evolution, Adaptation and Yield*. By L. T. EVANS. 23 x 15 cm. Pp. xi + 500 with 131 text-figures. Cambridge: Cambridge University Press, 1st paperback edition, 1996. ISBN 0 521 29558 0. New

Phytologist, 135(3), 567–574. <https://doi.org/10.1046/j.1469-8137.1997.00655.x>

EVANS, L. & BINGHAM, J. & JACKSON, P. & SUTHERLAND, JENNIFER. (2008). Effect of awns and drought on the supply of photosynthate and its distribution within wheat ears. *Annals of Applied Biology*. 70. 67 - 76. [10.1111/j.1744-7348.1972.tb04689.x](https://doi.org/10.1111/j.1744-7348.1972.tb04689.x).

EVERS, J. B., VOS, J., ANDRIEU, B., & STRUIK, P. C. (2006). Cessation of Tillering in Spring Wheat in Relation to Light Interception and Red : Far-red Ratio. *Annals of Botany*, 97(4), 649–658. <https://doi.org/10.1093/aob/mcl020>

Fan, X., Tang, Z., Tan, Y., Zhang, Y., Luo, B., Yang, M., Lian, X., Shen, Q., Miller, A. J., & Xu, G. (2016). Overexpression of a pH-sensitive nitrate transporter in rice increases crop yields. *Proceedings of the National Academy of Sciences of the United States of America*, 113(26), 7118–7123. <https://doi.org/10.1073/PNAS.1525184113>

FAO. (2009). How to Feed the World in 2050. In *Insights from an expert meeting at FAO (Vol. 2050, Issue 1)*. <https://doi.org/10.1111/j.1728-4457.2009.00312.x>

FAO. (2017). *FAO Cereal Supply and Demand Brief | World Food Situation | Food and Agriculture Organization of the United Nations*. <http://www.fao.org/worldfoodsituation/csdb/en/>

Ferrante, A., Cartelle, J., Savin, R., & Slafer, G. A. (2017). Yield determination, interplay between major components and yield stability in a traditional and a contemporary wheat across a wide range of environments. *Field Crops Research*, 203, 114–127. <https://doi.org/10.1016/j.fcr.2016.12.028>

Feuillet, C., Langridge, P., & Waugh, R. (2008). Cereal breeding takes a walk on the wild side. In *Trends in Genetics (Vol. 24, Issue 1, pp. 24–32)*. Elsevier Current Trends. <https://doi.org/10.1016/j.tig.2007.11.001>

Fischer, R. A. (1983). Wheat in 'Proc. Symp. on Potential Productivity of Field Crops under Different Environments Sep 1980. In Crops.

http://books.irri.org/9711041146_content.pdf

Fischer, R. A. (1985). Number of kernels in wheat crops and the influence of solar radiation and temperature. *The Journal of Agricultural Science*, 105(02), 447. <https://doi.org/10.1017/S0021859600056495>

Fischer, R. A. (2007). Understanding the physiological basis of yield potential in wheat. *The Journal of Agricultural Science*, 145(02), 99.

<https://doi.org/10.1017/S0021859607006843>

Fischer, R. A. (2008). The importance of grain or kernel number in wheat: A reply to Sinclair and Jamieson. *Field Crops Research*, 105(1–2), 15–21.

<https://doi.org/10.1016/J.FCR.2007.04.002>

Fischer, R. A., & Edmeades, G. O. (2010). Breeding and cereal yield progress. *Crop Science*, 50(April), S-85-S-98.

<https://doi.org/10.2135/cropsci2009.10.0564>

Fischer, R. A., Rees, D., Sayre, K. D., Lu, Z.-M., Condon, A. G., & Saavedra, A. L. (1998). Wheat Yield Progress Associated with Higher Stomatal Conductance and Photosynthetic Rate, and Cooler Canopies. *Crop Science*, 38(6), 1467. <https://doi.org/10.2135/cropsci1998.0011183X003800060011x>

Fischer, R., Byerlee, D., & Edmeades, G. O. (2014). Crop Yields and Global Food Security. Will Yield Increase Continue to Feed the World? *European Review of Agricultural Economics*, 43(1), 191–192.

<https://doi.org/10.1093/erae/jbv034>

Fischer, R., & Stockman, Y. (1986). Increased Kernel Number in Norin 10-Derived Dwarf Wheat: Evaluation of the Cause. *Australian Journal of Plant Physiology*, 13(6), 767. <https://doi.org/10.1071/PP9860767>

Foulkes, M. J., Slafer, G. A., Davies, W. J., Berry, P. M., Sylvester-Bradley, R., Martre, P., Calderini, D. F., Griffiths, S., & Reynolds, M. P. (2011). Raising yield potential of wheat. III. Optimizing partitioning to grain while maintaining lodging resistance. *Journal of Experimental Botany*, 62(2), 469–486. <https://doi.org/10.1093/JXB/ERQ300>

Foulkes, M. J., Snape, J. W., Shearman, V. J., & Sylvester-Bradley, R. (2007). Physiological Processes Associated with Winter Wheat Yield Potential Progress. *Wheat Production in Stressed Environments*, 591–597.
https://doi.org/10.1007/1-4020-5497-1_71

Foulkes, M. J., Sylvester-Bradley, R., Weightman, R., & Snape, J. W. (2007). Identifying physiological traits associated with improved drought resistance in winter wheat. *Field Crops Research*, 103(1), 11–24.
<https://doi.org/10.1016/J.FCR.2007.04.007>

Gaju, O., DeSilva, J., Carvalho, P., Hawkesford, M. J., Griffiths, S., Greenland, A., & Foulkes, M. J. (2016). Leaf photosynthesis and associations with grain yield, biomass and nitrogen-use efficiency in landraces, synthetic-derived lines and cultivars in wheat. *Field Crops Research*, 193, 1–15.
<https://doi.org/10.1016/j.fcr.2016.04.018>

Gaju, O., Reynolds, M. P., Sparkes, D. L., & Foulkes, M. J. (2009). Relationships between Large-Spike Phenotype, Grain Number, and Yield Potential in Spring Wheat. *Crop Science*, 49(3), 961.
<https://doi.org/10.2135/cropsci2008.05.0285>

Gaju, O., Reynolds, M. P., Sparkes, D. L., Mayes, S., Ribas-Vargas, G., Crossa, J., & Foulkes, M. J. (2014). Relationships between physiological traits, grain number and yield potential in a wheat DH population of large spike phenotype. *Field Crops Research*.
<https://doi.org/10.1016/j.fcr.2014.05.015>

Gallagher, J. N., & Biscoe, P. v. (1978). Radiation absorption, growth and yield of cereals. *The Journal of Agricultural Science*, 91(01), 47.
<https://doi.org/10.1017/S0021859600056616>

Gao, X., Pal, J. S., & Giorgi, F. (2006). Projected changes in mean and extreme precipitation over the Mediterranean region from a high resolution double nested RCM simulation. *Geophysical Research Letters*, 33(3), L03706.
<https://doi.org/10.1029/2005GL024954>

García, G. A., Serrago, R. A., González, F. G., Slafer, G. A., Reynolds, M. P., & Miralles, D. J. (2014). Wheat grain number: Identification of favourable

- physiological traits in an elite doubled-haploid population. *Field Crops Research*, 168, 126–134. <https://doi.org/10.1016/J.FCR.2014.07.018>
- Gebbing, T., & Schnyder, H. (1999). Pre-Anthesis Reserve Utilization for Protein and Carbohydrate Synthesis in Grains of Wheat. *Plant Physiology*, 121(3), 871–878. <https://doi.org/10.1104/PP.121.3.871>
- Gerard, G. S., Alqudah, A., Lohwasser, U., Börner, A., & Simón, M. R. (2020). Uncovering the genetic architecture of fruiting efficiency in bread wheat (*Triticum aestivum* L.): a viable alternative to increase yield potential. *Crop Science*, 59(5), 1853–1869. <https://doi.org/10.2135/CROPSCI2018.10.0639>
- Gianibelli, M. C., Wrigley, C. W., & MacRitchie, F. (2002). Polymorphism of Low Mr Glutenin Subunits in *Triticum tauschii*. *Journal of Cereal Science*, 35(3), 277–286. <https://doi.org/10.1006/jcrs.2001.0424>
- Gibb, D. J., Hao, X., & McAllister, T. A. (2008). Effect of dried distillers' grains from wheat on diet digestibility and performance of feedlot cattle. *Canadian Journal of Animal Science*, 88(4), 659–665. <https://doi.org/10.4141/CJAS08040>
- Gill, B. S., & Friebe, B. (2002). Cytogenetics , phylogeny and evolution of cultivated wheats. *Bread Wheat Improvement and Production*, 30, 71–88. <http://www.fao.org/docrep/006/y4011e/y4011e07.htm>
- Giunta, F., Pruneddu, G., & Motzo, R. (2009). Radiation interception and biomass and nitrogen accumulation in different cereal and grain legume species. *Field Crops Research*, 110(1), 76–84. <https://doi.org/10.1016/J.FCR.2008.07.003>
- González, F. G., Slafer, G. A., & Miralles, D. J. (2003). Grain and floret number in response to photoperiod during stem elongation in fully and slightly vernalized wheats. *Field Crops Research*, 81(1), 17–27. [https://doi.org/10.1016/S0378-4290\(02\)00195-8](https://doi.org/10.1016/S0378-4290(02)00195-8)
- González, F. G., Terrile, I. I., & Falcón, M. O. (2011). Spike fertility and duration of stem elongation as promising traits to improve potential grain number (and yield): Variation in modern Argentinean wheats. *Crop Science*, 51(4), 1693–1702. <https://doi.org/10.2135/CROPSCI2010.08.0447>

Gonzalez-Navarro, O. E., Griffiths, S., Molero, G., Reynolds, M. P., & Slafer, G. A. (2016). Variation in developmental patterns among elite wheat lines and relationships with yield, yield components and spike fertility. *Field Crops Research*, 196, 294–304. <https://doi.org/10.1016/j.fcr.2016.07.019>

Graybosch, R. A., & Peterson, C. J. (2010). Genetic improvement in winter wheat yields in the Great Plains of North America, 1959-2008. *Crop Science*, 50(5), 1882–1890. <https://doi.org/10.2135/cropsci2009.11.0685>

Gregg, J. S., Bolwig, S., Hansen, T., Solér, O., Amer-Allam, S. ben, Viladecans, J. P., Klitkou, A., & Fevolden, A. (2017). Value chain structures that define European cellulosic ethanol production. *Sustainability (Switzerland)*, 9(1), 1–17. <https://doi.org/10.3390/su9010118>

Guo, Z., Slafer, G. A., & Schnurbusch, T. (2016). Genotypic variation in spike fertility traits and ovary size as determinants of floret and grain survival rate in wheat. *Journal of Experimental Botany*, 67(14), 4221–4230. <https://doi.org/10.1093/JXB/ERW200>

Haas, M., Schreiber, M., & Mascher, M. (2019). Domestication and crop evolution of wheat and barley: Genes, genomics, and future directions. *Journal of Integrative Plant Biology*, 61(3), 204–225. <https://doi.org/10.1111/JIPB.12737>

Hanssen-bauer, I., & Førland, E. (2000). TEMPERATURE AND PRECIPITATION VARIATIONS IN NORWAY 1900 – 1994 AND THEIR LINKS TO ATMOSPHERIC CIRCULATION. *INTERNATIONAL JOURNAL OF CLIMATOLOGY Int. J. Climatol*, 17(8), 1693–1708. http://jostemikk.com/PDF/Hanssen-Bauer_et_al-2000-International_Journal_of_Climatology.pdf

Hassan, M. A., Yang, M., Rasheed, A., Yang, G., Reynolds, M., Xia, X., Xiao, Y., & He, Z. (2019). A rapid monitoring of NDVI across the wheat growth cycle for grain yield prediction using a multi-spectral UAV platform. *Plant Science*, 282, 95–103. <https://doi.org/10.1016/J.PLANTSCI.2018.10.022>

Hedden, P. (2003). The genes of the Green Revolution. *Trends Genet*, 19(1), 5–9. [https://doi.org/10.1016/s0168-9525\(02\)00009-4](https://doi.org/10.1016/s0168-9525(02)00009-4)

Hew, L. I., Ravindran, V., Mollah, Y., & Bryden, W. L. (1998). Influence of exogenous xylanase supplementation on apparent metabolisable energy and amino acid digestibility in wheat for broiler chickens. *Animal Feed Science and Technology*, 75(2), 83–92. [https://doi.org/10.1016/S0377-8401\(98\)00206-5](https://doi.org/10.1016/S0377-8401(98)00206-5)

Hoffstetter, A., Cabrera, A., & Sneller, C. (2016). Identifying quantitative trait loci for economic traits in an elite soft red winter wheat population. *Crop Science*, 56(2), 547–558. <https://doi.org/10.2135/CROPSCI2015.06.0332>

Hoisington, D., Bohorova, N., Fennell, S., Khairallah, M., Pellegrineschi, A., & Ribaut, J. M. (2007). The application of biotechnology to wheat improvement. *Bread Wheat Improvement and Production. Plant Production and Protection*, 1–21. <http://www.fao.org/docrep/006/Y4011E/y4011e0d.htm#bm13>

Horton, P., Ruban, A. v., & Wentworth, M. (2000). Allosteric regulation of the light-harvesting system of photosystem II. *Philosophical Transactions of the Royal Society of London. Series B: Biological Sciences*, 355(1402), 1361–1370. <https://doi.org/10.1098/RSTB.2000.0698>

Hu, B., Wang, W., Ou, S., Tang, J., Li, H., Che, R., Zhang, Z., Chai, X., Wang, H., Wang, Y., Liang, C., Liu, L., Piao, Z., Deng, Q., Deng, K., Xu, C., Liang, Y., Zhang, L., Li, L., & Chu, C. (2015). Variation in NRT1.1B contributes to nitrate-use divergence between rice subspecies. *Nature Genetics*, 47(7), 834–838. <https://doi.org/10.1038/NG.3337>

Huang, J., Wang, H., Dai, Q., & Han, D. (2014). Analysis of NDVI data for crop identification and yield estimation. *IEEE Journal of Selected Topics in Applied Earth Observations and Remote Sensing*, 7(11), 4374–4384. <https://doi.org/10.1109/JSTARS.2014.2334332>

Hubbart, S., Smillie, I. R. A., Heatley, M., Swarup, R., Foo, C. C., Zhao, L., & Murchie, E. H. (2018). Enhanced thylakoid photoprotection can increase yield and canopy radiation use efficiency in rice. *Communications Biology* 2018 1:1, 1(1), 1–12. <https://doi.org/10.1038/s42003-018-0026-6>

Jabłoński B, Ogonowska H, Szala K, Bajguz A, Orczyk W, Nadolska-Orczyk A. Silencing of *TaCKX1* Mediates Expression of Other *TaCKX* Genes to Increase Yield Parameters in Wheat. *Int J Mol Sci*.

2020 Jul 7;21(13):4809. doi: 10.3390/ijms21134809. PMID: 32645965; PMCID: PMC7369774.

Karl, T. R., Knight, R. W., Karl, T. R., & Knight, R. W. (1998). Secular Trends of Precipitation Amount, Frequency, and Intensity in the United States. *Bulletin of the American Meteorological Society*, 79(2), 231–241. [https://doi.org/10.1175/1520-0477\(1998\)079<0231:STOPAF>2.0.CO;2](https://doi.org/10.1175/1520-0477(1998)079<0231:STOPAF>2.0.CO;2)

Kimber, G., & Riley, R. (1963). THE RELATIONSHIPS OF THE DIPLOID PROGENITORS OF HEXAPLOID WHEAT. *Canadian Journal of Genetics and Cytology*, 5(1), 83–88. <https://doi.org/10.1139/g63-012>

King, M., Altdorff, D., Li, P. et al. Northward shift of the agricultural climate zone under 21st-century global climate change. *Sci Rep* 8, 7904 (2018). <https://doi.org/10.1038/s41598-018-26321-8>

Kirby, E. J. M., Appleyard, M., & Simpson, N. A. (1994). Co-ordination of stem elongation and Zadoks growth stages with leaf emergence in wheat and barley. *Journal of Agricultural Science*, 122(01), 21–29. <https://doi.org/10.1017/S0021859600065746>

Korte, A., & Farlow, A. (2013). The advantages and limitations of trait analysis with GWAS: a review. *Plant Methods*, 9(1), 29. <https://doi.org/10.1186/1746-4811-9-29>

Kromdijk, J., Głowacka, K., Leonelli, L., Gabilly, S. T., Iwai, M., Niyogi, K. K., & Long, S. P. (2016). Improving photosynthesis and crop productivity by accelerating recovery from photoprotection. *Science*, 354(6314), 857–861. https://doi.org/10.1126/SCIENCE.AAI8878/SUPPL_FILE/KROMDIJK-SM.PDF

Kumar, S., Banks, T. W., & Cloutier, S. (2012). SNP Discovery through Next-Generation Sequencing and Its Applications. *International Journal of Plant Genomics*, 2012, 15. <https://doi.org/10.1155/2012/831460>

Lambin, E. F., & Meyfroidt, P. (2011). Global land use change, economic globalization, and the looming land scarcity. *Proceedings of the National Academy of Sciences of the United States of America*, 108(9), 3465–3472. <https://doi.org/10.1073/pnas.1100480108>

Lantican, M. A., Dubin, H. J., & Morris, M. L. (2005). Impacts of International Wheat Breeding Research in the Developing Countries. In *Developing World. CIMMYT*.

<http://repository.cimmyt.org/xmlui/bitstream/handle/10883/1048/81297.pdf?sequence=4&isAllowed=y>

Large, E. C. (1954). GROWTH STAGES IN CEREALS ILLUSTRATION OF THE FEEKES SCALE. *Plant Pathology*, 3(4), 128–129.

<https://doi.org/10.1111/j.1365-3059.1954.tb00716.x>

Lazaro, L., & Abbate, P. E. (2011). Cultivar effects on relationship between grain number and photothermal quotient or spike dry weight in wheat.

Journal of Agricultural Science, 150, 442–459.

<https://doi.org/10.1017/s0021859611000736>

Lehner, B., Döll, P., Alcamo, J., Henrichs, T., & Kaspar, F. (2006). Estimating the impact of global change on flood and drought risks in Europe: A continental, integrated analysis. *Climatic Change*, 75(3), 273–299.

<https://doi.org/10.1007/s10584-006-6338-4>

Lev-Yadun, S. (2000). ARCHAEOLOGY:Enhanced: The Cradle of Agriculture. *Science*, 288(5471), 1602–1603.

<https://doi.org/10.1126/science.288.5471.1602>

Li, X., Guo, T., Wang, J., Bekele, W. A., Sukumaran, S., Vanous, A. E., McNellie, J. P., Cortes, L. T., Lopes, M. S., Lamkey, K. R., Westgate, M. E., McKay, J. K., Archontoulis, S. v., Reynolds, M. P., Tinker, N. A., Schnable, P. S., & Yu, J. (2021). An integrated framework reinstating the environmental dimension for GWAS and genomic selection in crops. *Molecular Plant*, 14(6), 874–887. <https://doi.org/10.1016/J.MOLP.2021.03.010>

Liakat Ali, M., Stephen Baenziger, P., al Ajlouni, Z., Todd Campbell, B., Gill, K. S., Eskridge, K. M., Mujeeb-Kazi, A., & Dweikat, I. (2011). Mapping QTL for agronomic traits on wheat chromosome 3A and a comparison of recombinant inbred chromosome line populations. *Crop Science*, 51(2), 553–566. <https://doi.org/10.2135/CROPSCI2010.06.0359>

Liu, B., Zhang, B., Yang, Z., Liu, Y., Yang, S., Shi, Y., Jiang, C., & Qin, F. (2021). Manipulating ZmEXPA4 expression ameliorates the drought-induced

prolonged anthesis and silking interval in maize. *The Plant Cell*, 33(6), 2058–2071. <https://doi.org/10.1093/PLCELL/KOAB083>

Li, Y., Song, G., Gao, J. et al. Enhancement of grain number per spike by RNA interference of cytokinin oxidase 2 gene in bread wheat. *Hereditas* 155, 33 (2018). <https://doi.org/10.1186/s41065-018-0071-7>

Lobell, D. B., & Field, C. B. (2007). Global scale climate–crop yield relationships and the impacts of recent warming. *Environmental Research Letters*, 2(1), 014002. <https://doi.org/10.1088/1748-9326/2/1/014002>

Lobell, D. B., Schlenker, W., & Costa-Roberts, J. (2011). Climate trends and global crop production since 1980. *Science*, 333(6042), 616–620. <https://doi.org/10.1126/SCIENCE.1204531>

Lopes, M. S., Reynolds, M. P., Jalal-Kamali, M. R., Moussa, M., Feltaous, Y., Tahir, I. S. A., Barma, N., Vargas, M., Mannes, Y., & Baum, M. (2012). The yield correlations of selectable physiological traits in a population of advanced spring wheat lines grown in warm and drought environments. *Field Crop Res*, 128, 129–136. <https://doi.org/10.1016/j.fcr.2011.12.017>

Lopes, M. S., Reynolds, M. P., Manes, Y., Singh, R. P., Crossa, J., & Braun, H. J. (2012). Genetic yield gains and changes in associated traits of CIMMYT spring bread wheat in a “historic” set representing 30 years of breeding. *Crop Sci*, 52(3), 1123. <https://doi.org/10.2135/cropsci2011.09.0467>

Loss, S. P., & Siddique, K. H. M. (1994). Morphological and Physiological Traits Associated with Wheat Yield Increases in Mediterranean Environments. *Advances in Agronomy*, 52(C), 229–276. [https://doi.org/10.1016/S0065-2113\(08\)60625-2](https://doi.org/10.1016/S0065-2113(08)60625-2)

Love, Bethany (2022) *Plant hormones associated with increasing grain number and yield potential in wheat (Triticum aestivum L.) and their genetic regulation*. PhD thesis, University of Nottingham

Lucas, H. (2012). Breakout session P1.1 National Food Security – The Wheat Initiative – an International Research Initiative for Wheat Improvement Context – the problems being addressed. GCARD - Second Global Conference on Agricultural Research for Development, September, 1–3.

[http://www.fao.org/docs/eims/upload/306175/Briefing Paper \(3\)-Wheat Initiative - H el ene Lucas.pdf](http://www.fao.org/docs/eims/upload/306175/Briefing Paper (3)-Wheat Initiative - H el ene Lucas.pdf)

Luo, M. C., Yang, Z. L., You, F. M., Kawahara, T., Waines, J. G., & Dvorak, J. (2007). The structure of wild and domesticated emmer wheat populations, gene flow between them, and the site of emmer domestication. *Theoretical and Applied Genetics*, 114(6), 947–959. <https://doi.org/10.1007/s00122-006-0474-0>

Ma, F., Xu, Y., Ma, Z., Li, L., & An, D. (2018). Genome-wide association and validation of key loci for yield-related traits in wheat founder parent Xiaoyan 6. *Molecular Breeding*, 38(7). <https://doi.org/10.1007/S11032-018-0837-7>

Ma, H., Xu, S. P., Luo, D., Xu, Z. H., & Xue, H. W. (2004). OsPIP1K1, a rice phosphatidylinositol monophosphate kinase, regulates rice heading by modifying the expression of floral induction genes. *Plant Molecular Biology*, 54(2), 295–310. <https://doi.org/10.1023/B:PLAN.0000028796.14336.24>

Ma, J., Ding, P., Liu, J., Li, T., Zou, Y., Habib, A., Mu, Y., Tang, H., Jiang, Q., Liu, Y., Chen, G., Wang, J., Deng, M., Qi, P., Li, W., Pu, Z., Zheng, Y., Wei, Y., & Lan, X. (2019). Identification and validation of a major and stably expressed QTL for spikelet number per spike in bread wheat. *Theoretical and Applied Genetics*, 132(11), 3155–3167. <https://doi.org/10.1007/S00122-019-03415-Z/FIGURES/5>

Mall, R. K., Singh, R., Gupta, A., Srinivasan, G., & Rathore, L. S. (2006). Impact of Climate Change on Indian Agriculture: A Review. *Climatic Change*, 78(2–4), 445–478. <https://doi.org/10.1007/s10584-005-9042-x>

Man es, Y., Gomez, H. F., Puhl, L., Reynolds, M., Braun, H. J., & Trethowan, R. (2012). Genetic Yield Gains of the CIMMYT International Semi-Arid Wheat Yield Trials from 1994 to 2010. *Crop Science*, 52(4), 1543. <https://doi.org/10.2135/cropsci2011.10.0574>

Meehl, G. A., Arblaster, J. M., & Tebaldi, C. (2005). Understanding future patterns of increased precipitation intensity in climate model simulations. *Geophysical Research Letters*, 32(18), 1–4. <https://doi.org/10.1029/2005GL023680>

- Melrose, J., Perroy, R., & Careas, S. (2015). World population prospects. United Nations, 1(6042), 587–592.
<https://doi.org/10.1017/CBO9781107415324.004>
- Meng, J., Du, X., & Wu, B. (2013). Generation of high spatial and temporal resolution NDVI and its application in crop biomass estimation. *Http://Dx.Doi.Org/10.1080/17538947.2011.623189*, 6(3), 203–218.
<https://doi.org/10.1080/17538947.2011.623189>
- Miralles, D. J., & Slafer, G. A. (2007). Sink limitations to yield in wheat : how could it be reduced?
<https://doi.org/https://doi.org/10.1017%2fs0021859607006752>
- MIRALLES, D. J., SLAFER, G. A., & RICHARDS, R. A. (2003). Influence of historic photoperiod during stem elongation on the number of fertile florets in wheat. *The Journal of Agricultural Science*, 141(2), 155–158.
<https://doi.org/10.1017/S0021859603003551>
- Mkhabela, M. S., Bullock, P., Raj, S., Wang, S., & Yang, Y. (2011). Crop yield forecasting on the Canadian Prairies using MODIS NDVI data. *Agricultural and Forest Meteorology*, 151(3), 385–393.
<https://doi.org/10.1016/J.AGRFORMET.2010.11.012>
- Neumann, K., Kobiljski, B., Denčić, S., Varshney, R. K., & Börner, A. (2011). Genome-wide association mapping: a case study in bread wheat (*Triticum aestivum* L.). *Mol Breed*, 27(1), 37–58. <https://doi.org/10.1007/s11032-010-9411-7>
- Nikulin, G., Kjellström, E., Hansson, U., Strandberg, G., & Ullerstig, A. (2011). Evaluation and future projections of temperature, precipitation and wind extremes over Europe in an ensemble of regional climate simulations. *Tellus, Series A: Dynamic Meteorology and Oceanography*, 63(1), 41–55.
<https://doi.org/10.1111/j.1600-0870.2010.00466.x>
- Ogbonnaya, F. C., Rasheed, A., Okechukwu, E. C., Jighly, A., Makdis, F., Wuletaw, T., Hagra, A., Uguru, M. I., & Agbo, C. U. (2017). Genome-wide association study for agronomic and physiological traits in spring wheat evaluated in a range of heat prone environments. *Theoretical and Applied Genetics*, 130(9), 1819–1835. <https://doi.org/10.1007/S00122-017-2927-Z>

- Olesen, J. E., & Bindi, M. (2002). Consequences of climate change for European agricultural productivity, land use and policy. In *European Journal of Agronomy* (Vol. 16, Issue 4, pp. 239–262). Elsevier.
[https://doi.org/10.1016/S1161-0301\(02\)00004-7](https://doi.org/10.1016/S1161-0301(02)00004-7)
- Pask, A. (2009). Optimising nitrogen storage in wheat canopies for genetic reduction in fertiliser nitrogen inputs. <http://eprints.nottingham.ac.uk/12567/>
- Payne, P. I., Nightingale, M. A., Krattiger, A. F., & Holt, L. M. (1987). The relationship between HMW glutenin subunit composition and the bread making quality of British grown wheat varieties. *Journal of the Science of Food and Agriculture*, 40(1), 51–65.
- Peltonen-Sainio, P., Jauhiainen, L., & Laurila, I. P. (2009). Cereal yield trends in northern European conditions: Changes in yield potential and its realisation. *Field Crops Research*, 110(1), 85–90.
<https://doi.org/10.1016/J.FCR.2008.07.007>
- Peng, J., Richards, D. E., Hartley, N. M., Murphy, G. P., Devos, K. M., Flintham, J. E., Beales, J., Fish, L. J., Worland, A. J., Pelica, F., Sudhakar, D., Christou, P., Snape, J. W., Gale, M. D., & Harberd, N. P. (1999). 'Green revolution' genes encode mutant gibberellin response modulators. *Nature*, 400(6741), 256–261. <https://doi.org/10.1038/22307>
- Piao, S., Ciais, P., Huang, Y., Shen, Z., Peng, S., Li, J., Zhou, L., Liu, H., Ma, Y., Ding, Y., Friedlingstein, P., Liu, C., Tan, K., Yu, Y., Zhang, T., & Fang, J. (2010). The impacts of climate change on water resources and agriculture in China. *Nature*, 467(7311), 43–51. <https://doi.org/10.1038/nature09364>
- Piñera-Chavez, F. J., Berry, P. M., Foulkes, M. J., Molero, G., & Reynolds, M. P. (2016). Avoiding lodging in irrigated spring wheat. II. Genetic variation of stem and root structural properties. *Field Crops Research*, 196, 64–74.
<https://doi.org/10.1016/J.FCR.2016.06.007>
- Pinto, R. S., Reynolds, M. P., Mathews, K. L., McIntyre, C. L., Olivares-Villegas, J. J., & Chapman, S. C. (2010). Heat and drought adaptive QTL in a wheat population designed to minimize confounding agronomic effects. *Theor Appl Genet*, 121(6), 1001–1021. <https://doi.org/10.1007/s00122-010-1351-4>

PJ, L. V., DJ, M., & RA, S. (n.d.). Genetic progress in Argentine bread wheat varieties released between 1918 and 2011: Changes in physiological and numerical yield components. *Field Crops Research*, 221, 314–321.

Pradhan, S., Babar, M. A., Robbins, K., Bai, G., Mason, R. E., Khan, J., Shahi, D., Avci, M., Guo, J., Maksud Hossain, M., Bhatta, M., Mergoum, M., Asseng, S., Amand, P. S., Gezan, S., Baik, B. K., Blount, A., & Bernardo, A. (2019). Understanding the Genetic Basis of Spike Fertility to Improve Grain Number, Harvest Index, and Grain Yield in Wheat Under High Temperature Stress Environments. *Frontiers in Plant Science*, 10, 1481. <https://doi.org/10.3389/FPLS.2019.01481/BIBTEX>

Preston, J. C., & Hileman, L. C. (2013). Functional evolution in the plant SQUAMOSA-PROMOTER BINDING PROTEIN-LIKE (SPL) gene family. *Frontiers in Plant Science*, 4(APR), 80. <https://doi.org/10.3389/FPLS.2013.00080/ABSTRACT>

Pretini, N., Alonso, M. P., Vanzetti, L. S., Pontaroli, A. C., & González, F. G. (2021). The physiology and genetics behind fruiting efficiency: a promising spike trait to improve wheat yield potential. *Journal of Experimental Botany*, 72(11), 3987–4004. <https://doi.org/10.1093/JXB/ERAB080>

Qaseem, M. F., Qureshi, R., Muqaddasi, Q. H., Shaheen, H., Kousar, R., & Röder, M. S. (2018). Genome-wide association mapping in bread wheat subjected to independent and combined high temperature and drought stress. *PLoS ONE*, 13(6). <https://doi.org/10.1371/JOURNAL.PONE.0199121>

Qaseem MF, Qureshi R, Shaheen H, Shafqat N (2019) Genome-wide association analyses for yield and yield-related traits in bread wheat (*Triticum aestivum* L.) under pre-anthesis combined heat and drought stress in field conditions. *PLOS ONE* 14(3): e0213407. <https://doi.org/10.1371/journal.pone.0213407>

Rabinovich, S. v. (1998). Importance of wheat-rye translocations for breeding modern cultivars of *Triticum aestivum* L. (Reprinted from *Wheat: Prospects for global improvement*, 1998). *Euphytica*, 100(1/3), 323–340. <https://doi.org/10.1023/a:1018361819215>

Radhouane, L. (2013). Climate change impacts on North African countries and on some Tunisian economic sectors. *Journal of Agriculture and Environment for International Development (JAEID)*, 107(1), 101–113. <https://doi.org/10.12895/JAEID.20131.123>

Rajala, A., Hakala, K., Mäkelä, P., Muurinen, S., & Peltonen-Sainio, P. (2009). Spring wheat response to timing of water deficit through sink and grain filling capacity. *Field Crops Research*, 114(2), 263–271. <https://doi.org/10.1016/J.FCR.2009.08.007>

Rajkumara, S. (2008). Lodging in Cereals- A review. *Agric. Rev.*, 29(1), 55–60. <http://www.arccjournals.com/journal/agricultural-reviews/ARCC2487>

Reitan, L. (1980). Genetical aspects of seed dormancy in wheat related to seed coat colour in an 8 X 8 diallele cross. *Cereal Research Communications*, 8(1), 272–285. <https://www.cabdirect.org/cabdirect/abstract/19801689244>

Rejesus, R. M., Heisey, P. W., & Smale, M. (1999). Sources of Productivity Growth in Wheat: A Review of Recent Performance and Medium- to Long-Term Prospects. CIMMYT Economics Paper 99-05. <http://repository.cimmyt.org/xmlui/bitstream/handle/10883/982/67583.pdf?sequence=1&isAllowed=y>

Reynolds, M., Balota, M., Delgado, M., Amani, I., & Fischer, R. (1994). Physiological and Morphological Traits Associated With Spring Wheat Yield Under Hot, Irrigated Conditions. *Australian Journal of Plant Physiology*, 21(6), 717. <https://doi.org/10.1071/PP9940717>

Reynolds, M., Bonnett, D., Chapman, S. C., Furbank, R. T., Manès, Y., Mather, D. E., & Parry, M. A. J. (2011). Raising yield potential of wheat. I. Overview of a consortium approach and breeding strategies. *Journal of Experimental Botany*, 62(2), 439–452. <https://doi.org/10.1093/jxb/erq311>

Reynolds, M., Foulkes, J., Furbank, R., Griffiths, S., King, J., Murchie, E., Parry, M., & Slafer, G. (2012). Achieving yield gains in wheat. *Plant, Cell and Environment*, 35(10), 1799–1823. <https://doi.org/10.1111/j.1365-3040.2012.02588.x>

Reynolds, M., Foulkes, M. J., Slafer, G. A., Berry, P., Parry, M. A. J., Snape, J. W., & Angus, W. J. (2009). Raising yield potential in wheat. In *Journal of Experimental Botany* (Vol. 60, Issue 7, pp. 1899–1918). Oxford University Press. <https://doi.org/10.1093/jxb/erp016>

Reynolds, M., & Langridge, P. (2016). Physiological breeding. In *Current Opinion in Plant Biology* (Vol. 31, pp. 162–171). Elsevier Current Trends. <https://doi.org/10.1016/j.pbi.2016.04.005>

Rivera-Amada, C., Trujillo-Negrellos, E., Sylvester-Bradley, R., Molero, G., Sierra-Gonzalez, A., Reynolds, M. P., & Foulkes, M. J. (2016). Achieving increases in spike growth, fruiting efficiency, and harvest index in high biomass wheat cultivar. *Proceedings of the 2nd International TRIGO (Wheat) Yield Potential Workshop 2016*, 70–76. <http://repository.cimmyt.org/xmlui/bitstream/handle/10883/18171/58303.pdf?sequence=1&isAllowed=y#page=76>

Rivera-Amado, A. C. (2015). Identifying physiological traits to optimize assimilate partitioning and spike fertility for yield potential in wheat (*Triticum aestivum* L.) genotypes. PhD Thesis, University of Nottingham School of Biosciences, Sutton Bonnington Campus, Leicestershire, UK, September.

Rodrigues, O., Teixeira, M. C. C., Costenaro, E. R., Vargas, L., & Damo, R. (2014). Influence of Vernalization and Photoperiod on the Duration of Stem Elongation and Spikelet Fertility in Wheat. *Agricultural Sciences*, 05(December), 1547–1557. <https://doi.org/10.4236/as.2014.514166>

Rosegrant, M. W., Paisner, M. S., Meijer, S., & Witcover, J. (2001). 2020 Global Food Outlook Trends, Alternatives, and Choices A 2020 Vision for Food, Agriculture, and the Environment Initiative. *Bread Wheat Improvement and Production*. <https://ageconsearch.umn.edu/bitstream/15916/1/mi01ro01.pdf>

Sadras, V. O., & Lawson, C. (2011). Genetic gain in yield and associated changes in phenotype, trait plasticity and competitive ability of South Australian wheat varieties released between 1958 and 2007. *Crop and Pasture Science*, 62(7), 533–549. <https://doi.org/10.1071/CP11060>

- SANCHEZ-GARCIA, M., ROYO, C., APARICIO, N., MARTÍN-SÁNCHEZ, J. A., & ÁLVARO, F. (2013). Genetic improvement of bread wheat yield and associated traits in Spain during the 20th century. *The Journal of Agricultural Science*, 151(01), 105–118. <https://doi.org/10.1017/S0021859612000330>
- Sayre, K. D., Rajaram, S., & Fischer, R. A. (1997). Yield potential progress in short bread wheats in northwest Mexico. *Crop Science*, 37(1), 36–42. <https://doi.org/10.2135/cropsci1997.0011183X003700010006x>
- Schachtman, D. P., Lagudah, E. S., & Munns, R. (1992). The expression of salt tolerance from *Triticum tauschii* in hexaploid wheat. *Theoretical and Applied Genetics*, 84(5–6), 714–719. <https://doi.org/10.1007/BF00224174>
- Schlegel, R., & Korzun, V. (1997). About the origin of 1RS.1BL wheat-rye chromosome translocations from Germany. *Plant Breeding*, 116(6), 537–540. <https://doi.org/10.1111/j.1439-0523.1997.tb02186.x>
- Sears, E. (1944). Cytogenetic studies with polyploid species of wheat. II. Additional chromosomal aberrations in *Triticum vulgare*. *Genetics*, 29, 232–246. <https://www.ncbi.nlm.nih.gov/pmc/articles/PMC1209244/pdf/232.pdf>
- Sehgal, D., Singh, R., & Rajpal, V. R. (2016). Quantitative Trait Loci Mapping in Plants: Concepts and Approaches. 31–59. https://doi.org/10.1007/978-3-319-27090-6_2
- Sharma, R. C. (1995). Tiller mortality and its relationship to grain yield in spring wheat. *Field Crops Research*, 41(1), 55–60. [https://doi.org/10.1016/0378-4290\(94\)00109-P](https://doi.org/10.1016/0378-4290(94)00109-P)
- Sharma, R. C., Crossa, J., Velu, G., Huerta-Espino, J., Vargas, M., Payne, T. S., & Singh, R. P. (2012). Genetic gains for YLD in CIMMYT spring bread wheat across international environments. *Crop Sci*, 52(4), 1522. <https://doi.org/10.2135/cropsci2011.12.0634>
- Shearman, V. J., Sylvester-Bradley, R., Scott, R. K., & Foulkes, M. J. (2005). Physiological processes associated with wheat yield progress in the UK. *Crop Science*, 45(1), 175–185. <https://doi.org/10.2135/cropsci2005.0175>
- Shen, C., Yuan, J., Qiao, H., Wang, Z., Liu, Y., Ren, X., Wang, F., Liu, X., Zhang, Y., Chen, X., & Ou, X. (2020). Transcriptomic and anatomic profiling

reveal the germination process of different wheat varieties in response to waterlogging stress. *BMC Genetics*, 21(1). <https://doi.org/10.1186/S12863-020-00901-Y>

Shewry, W. P. R. (2009). DARWIN REVIEW. *Journal of Experimental Botany*, 60(6), 1537–1553. <https://doi.org/10.1093/jxb/erp058>

Shiferaw, B., Smale, M., Braun, H.-J., Duveiller, E., Reynolds, M., & Muricho, G. (2013). Crops that feed the world 10. Past successes and future challenges to the role played by wheat in global food security. *Food Security*, 5(3), 291–317. <https://doi.org/10.1007/s12571-013-0263-y>

Shinozuka, H., Cogan, N. O. I., Spangenberg, G. C., & Forster, J. W. (2012). Quantitative Trait Locus (QTL) meta-analysis and comparative genomics for candidate gene prediction in perennial ryegrass (*Lolium perenne* L.). *BMC Genetics*, 13(1), 1–12. <https://doi.org/10.1186/1471-2156-13-101/FIGURES/3>

Siddique, K. H. M., Kirby, E. J. M., & Perry, M. W. (1989). Ear: Stem ratio in old and modern wheat varieties; relationship with improvement in number of grains per ear and yield. *Field Crops Research*, 21(1), 59–78. [https://doi.org/10.1016/0378-4290\(89\)90041-5](https://doi.org/10.1016/0378-4290(89)90041-5)

Sierra-Gonzalez, A., Molero, G., Rivera-Amado, C., Babar, M. A., Reynolds, M. P., & Foulkes, M. J. (2021). Exploring genetic diversity for grain partitioning traits to enhance yield in a high biomass spring wheat panel. *Field Crops Research*, 260, 107979. <https://doi.org/10.1016/J.FCR.2020.107979>

Sinclair, T. R., & Jamieson, P. D. (2008). Yield and grain number of wheat: A correlation or causal relationship?: Authors' response to "The importance of grain or kernel number in wheat: A reply to Sinclair and Jamieson" by R.A. Fischer. *Field Crops Research*, 105(1–2), 22–26. <https://doi.org/10.1016/J.FCR.2007.07.003>

Slafer, G. A., & Andrade, F. H. (1993). Physiological attributes related to the generation of grain yield in bread wheat cultivars released at different eras. *Field Crops Research*, 31(3–4), 351–367. [https://doi.org/10.1016/0378-4290\(93\)90073-V](https://doi.org/10.1016/0378-4290(93)90073-V)

Slafer, G. A., Andrade, F. H., & Feingold, S. E. (1990). Genetic improvement of bread wheat (*Triticum aestivum* L.) in Argentina: relationships between nitrogen and dry matter. *Euphytica* 1990 50:1, 50(1), 63–71.

<https://doi.org/10.1007/BF00023162>

Slafer, G. A., Elia, M., Savin, R., García, G. A., Terrile, I. I., Ferrante, A., Miralles, D. J., & González, F. G. (2015). Fruiting efficiency: An alternative trait to further rise wheat yield. *Food and Energy Security*, 4(2), 92–109.

<https://doi.org/10.1002/FES3.59>

Slafer, G., & Araus, J. (2007). Physiological traits for improving wheat yield under a wide range of conditions. *Scale and Complexity in Plant Systems*, 147–156. <https://doi.org/10.1007/1-4020-5906-X>

Slafer, G., & Rawson, H. (1994). Sensitivity of Wheat Phasic Development to Major Environmental Factors: a Re-Examination of Some Assumptions Made by Physiologists and Modellers. *Australian Journal of Plant Physiology*, 21(4), 393. <https://doi.org/10.1071/PP9940393>

Slewinski, T. L. (2012). Non-structural carbohydrate partitioning in grass stems: a target to increase yield stability, stress tolerance, and biofuel production. *Journal of Experimental Botany*, 63(13), 4647–4670.

<https://doi.org/10.1093/jxb/ers124>

Smith, P., Gregory, P. J., van Vuuren, D., Obersteiner, M., Havlík, P., Rounsevell, M., Woods, J., Stehfest, E., & Bellarby, J. (2010). Competition for land. *Philosophical Transactions of the Royal Society of London. Series B, Biological Sciences*, 365(1554), 2941–2957.

<https://doi.org/10.1098/rstb.2010.0127>

Soto-Cerda, B. J., & Cloutier, S. (n.d.). Association Mapping in Plant Genomes. <https://doi.org/10.5772/33005>

Stockman, Y. M., Fischer, R. A., & Brittain, E. G. (1983). Assimilate Supply and Floret Development Within the Spike of Wheat (*Triticum aestivum* L.). *Australian Journal of Plant Physiology*, 10(6), 585–594.

<https://doi.org/10.1071/PP9830585>

- Streck, N. A., Weiss, A., & Baenziger, P. S. (2003). A generalized vernalization response function for winter wheat. *Agronomy Journal*, 95(1), 155–159. <https://doi.org/10.2134/agronj2003.0155>
- Sukumaran, S., Dreisigacker, S., Lopes, M., Chavez, P., & Reynolds, M. P. (2014). Genome-wide association study for grain yield and related traits in an elite spring wheat population grown in temperate irrigated environments. *Theoretical and Applied Genetics* 2014 128:2, 128(2), 353–363. <https://doi.org/10.1007/S00122-014-2435-3>
- Sukumaran, S., Dreisigacker, S., Lopes, M., Chavez, P., & Reynolds, M. P. (2015). Genome-wide association study for grain yield and related traits in an elite spring wheat population grown in temperate irrigated environments. *Theoretical and Applied Genetics*, 128(2), 353–363. <https://doi.org/10.1007/S00122-014-2435-3>
- Sukumaran, S., Lopes, M., Dreisigacker, S., & Reynolds, M. (2018). Genetic analysis of multi-environmental spring wheat trials identifies genomic regions for locus-specific trade-offs for grain weight and grain number. *Theoretical and Applied Genetics*, 131(4), 985–998. <https://doi.org/10.1007/S00122-017-3037-7/TABLES/7>
- Sun, C., Zhang, F., Yan, X., Zhang, X., Dong, Z., Cui, D., & Chen, F. (2017). Genome-wide association study for 13 agronomic traits reveals distribution of superior alleles in bread wheat from the Yellow and Huai Valley of China. *Plant Biotechnology Journal*, 15(8), 953–969. <https://doi.org/10.1111/PBI.12690>
- Tattaris, M., Reynolds, M. P., & Chapman, S. C. (2016). A Direct Comparison of Remote Sensing Approaches for High-Throughput Phenotyping in Plant Breeding. *Frontiers in Plant Science*, 7(August), 1–9. <https://doi.org/10.3389/fpls.2016.01131>
- Terrile, I. I., Miralles, D. J., & González, F. G. (2017). Fruiting efficiency in wheat (*Triticum aestivum* L): Trait response to different growing conditions and its relation to spike dry weight at anthesis and grain weight at harvest. *Field Crops Research*, 201, 86–96. <https://doi.org/10.1016/j.fcr.2016.09.026>

van Ginkel, M., & Ogonnaya, F. (2007). Novel genetic diversity from synthetic wheats in breeding cultivars for changing production conditions. *Field Crops Research*, 104(1–3), 86–94. <https://doi.org/10.1016/j.fcr.2007.02.005>

Vernotte, C., Etienne, A. L., & Briantais, J. M. (1979). Quenching of the System II chlorophyll fluorescence by the plastoquinone pool. *Biochimica et Biophysica Acta (BBA) - Bioenergetics*, 545(3), 519–527. [https://doi.org/10.1016/0005-2728\(79\)90160-9](https://doi.org/10.1016/0005-2728(79)90160-9)

Villareal, R. L., Rajaram, S., Mujeeb-Kazi, A., & del Toro, E. (1991). The Effect of Chromosome 1B/1R Translocation on the Yield Potential of Certain Spring Wheats (*Triticum aestivum* L.). *Plant Breeding*, 106(1), 77–81. <https://doi.org/10.1111/j.1439-0523.1991.tb00482.x>

Voss-Fels, K. P., Stahl, A., Wittkop, B., Lichthardt, C., Nagler, S., Rose, T., Chen, T. W., Zetzsche, H., Seddig, S., Majid Baig, M., Ballvora, A., Frisch, M., Ross, E., Hayes, B. J., Hayden, M. J., Ordon, F., Leon, J., Kage, H., Friedt, W., ... Snowdon, R. J. (2019). Breeding improves wheat productivity under contrasting agrochemical input levels. *Nature Plants* 2019 5:7, 5(7), 706–714. <https://doi.org/10.1038/s41477-019-0445-5>

W Tadesse, F. O. A. J. M. S.-G. Q. S. S. R. M. B. (2015). Genome-wide association mapping of yield and grain quality traits in winter wheat genotypes. *PLOS ONE*.

Waddington, S. R., Ransom, J. K., Osmanzai, M., & Saunders, D. A. (1986). Improvement in the yield potential of bread wheat adapted to northwest Mexico. *Crop Science*, 26(4), 698–703. <https://doi.org/10.2135/cropsci1986.0011183X002600040012x>

Walkowiak, S., Gao, L., Monat, C., Haberer, G., Kassa, M. T., Brinton, J., Ramirez-Gonzalez, R. H., Kolodziej, M. C., Delorean, E., Thambugala, D., Klymiuk, V., Byrns, B., Gundlach, H., Bandi, V., Siri, J. N., Nilsen, K., Aquino, C., Himmelbach, A., Copetti, D., ... Pozniak, C. J. (2020). Multiple wheat genomes reveal global variation in modern breeding. *Nature* 2020 588:7837, 588(7837), 277–283. <https://doi.org/10.1038/s41586-020-2961-x>

Wang, H., He, Y., Qian, B., McConkey, B., Cutforth, H., McCaig, T., McLeod, G., Zentner, R., DePauw, R., Lemke, R., Brandt, K., Liu, T., Qin, X., White, J., Hunt, T., & Hoogenboom, G. (2012). Short Communication: Climate change and biofuel wheat: A case study of southern Saskatchewan. *Canadian Journal of Plant Science*, 92(3), 421–425. <https://doi.org/10.4141/cjps2011-192>

Wang, S. X., Zhu, Y. L., Zhang, D. X., Shao, H., Liu, P., Hu, J. B., Zhang, H., Zhang, H. P., Chang, C., Lu, J., Xia, X. C., Sun, G. lou, & Ma, C. X. (2017). Genome-wide association study for grain yield and related traits in elite wheat varieties and advanced lines using SNP markers. *PLoS ONE*, 12(11). <https://doi.org/10.1371/JOURNAL.PONE.0188662>

Wang, Y. Y., Cheng, Y. H., Chen, K. E., & Tsay, Y. F. (2018). Nitrate Transport, Signaling, and Use Efficiency. *Annual Review of Plant Biology*, 69, 85–122. <https://doi.org/10.1146/ANNUREV-ARPLANT-042817-040056>

Whitechurch, E. M., Slafer, G. A., & Miralles, D. J. (2007). Variability in the duration of stem elongation in wheat genotypes and sensitivity to photoperiod and vernalization. *Journal of Agronomy and Crop Science*, 193(2), 131–137. <https://doi.org/10.1111/j.1439-037X.2007.00259.x>

Whitest, E. M., & Wilson, F. E. A. (2006). Responses of grain yield, biomass and harvest index and their rates of genetic progress to nitrogen availability in ten winter wheat varieties. *Irish Journal of Agricultural and Food Research*, 45(1), 85–101.

Wik, M., Pingali, P., & Broca, S. (2008). Global Agricultural Performance: Past Trends and Future Prospects. *World Development Report 2008*, 1–39. <https://openknowledge.worldbank.org/handle/10986/9122>

William, H. M., Trethowan, A. R., & Crosby-Galvan, A. E. M. (2007). Wheat breeding assisted by markers: CIMMYT's experience. <https://doi.org/10.1007/s10681-007-9405-7>

Wu, J., Carver, B. F., & Goad, C. L. (1999). Kernel color variability of hard white and hard red winter wheat. *Crop Science*, 39(3), 634–638. <https://doi.org/10.2135/cropsci1999.0011183X003900020003x>

Yan, L., Loukoianov, A., Blechl, A., Tranquilli, G., Ramakrishna, W., SanMiguel, P., Bennetzen, J. L., Echenique, V., & Dubcovsky, J. (2004). The wheat VRN2 gene is a flowering repressor down-regulated by vernalization. *Science (New York, N.Y.)*, 303(5664), 1640–1644. <https://doi.org/10.1126/science.1094305>

Yan, L., Loukoianov, A., Tranquilli, G., Helguera, M., Fahima, T., & Dubcovsky, J. (2003). Positional cloning of the wheat vernalization gene VRN1. *Proceedings of the National Academy of Sciences of the United States of America*, 100(10), 6263–6268. <https://doi.org/10.1073/pnas.0937399100>

Yang, W., Liu, D., Li, J., Zhang, L., Wei, H., Hu, X., Zheng, Y., He, Z., & Zou, Y. (2009). Synthetic hexaploid wheat and its utilization for wheat genetic improvement in China. *Journal of Genetics and Genomics*, 36(9), 539–546. [https://doi.org/10.1016/S1673-8527\(08\)60145-9](https://doi.org/10.1016/S1673-8527(08)60145-9)

You, L., Rosegrant, M. W., Wood, S., & Sun, D. (2009). Impact of growing season temperature on wheat productivity in China. *Agricultural and Forest Meteorology*, 149(6–7), 1009–1014. <https://doi.org/10.1016/j.agrformet.2008.12.004>

Yu, L. X., Lorenz, A., Rutkoski, J., Singh, R. P., Bhavani, S., Huerta-Espino, J., & Sorrells, M. E. (2011). Association mapping and gene-gene interaction for stem rust resistance in CIMMYT spring wheat germplasm. *Theor Appl Genet*, 123(8), 1257–1268. <https://doi.org/10.1007/s00122-011-1664-y>

Yue, B., Xue, W., Xiong, L., Yu, X., Luo, L., Cui, K., Jin, D., Xing, Y., & Zhang, Q. (2006). Genetic basis of drought resistance at reproductive stage in rice: separation of drought resistance from drought avoidance. *Genetics*, 172(2), 1213–1228. <https://doi.org/10.1534/genetics.105.045062>

YuMin, Y., QingYu, Z., Jun, L., HuiTing, W., XiaoRong, H., ZhengSong, P., & WuYun, Y. (2012). Detection of the introgression loci in *Triticum aestivum* transferred from *Aegilops tauschii* by simple sequence repeat (SSR) markers. *African Journal of Biotechnology*, 11(58 PG-12167–12172), 12167–12172. <https://doi.org/10.5897/AJB12.677>

- Zadoks, J. C., Chang, T. T., & Konzak, C. F. (1974). A decimal code for the growth stages of cereals. *Weed Research*, 14(6), 415–421.
<https://doi.org/10.1111/j.1365-3180.1974.tb01084.x>
- Zhai, P., Zhang, X., Wan, H., & Pan, X. (2005). Trends in total precipitation and frequency of daily precipitation extremes over China. *Journal of Climate*, 18(7), 1096–1108. <https://doi.org/10.1175/JCLI-3318.1>
- [Xiao Zhang and Ximing Cai \(2011\). Climate change impacts on global agricultural land availability Environmental. Research. Letters. 6 014014.](#)
<https://doi.org/10.1088/1748-9326/6/1/014014>
- Zheng C, Zhu Y, Wang C, Guo T (2016) Wheat Grain Yield Increase in Response to Pre-Anthesis Foliar Application of 6-Benzylaminopurine Is Dependent on Floret Development. *PLOS ONE* 11(6):
e0156627. <https://doi.org/10.1371/journal.pone.0156627>
- Zhu, C., Gore, M., Buckler, E. S., & Yu, J. (2008). Status and prospects of association mapping in plants. *Plant Genome J*, 1(1), 5.
<https://doi.org/10.3835/plantgenome2008.02.0089>
- Zohary, Daniel., Hopf, Maria., & Weiss, Ehud. (2012). *Domestication of plants in the Old World: the origin and spread of cultivated plants in south-west Asia, Europe, and the Mediterranean Basin*. Oxford University Press.
<https://global.oup.com/academic/product/domestication-of-plants-in-the-old-world-9780199549061?cc=gb&lang=en&>

8. Appendix

Appendix Table 7.1 KWS Panel genotypes and parental backgrounds

Entrynumber_Original	Genotype Original	Pedigree Original
1	Gravity	KWS Santiago x Oakley x Scout
2	Graham	Expert x Premio
3	Gleam	Hereford x KWS Kielder
4	Skyscapper	Cassius x KWS Santiago x NAWW29
5	Kerrin	KWS Santiago x W177
6	Silverstone	KWS Sterling x JB_Diego
7	W346	KWS Silverstone x Reflection
8	Barrel	Bantam x Viscount
9	Basset	Cassius x Scout
10	Cordiale	Reaper x Cadenza x Malacca
11	Crispin	Conqueror x W134
12	Croft	(Deben x Robigus) x Robigus
13	Grafton	Cordiale x W97

14	Humber	Anglo x Krakatoa
15	Jackal	Santiago x W177
16	Kielder	Brompton x Oakley
17	Leeds	ISTABRACQ x ROBIGUS
18	Lili	Horizon x W134
19	Robigus	1366 Putch x Capet
20	Santiago	Sherborne x Oakley
21	Siskin	Sterling x W 134
22	Trinity	(Grafton x Einstein) x W134
23	Zyatt	Hereford x KWS Quartz
24	Huckerby	W191 x Humber
25	Solo	CPBT W105 x Istabraq
26	Tempo	W151 x W134
27	JB_Diego	3351B2 x STRU2374
28	Costello	W151 x W134
29	Crusoe	Cordiale x Gulliver
30	Reflection	DENMAN x OAKLEY
31	Revelation	(Alchemy x Claire) x Shepherd
32	Skyfall	C4148 x Hurricane
33	Stigg	(Biscay x Septoria resistant line) x Tanker
34	TC16_118	Cougar x Rowan
35	TC16_125	W215 x Leeds
36	TC16_128	W220 x Santiago
37	TC16_133	W222 x Sterling

38	TC16_149	(Tuxedo x Rowan) x Beluga
39	TC16_166	Kielder x Dickens
40	TC16_171	Tempo x Santiago
41	TC16_175	Gator x Reflection
42	TC16_193	Kielder x Basset
43	TC16_315	Basmati(MH09-16) x Cashel
44	TC16_330	Revelation x JBDiego
45	TC16_332	Relay x Horatio
46	TC16_335	Tuxedo x Rowan
47	TC16_358	Kielder x Horatio
48	TC16_371	W218 x Kielder
49	TC16_374	W220 x Kielder
50	TC16_407	Grafton x Evolution
51	TC16_415	Solstice x Costello
52	TC16_417	Solstice x Trinity
53	TC16_441	Twister x Tu x edo
54	TC16_466	Croft x Costello
55	TC16_479	Kielder x Dickens
56	TC16_484	W192 x Costello
57	TC16_493	Bonham x Costello
58	TC16_514	W213 x Costello
59	TC16_526	Tempo x Kielder
60	TC16_536	Crispin x Santiago
61	TC16_537	Crispin x Gator
62	TC16_547	W234 x Tu x edo

63	TC16_602	(Cougar x Tu x edo) x Leeds
64	TC16_622	(W218 x Tu x edo) x Invicta
65	TC16_82	Viscount x Croft
66	TC16_84	KWDH10109-07 x 09-6
67	TC16_97	Twister x Tuxedo
68	W279	Horizon x Santiago
69	W295	Horizon x KWS W194
70	W309	Denman x Sterling
71	W310	W177 x JBDiego
72	W312	Horizon x Cleveland
73	W320	Cougar x Rowan
74	W321	Cougar x Rowan
75	Skyfall (1)	C4148 x Hurricane
76	W344	KWS Gator x Reflection
77	St16_36647	Santiago x Zulu
78	St16_37680	Revelation x Costello
79	St16_38736	Twister x Tempo
80	St16_38763	Twister x Tempo
81	St16_38812	Twister x Tempo
82	St16_38839	Twister x Tempo
83	St16_38855	Twister x Tempo
84	St16_39414	Kielder x Silverstone
85	St16_40182	Evolution x Lili
86	St16_40243	Evolution x Lili
87	St16_40667	Revelation x Costello

88	St16_41130	Leeds x Revelation
89	St16_41346	Leeds x Revelation
90	St16_41372	Leeds x Revelation
91	St16_41581	Leeds x Revelation
92	St16_41754	Silverstone x Reflection
93	St16_41954	Reflection x Lili
94	St15_34646	Leeds x W235
95	St15_34755	Croft x SY111978
96	St15_34760	Croft x SY111978
97	St15_34762	Croft x SY111978
98	St15_34957	W236 x SY111978
99	St15_35050	W237 x SY111978
100	St15_35217	Leeds x Revelation
101	St15_35289	Croft x SY111978
102	St15_35489	W237 x SY111978
103	St15_35594	Leeds x W235
104	St15_35598	Leeds x W235
105	St15_35607	Leeds x W235
106	St15_35701	W227 x W239
107	St15_35704	W227 x W239
108	St15_35866	SEWC111 x SY111978
109	St15_35870	SEWC111 x SY111978
110	St15_36102	Evolution x SY111978
111	St15_36207	Croft x SY111978
112	St15_36393	SEWC111 x SY111978

113	St15_36407	Zulu x SY111978
114	St15_36413	Evolution x SY111978
115	St14_34872	Kielder x Basset
116	St13_23212	W192 x W207
117	St13_23343	W193 x Relay
118	St13_23580	W196 x Beluga
119	St13_23780	Horatio x Tu x edo
120	St13_24090	W178 x MH09_28
121	St13_24200	W193 x Relay
122	St13_24243	W196 x Beluga
123	St13_24317	Horatio x Tuxedo
124	St13_24687	W192 x W207
125	St13_24860	W196 x Beluga
126	St13_25110	Horatio x Tuxedo
127	St12_18408	W165 x W189
128	St12_18726	W156 x W192
129	St12_18766	W178 x Gravitas
130	St12_18798	W178 x Gravitas
131	St12_19045	Sterling x W193
132	St12_19183	W156 x W191
133	St12_19379	W178 x Gravitas
134	St12_19652	W156 x W191
135	St12_19840	Horizon x W194
136	SEWC123	(Panorama x Quartz) x Sterling
137	Spotlight	Horatio x Scribe

138	Robigus	1366 Putch x Capet
-----	---------	--------------------